Mining Crowdsourced Data for Pavement Maintenance, Incident Management, and Traffic Monitoring

A Dissertation Presented for the
Doctor of Philosophy
Degree
The University of Tennessee, Knoxville

Yangsong Gu
May 2023

DEDICATION

This dissertation is dedicated to my parents, Zhixin Gu and Xinhui Xu, and my extended family, including my grandparents, my uncles, and my aunts for their nurture and love.

I believe that:

The subjective agency recognizes that individuals are not passive recipients of external forces, but rather active agents who have the power to shape their own lives and the world around them.

ACKNOWLEDGEMENTS

As I am approaching the end of my Ph.D. training journey, I would like to express my sincere gratitude to all the people who helped me along the way and made my journey meaningful and memorable.

First, my advisor Dr. Lee D. Han, he’s my best research advisor and spiritual mentor ever. Without his recognition of me four years ago, I don’t even know where I would be now. Transitioning from an undergraduate lifestyle directly to a Ph.D. research life was quite challenging for me. It is his patient guidance and support no matter in my project or research studies that motivate me to grow quickly. His teaching style perfectly embodies the philosophy concept in the term of a Ph.D. I was always encouraged to try new techniques and research related to transportation. Besides, his research spirit, creative thinking, aesthetics, reasoning, open-mindedness, and resourcefulness had a profound impact on my thoughts and actions. The most impressive and powerful saying he spoke to me is “If I were you, I would …”. Whenever I face challenges or make decisions in my projects and research, I often think about how my advisor would approach the situation to make a better choice. In my life, he’s more like a parent to me. Whenever I experienced depression about my research, he would attentively listen to my concerns and comfort me. When I fell sick or was unable to work due to health reasons, he would show his concern by checking in on me regularly. From Dr. Han, I learned not only how to do research and communicate ideas and results, but more importantly, I learned how to become mature and a greater man from time to time. Words will never suffice to express my deepest gratitude for the effort and time that he put into me.

Besides, I would like to thank Dr. Asad Khattak, Dr. Hyun Kim, and Dr. Russell Zaretzki for serving on my committee. As experts from different research fields, they provided me with much professional feedback to enhance the quality of my dissertation.

My deep appreciation also goes out to Dr. Cheng Liu and Dr. Kwai Wong who are my mentors in Research Experience for Undergraduate (REU) summer internship program in 2018. I am grateful to Dr. Wong for giving me the opportunity to take part in the research program. It is this program that inspires my research interests and passion. In addition, I have vivid memories of Dr. Liu's patient guidance in teaching me C programming, carefully examining each line of code in both C and MATLAB. He also devoted extensive time to reviewing complex mathematical models with me. I was greatly influenced by his passion for research and his eagerness and persistence to tackle challenging problems. Moreover, I was so lucky that I had the opportunity to continue staying with him for one more month after the internship. During that time, we engaged in various enjoyable activities such as cooking, dining out at restaurants, making and playing his invented version of Chinese chess, assembling parallel machines, and so many more.

I was fortunate to have the opportunity to participate in various research projects funded by the Tennessee Department of Transportation (TDOT), which are fundamental to my research endeavors. Through these projects, I had the pleasure of meeting many excellent transportation engineers, leaders, and practitioners. Honestly, many research ideas and work motivations come from the communication and discussion with Brad

Freeze, Nathan Vatter, Michelle Nickerson, and Jon Storey who are contributing to the development of transportation for the state of Tennessee.

Furthermore, I am appreciative of my entire group. I was so lucky to work with exceptional groupmates: Dr. Yuandong Liu, Dr. Zhihua Zhang, Dr. Nima Hoseinzadeh, Hairuilong Zhang, Ruqing Huang, Diyi Liu, John Stanford, Lanmin Liu, and Mohammad Khojastehpour. Not only did we assist each other with projects and research, but we also had a lot of fun together during the pandemic. I am particularly grateful to Yuandong, Zhihua, and Nima for their tremendous help at the start of my Ph.D. journey. They assisted me with my projects and helped me in adapting to the research life.

Lastly, I would like to thank two other professors in the transportation program: Dr. Candace Brakewood, and Dr. Chris Cherry, and my amazing lab mates from other groups: Jing Guo, Yi Wen, Meredith King, Nitesh Shah, Abubakr Ziedian, Sameer Aryal, A. Latif Patwary, Steve Lee, Antora Moshena Haque, Mojdeh Azad, Saurav Parajuli and many others. Staying with them was a fantastic experience on my Ph.D. journey.

ABSTRACT

Crowdsourcing has been a prevailing fashion of data acquisition thanks to the proliferation of smart devices and wireless communication techniques. In the transportation field, emerging crowdsourcing data could potentially facilitate traffic operation and management. A motiving example is Waze, which is a navigation app that allows Waze users (Wazers) to report different types of traffic incidents e.g., accidents, jams, potholes, disabled vehicles, and so on. Crowdsourced data has many advantages over existing fixed location sensors: cost-effective, extensive geographic coverage, high resolution, and real-time. Moreover, it assembles the human's perception and judgment of traffic incidents, which is more straightforward compared to raw data output from detectors.

This dissertation centers on exploring the application of crowdsourced Waze data in pavement maintenance, incident management, and truck traffic monitoring. Specifically, the first chapter exploited pothole reports to evaluate the pothole spatiotemporal occurrence and hotspot. The pothole reports were compared to the pothole work request and work record from the pavement management system. The second chapter investigated both the association and causation between potholes and flat tire frequency on highways and discussed the spatiotemporal heterogeneous effect of potholes on flat tire frequency. The third chapter made use of accident and jam reports to estimate traffic recovery time after the crash is cleared. This chapter developed a spatiotemporal statistics model to reveal how factors influence the total crash-induced impact duration. Lastly, the dissertation presented a method to estimate the long truck volume by harnessing crowdsourced speed data as well as traffic detector data. In summary, this dissertation contributes to expanding the potential uses of crowdsourcing for managing pavement and incidents, as well as monitoring traffic.

Keywords*: Crowdsourcing, pothole, traffic incident, spatiotemporal heterogeneity, truck traffic*

TABLE OF CONTENTS

LIST OF TABLES

LIST OF FIGURES

INTRODUCTION

Motivation

Crowdsourcing has been a prevailing fashion of data acquisition thanks to the proliferation of smart devices and wireless communication techniques. Crowdsourcing refers to gathering data of interest via many people or vehicles active in different places. There are two motivating examples in the transportation field. One is the navigation app Waze, which has over 30 million monthly active users in the US according to the latest (till 2023) fact sheet (*1*). Waze users are encouraged to share the real-time traffic status, accidents, and other roadway incident information through the app report portal. In addition to Waze, some social media such as Twitter and Facebook, and smart mobile apps such as Google Maps also play important roles in sharing traffic information with the public. The other is crowdsourced probe vehicles. As a small part of road traffic, they are usually equipped with advanced wireless communications to collect and share real-time traffic data (e.g., speed and location). There is no doubt that crowdsourced data paves the way toward a new era of proposing innovative ideas and solutions for traffic management and operation systems.

Crowdsourcing breaks through many limitations of conventional data acquisition in the transportation field. Firstly, it reduces the cost of data collection. For instance, traffic data such as flow, density, and speed are usually collected by infrastructure-mounted sensors such as loop detectors, and radar detectors. Therefore, massive detectors are required to ensure large wide traffic monitoring. However, under crowdsourcing circumstances, everyone can serve as a volunteer to report traffic events through the mobile app. Secondly, it breaks through the geofence of data collection. Traffic detectors are usually prioritized at locations (e.g., urban highways) of great importance to traffic monitoring, whereas other road sections such as rural areas or locations between detectors might be largely unnoticed. Crowdsourcing can complement this gap wherever there is the presence of road users. Thirdly, it characterizes traffic events by the user's perception and judgment. Data collected from traffic detectors usually are quantitative indicators (e.g., electronic format) of traffic status whereas the crowdsourced data could provide qualitative descriptions of traffic events. By contrast, the road user's perception can explicitly reflect the road conditions.

Aside from the existing studies, this study aims to propose innovative solutions to employ crowdsourced data for pavement maintenance, traffic incident analysis, and vehicle classification. To this end, four different studies are designed. First, pothole reports from Waze were employed to identify the locations and lifetime of pavement potholes. This will help pavement crews to locate the pavement pothole distress more efficiently and promptly. Second, the study is trying to untangle the association and causation between pothole distress and flat tire events. The pothole distress is represented by the pothole complaints from users per road length. Third, the jam reports are utilized for estimating the incident recovery time thereby completing the graph of the entire incident impact duration. Fourth, an innovative method was proposed to estimate large truck volume from a loop detector system and crowdsourced speed. This will help traffic management and the operation center monitor network-wide truck traffic using existing data sources.

Data

The data sourced employed in this dissertation are briefly described as follows.

Waze Reports

Waze provides many reports such as crash, congestion, weather, road hazard, and so on. Correspondingly, they can be used for different scenarios such as primary (secondary) crash detection and queueing analysis. Different from conventional traffic detector data, Waze collects traffic events wherever and whenever riders use the app.
Besides, the traffic events including the severity were reflected based on the user's perception and judgment, which can be used to characterize the travel circumstance semantically. The data is obtained through the Waze for Cities (W4C) program. Two types of Waze reports, including pothole (road hazard) and traffic jam reports (heavy, moderate, standstill, or light) are utilized in this dissertation. Especially, the author is among the first to extract useful information from pothole reports in the existing studies. This pothole reports data will be used in **Chapters** I and II. Besides, the Jam reports will be used for incident recovery time estimation in **Chapter** III.

Waze Speed

When Waze users keep the app open for navigation, they can implicitly tell the Waze app the vehicle's operating speed on a specific stretch of the road. The road speed, along with historical information, is measured by real-time updates from multiple Waze users (*2*). Similar to Waze reports, Waze speed is available where there are Waze users. This merit expands the geographic coverage of vehicle speed. Under the traffic view of the Waze partners platform, contract partners can monitor travel speed for any designated routes. In this dissertation, the speed will be utilized for estimating large truck volume in **Chapter** IV.

Pavement Management System Data

The pavement management system provides the work request and work records of pavement repair and construction activities. They are important ground truths for assessing the performance of pothole detection from Waze reports. The data includes when and where (e.g., Interstate 40 mile-maker 201 to mile-marker 204) the pavement was repaired by which work (e.g., in-house resurfacing). The data was originally obtained through the project collaborated with TDOT and it will be applied in **Chapter** I.

Incidents Data

The incident data used in this dissertation comprises operation logs for disabled vehicles and characteristics of single/multiple vehicle crashes. The occurrence of a flat tire is considered an atypical incident and is classified as a disabled vehicle in the TDOT database. Therefore, the operation log data is scrutinized to identify instances of flat tire incidents by searching for relevant keywords such as "flat tire" or "change tire" in the incident operation log. The operation log data is applied in **Chapter** II. In addition, each incident record includes the information of time, location (e.g., latitude longitude, or mile markers), incident type, incident duration, number of lanes closed, and others. All the incident data was obtained through the project collaboration with TDOT. This data will be employed for estimating incident duration in **Chapter** IV.

Miscellaneous data sources

In addition to the abovementioned three main data sources, the other miscellaneous data sources are used to constitute built-environment variables for regression analysis. They comprise roadway characteristics from E-Trims, traffic exposure from Radar Detectors, weather conditions from underground weather, and NPMRDS data from INRIX.

Dissertation Structure

This dissertation includes four chapters. In the following, each chapter will be briefly discussed. **Figure 1** shows the framework of the dissertation.

Chapter I: Towards a crowdsourcing-based pothole detection and evaluation.

This study proposed two using scenarios of crowdsourced pothole reports in facilitating pavement management and maintenance. The spatiotemporal density model is preferred because of two reasons. Firstly, the presence of potholes demonstrates inherent spatiotemporal tendencies. Secondly, the frequency of reports regarding potholes within a particular location and timeframe indicates a higher probability of pothole occurrence. The model should also be robust against false reports. Hence, a spatiotemporal kernel density estimation was implemented to highlight the pothole hotspots. Followed by that, a spatiotemporal density-based clustering approach was conducted to identify potholes from the crowdsourced reports. The performance of detection was evaluated by pavement work requests and work records from Pavement Management System (PMS).

Chapter II: Association and causation between potholes and flat tire incidents.

This chapter intends to uncover the association and causation between potholes and flat tire incidents. In other words, the study tried to answer two questions: 1) Does pothole occurrence correlate with flat tire frequencies? 2) Do more potholes cause more flat tire incidents? To this end, the study developed a spatiotemporal regression model and a fixed effects model to tackle the correlation and causation between potholes and flat tire incidents, respectively. The pothole information was extracted from Waze pothole reports and flat tire incidents were obtained from Tennessee Department of Transportation (TDOT) incidents operation notes.

Chapter III: Estimate incident time to normal traffic duration from crowdsourced data.

This study primarily aims to propose an innovative way to estimate the recovery time of traffic incidents thereby completing the graph of incident impact measured by the time to return to normal flow. Furthermore, the spatiotemporal heterogeneity of observed factors was uncovered by a spatiotemporal local model. To estimate incident recovery time, Waze Jam reports were employed to capture the end of the queue. Besides, this study makes methodological contributions by introducing an advanced modeling approach that integrates geographical regression with survival analysis.

Chapter IV: Estimate truck volume from traffic flow fundamentals.

This chapter proposed an innovative way to estimate large truck volume solely based on traffic fundamental elements: flow, speed, and occupancy. The truck presence was inferred by intrinsic relationships between those three elements. The study put forth two new methods and evaluated their performance against two established methods in the existing studies. The first proposed method breaks through the traditional proportion concept and innovatively formulates vehicle classification as an optimization model. The second proposed method employed the external speed which gets rid of assumptions for speed estimation. To this end, traffic detector data (occupancy and volume) and crowdsourced speed were utilized.

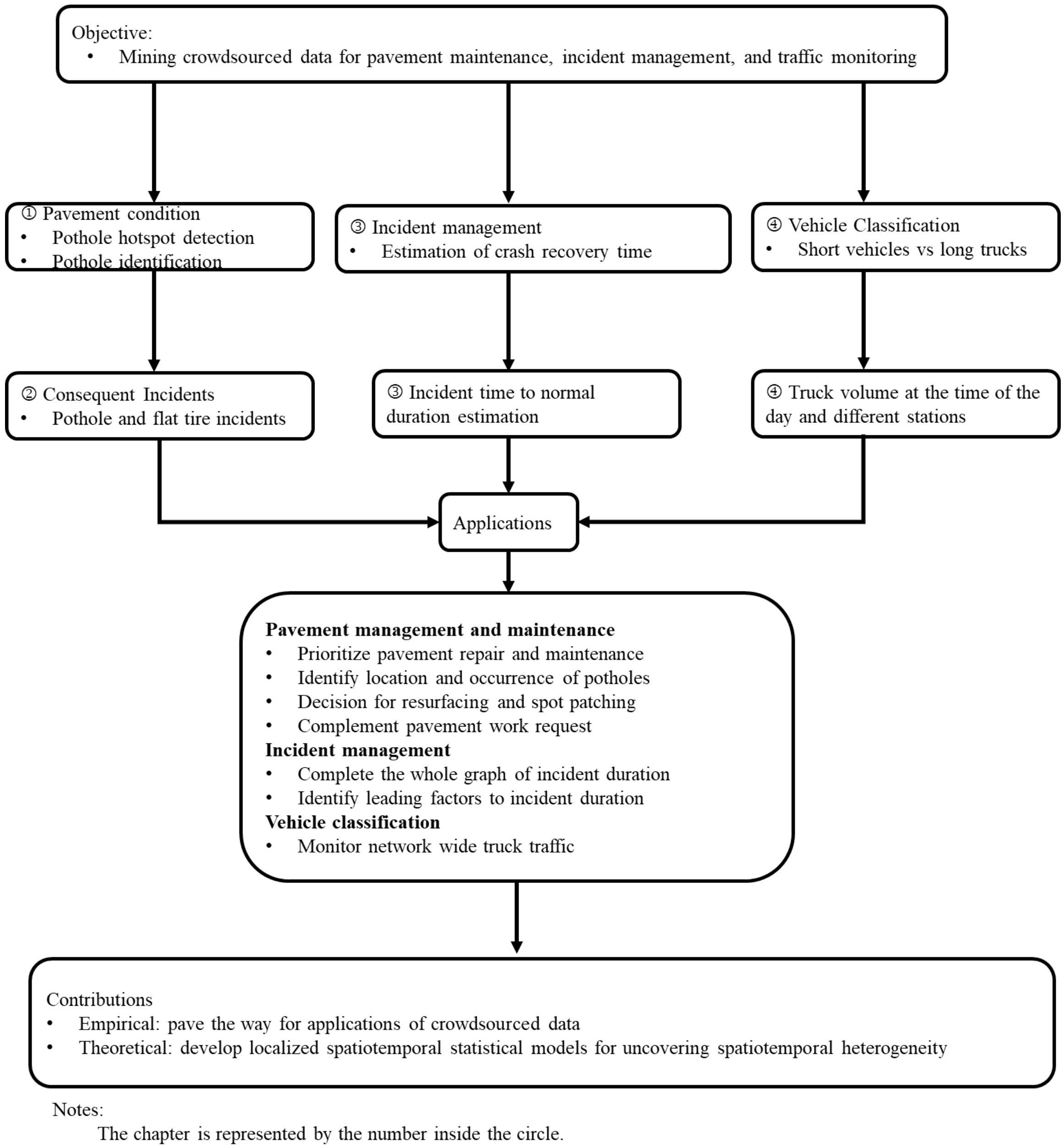

Figure 1. Dissertation framework.

CHAPTER I. SPATIOTEMPORAL KERNEL DENSITY CLUSTERING FOR NOISY CROWDSOURCING DATA FOR WIDE AREA NEAR REAL-TIME POTHOLE DETECTION

A version of this chapter was presented by Yangsong Gu at the 2023 TRB Annual Meeting, and it is under review in Expert Systems with Applications.

Abstract

Identifying and fixing roadway potholes promptly can improve roadway safety and decrease vehicular damage, which is essential in transportation infrastructure management. Transportation agencies are constantly looking for efficient solutions for pavement intelligent management and maintenance. Traditionally, laser scanning, accelerometers, and videos are the major detecting sources employed to diagnose pavement distress. However, the responsiveness of these methods is constrained by the limited amount of equipment and labor. By contrast, crowdsourced tools like the navigation app Waze provide citizens with a cost-effective way to feed real-time roadway information, which could facilitate the evaluation, detection, and repair of potholes. To examine these possibilities, the study collected the 2021 pothole reports for five critical corridors in Nashville, Tennessee. Firstly, a Spatiotemporal Kernel Density Estimation (STKDE) was proposed to estimate the likelihood of potholes over space and time. The results highlight the spatiotemporal variation of pothole propensity. Furthermore, the hotspots recognized at a 95% confidence level revealed the significantly vulnerable areas and times, such as I-40 Westbound near log mile marker 13 from January to June 2021. Secondly, based on the optimal bandwidths generated by STKDE, spatiotemporal DBSCAN clustering was performed to identify potholes. Two pothole patterns are identified and interpreted as isolated spots and pothole zones, respectively. It was also found that crowdsource reports come up much sooner than work requests in Pavement Management System (PMS). Moreover, these reports also identified several blind spots ignored by the maintenance team. This study contributes to facilitating pavement management and maintenance with emerging crowdsourced data.

Introduction

A pothole, as a type of pavement distress, typically appears during the winter and spring months after heavy rain and snow erode and freeze the pavement surface. According to a survey about pothole-related complaints in the past 17 years, Tennessee is ranked 8th in the states with the worst pothole problems (*3; 4*). Also, as estimated by American Automobile Association (*5*) data, drivers nationwide spend nearly $3 billion per year fixing damage such as punctured tires, bent wheels, and broken-down suspension systems (*5*). Therefore, there is an immediate need to find potholes and repair them as soon as possible.

In early 2022, the Tennessee Department of Transportation (*6*) launched a plan for pothole repairs after several winter storms hit Tennessee and many potholes emerged on highways and state routes (*6*). The statewide expenditures for pothole patching in the first 19 days of 2022 were $3.32M, which accounts for over one-third of the total budget (i.e., $9.16M) for 2022. TDOT has spent around $8M every year repairing potholes in the past three years (*6*). However, the majority of potholes are currently inspected by annual laser scanning (*7*) while the minority of them are reported by motorists through TDOT's maintenance request[1]. The former way can generate a reliable diagnosis of pavement conditions, but it involves massive labor and cost. The latter way is at the mercy of the user's perception of potholes. Compared to laser scanning, motorists cannot have a good sense of the location of potholes, especially when they pass the potholes rapidly. However, the crowdsourced reports from motorists might have a wider range and more frequent scanning of the road than TDOT's annual pavement patrol.

Different from filling in electronic forms to report potholes, the navigation app Waze makes it easy to report and share the location and time of potholes via built-in functionalities. Through Waze for Cities program, state and federal government and nonprofit agencies can access free reports (*8*). Many studies have investigated the valuable contribution of other Waze reports to real-time traffic operations (*9; 10*), accident detection (*11; 12*), disabled vehicle detection (*12; 13*), flooding alerts (*4; 14*), and others. However, there is currently no study looking into Waze pothole reports to the author's best knowledge. Therefore, the objective of this study is to investigate the potential of using crowdsourced pothole reports for better pavement management and maintenance.

The remainder of this paper is organized as follows: the literature review section reviewed the prior studies related to the Waze report characteristics and relevant processing methods. In the methodology section, we elaborated on two spatiotemporal methods for exploring pothole reports. Then, the results of the two models are highlighted and discussed, followed by the limitations and conclusions of this study.

Literature Review

Before employing the Waze reports, we must understand the characteristics of Waze reports, which will affect how to effectively use pothole reports to contribute to pavement condition evaluation and pothole detection. This part first reviews the studies about the Waze characteristics. Then, studies identifying pavement distress hotspots are summarized and the conventional pothole detection methods are reviewed. Finally, we discuss the research gaps in existing studies.

Waze Characteristics

Although crowdsourced data has inviting characteristics such as cost-effectiveness and wide coverage, unreliability and redundancy have been two major concerns when they are employed. Specifically, unreliability refers to false alarms. This is likely to happen when users intentionally report nonexistent incidents or misclassify the incident types (*15*). Note that the pothole report is the only option concerning pavement condition in the Waze app so users might report other types of pavement distress (e.g., cracks) as potholes. Therefore, some studies have been conducted to evaluate the validity of Waze reports. For instance, Goodall and Lee evaluated the accuracy of Waze crash and disabled vehicle reports along a 2.7-mile section of the urban freeway by comparing Waze reports with ground truth from video footage. Among 40 crashes associated with the Waze reports, 2 (5%) were confirmed false alarms. By

[1] TDOT Maintenance Request Form. https://www.tn.gov/tdot/maintenance/maintenance-request.html

contrast, disabled vehicle reports have more false alarms than crash reports. Of 560 disabled vehicle reports, 131 (23%) were identified as false alarms (*12*). The redundancy pertains to multiple users reporting the same incident. To mitigate the data redundancy, most of them applied a threshold-based approach. This is because those redundant reports tend to be located in the vicinity of the incident locale and close to the time of incident occurrence. For instance, Liu (*13*) enumerated all possible combinations of spatiotemporal thresholds to match disabled vehicle reports with official incident reports (i.e., Locate IM). It was found that matching rates would stabilize when the time threshold exceeds 50 minutes, and the space threshold exceeds one mile for disabled vehicles. Likewise, when dealing with pothole reports, unreliability, redundancy, and spatiotemporal accuracy should be considered as well.

Pavement Distress Hotspot Mapping

Hotspot mapping is important in prioritizing intervention. It highlights the location and severity of the event of interest. Roberts et al. quantified the area of distress and the percentage of road sections distressed to identify the vulnerable sections. The method is promising in assessing the severity of road sections. However, it is simply not possible to use on every road in the network because distress detection based on deep learning techniques is computationally demanding and time-consuming (*16*). Karimzadeh et al. applied the kernel density estimation to estimate the risk score of roadways thereby identifying the susceptible road sections (*17*). In their model, the parameter Risk Score (*18*) defined by the density of defects per square mile was interpolated for unobserved areas via kernel density estimation. Using the data from Long Term Pavement Performance (LTPP) program, Zhang and Wang employed the Getis-Ord G_i^* to identify the pavement distress hot and cold spots. They found that identified hotspots are closely correlated to environmental and traffic factors (*19*). However, these studies account only for the spatial variation of pavement distress while the temporal variation is not considered. The results might be misleading as climatic factors vary across the year and the amount of impact on pavement structural properties changes across the year accordingly (*20*).

Pavement Pothole Detection

To detect pavement potholes, transportation agencies, and researchers have made substantial efforts in researching advanced detectors and algorithms. Table 1 summarized prior studies of pothole detection. Vibration analysis, 3D construction, and image processing are the three main detection techniques. For each detection technique, we listed several representative studies and pointed out their merits and shortcomings. First, the accelerometer data are usually acquired from smartphones or vehicles embedded with accelerometer sensors, and the pothole event is identified by the characteristics of vehicle horizontal, lateral, and vertical acceleration (*21-24*). The advantage of a vibration-based approach is that little computation and data storage is required. Thus, it can be used in real-time detection. However, the major drawback of this method is that the sensor can only work well when the vehicle hits potholes. If potholes exist in the middle of the lane or the drivers intentionally avoid the potholes, the potholes are likely to be ignored by the accelerometers. Second, 3D construction relies on the advanced techniques of 3D laser scanners (*25-27*), Stereo vision (*26*), and Kinect sensors (*28*). Compared to the accelerometer sensors, 3D construction can typically observe more pavement conditions details and generate more accurate evaluation reports. However, the cost of detectors is still significant, and high computational effort is needed to perform a wide range of detections. Third, image-based methods benefit from emerging image-processing techniques. The image source is usually captured or clipped from the camera mounted on the vehicles. To distinguish the characteristics of potholes from other pavement distresses, earlier research focused on image segmentation and visual properties extraction (i.e., visual texture, shape, and dimension) (*29-31*). With the development of deep learning in recent years, growing studies employ Convolutional Neural Networks (CNN) and their extension models to classify pavement images with potholes (*32-37*). As for the characteristics of machine learning, a set of images with identified potholes is needed to train the model. Although it requires less labor and generates higher accuracy than earlier approaches, intensive computation is a bottleneck when it is applied for real-time detection. What's more, the storage requirement for the image or video collection is still non-negligible (*38*). These pavement pothole detection approaches tend to be cost-prohibitive or labor-intensive and are typical with limited geographical coverage or implementation frequency. An approach with more extensive spatiotemporal coverage of the roadway network and more affordable to public agencies is desired. To that end, the study presented in this paper examines a crowdsource data-based pothole detection approach.

Research Gaps

Several limitations have been identified in previous studies. Pothole appears as spatiotemporal characteristics due to seasonal weather conditions and uneven traffic load on the network, while the existing studies lack the consideration of the temporal variation of the pavement distress when identifying the hotspots. The Waze pothole report has not been extensively explored, despite the widespread use of other Waze reports (e.g., crash, jam) in transportation safety and operation research. This study aims to investigate the promise of using the Waze pothole reports for supporting pavement management and maintenance. Specifically, the study attempted to address the following research tasks:

1. Uncover the spatial and temporal hotspots of potholes.
2. Identify the potholes through crowdsourced pothole reports.

To this end, the researchers collected one year (i.e., 2021) of Waze pothole reports for the five important corridors in Nashville, Tennessee: Interstate 24, 40, 65, 440, and State Route 155 (hereinafter referred to as SR-155) as a case study. Motivated from the literature review. A spatiotemporal kernel density estimation approach was proposed for detecting the pothole likelihood concerning place and time, followed by a statistic test for hotspot recognition. Then, a spatiotemporal DBSCAN (density-based spatial clustering of applications with noise) clustering was implemented to identify potholes. The identified potholes are compared with the pothole work request and records from the Pavement Management System. Finally, a series of performance metrics are proposed to evaluate the contribution of Waze pothole reports.

Table 1. Summary of studies about pothole detection in the literature

No.	Type	Reference	Data Source	Method	Pros	Cons
1	Vibration-based	Kulkarni et al. *(39)*	Accelerometers data and official pothole data	Neural network	Real-time application	Subject to both technical limitations and human error
2		Yu and Yu *(21)*	Acceleration records	Statistical analysis based on level of vibration.	Small storage, cost-effective	Not available to distinguish distress type
3		Lekshmipathy, Velayudhan and Mathew *(22)*	Smartphone accelerometer data and video ground truth	Statistical analysis based on vehicle vertical jerk.	Accurate, real-time	Need to fix the smartphone at a certain location; Cannot detect the potholes in the middle of the lane
4		Bhatt et al. *(23)*	Smartphone gyroscope and accelerometer sensors	Classification model based on a Support vector machine	Real-time and high accuracy (92%)	Require sufficient data to build a reliable classifier
5		Egaji et al. *(24)*	Accelerometer data	Multiple machine learning models such as support vector machine, random forest, and so on.	Real-time application	Require a large number of training data
6	3D construction	Chang, Chang and Liu *(25)*	3D laser scanner	Clustering the 3D laser points	Estimate the area and volume of potholes.	Expensive.
7		Jog et al. *(27)*	3D laser scanner and 2D video	2D appearance-based recognition combined with 3D sparse points reconstruction and	Estimate the area and volume of potholes.	Off-time detection, computation demanding
8		Zhang et al. *(26)*	Stereo vision	Compare the difference between disparity points and fitted surfaces.	Estimate the size, volume, and position of potholes	A threshold is needed to outline the potholes.
9		Moazzam et al. *(28)*	Kinect sensor	Characterize the pothole from pavement depth images	Estimate the size and volume of potholes	Low accuracy
10	Image processing	Koch and Brilakis *(31)*	Pavement images	Image segmentation, morphological thinning, and elliptic regression	High accuracy	Image lightning and viewing can impact the detection.

Table 1. Continued

11		Ukhwah, Yuniarno and Suprapto *(33)*	Pavement images	Deep learning under the YOLO framework.	Fast detection	Need labeling the data for training parameters.
12		Ye et al. (*34)*	Pavement images	Convolutional Neural Network	High accuracy	Need many images to train the model.
13		Zhang et al. (*36)*	Pavement images	ShuttleNet Neural network	High accuracy	It has limitations in detecting giant patches and cannot detect all types of pavement distress.
14		Maeda et al. (*37)*	Pavement images	Generative adversarial network	Available for the small size of real training images	The accuracy partially relies on the amount of original training data.

Methodology

Given the specific shortcomings of Waze data mentioned in the above **Literature Review**, two density methods were proposed to eliminate the impact of redundant reports and possible false reports. The density-based methods, namely, detecting the area of interest according to the density of points, can effectively deal with these two challenges (*40*). The density-based models attach higher importance to the area with dense points of interest while lower importance to the area with few points of interest. Thus, the area with dense pothole reports would explicitly reflect the severity of potholes, and the area with few reports that potentially are false reports would be disregarded as they cannot form a dense area. The workflow to implement density-based models is shown in **Figure 2**, wherein the steps including from data collection (i.e., Waze and PMS ground truth) to model deployment. To examine the potential of Waze for hotspot discovery, only Waze data was used. Besides, the ground truth from PMS was employed to evaluate the performance of pothole detection. The first density model that estimates the pothole likelihood can reveal the vulnerable areas and periods, which further helps the pothole detection model in parameter selection. In the end, applications and lessons in using crowdsourcing data for monitoring potholes are discussed.

Spatiotemporal Kernel Density Estimation (STKDE)

Spatiotemporal kernel density estimation has been applied for estimating the risk or the likelihood of the events that have spatiotemporal patterns. Therefore, it is frequently used in crime (*41; 42*) and crash (*43; 44*) hotspot mapping analysis. The STKDE is also a predictive approach as it can estimate the likelihood of where the event of interest is not observed. This merit compensates for the Waze pothole report because Waze users might not be everywhere on the network; on the other hand, users may not observe every pothole. STKDE models the probability of an event as a function of space and time. Since the pavement work request and record were noted by project mile markers, we projected Waze reports from the 2-D space (i.e., latitude and longitude) to 1-D (i.e., log mile maker), thus the fundamental formula is written as (*42*):

$$f(x,t) = \frac{1}{nh_s^2 h_t}\sum_{i=1}^{n} k_s\left(\frac{x-x_i}{h_s}\right)k_t\left(\frac{t-t_i}{h_t}\right) \tag{1}$$

where $k_s(\cdot)$ and $k_t(\cdot)$ are the spatial and temporal kernels, respectively. h_s and valuableh_t are corresponding spatial and temporal bandwidth. The x_i and t_i represent the log mile and timestamp of a Waze pothole report.

Bandwidth selection is the crucial element of STKDE. The scale of bandwidth affects the smoothness of a fitted surface. A large bandwidth tends to produce over-smoothing, which will hide multi-modal distribution in space and time dimensions. On the contrary, a small bandwidth leads to increased variability, which is insufficient to interpolate the unobserved areas and periods. Inspired by the crime research of Hu et al. (*41*), this study implements the likelihood cross-validation method, which is a data-driven optimization approach. It can reflect the spatiotemporal pattern more accurately. This approach was proposed by Duin (*45*) in 1976. The optimal bandwidth is obtained by minimizing the Kullback-Leibler divergence which is the distance between the expected probability distribution and the estimated probability distribution. The Kullback-Leibler divergence (Remarked as the Integrated Mean Squared Error, **IMSE**) can be written as:

$$IMSE = d_{kl}(f,\hat{f}) = \int \ln\left[\frac{f(x,t)}{\hat{f}(x,t)}\right] f(x,t)dxdt \\ = \int \ln[f(x,t)]\, f(x,t)dxdt - \int \ln[\hat{f}(x,t)]\, f(x,t)dxdt \tag{2}$$

Since the first part is not related to the bandwidth, choosing *h* to minimize **Equation** (2) is, therefore, equivalent to maximizing the second term, which is the expectation of $\ln[\hat{f}(x,t)]$:

$$\hat{E}(\ln[\hat{f}(x,t)]) = \ln\,[\frac{1}{h_s h_t}\sum_{i=1}^{n} k(\frac{x-x_i}{h_s}) \times k(\frac{t-t_i}{h_t})] \tag{3}$$

Further, $\hat{f}(x,t)$ can be approximately estimated by its sample mean, which is:

$$\hat{f}_{-i}(x,t) = \frac{1}{(n-1)h_s h_t}\sum_{j=1,j\neq i}^{n} k(\frac{x-x_j}{h_s}) \times k(\frac{t-t_j}{h_t}) \tag{4}$$

Therefore, the optimal bandwidth h_s and h_t can be estimated by maximizing the sum of the log-likelihood of **Equation** (4), which is:

$$\sum_{i=1}^{n} \ln[\hat{f}_{-i}(x,t)] = \ln\,[\frac{1}{(n-1)h_s h_t}\sum_{j=1,j\neq i}^{n} k(\frac{x-x_j}{h_s}) \times k(\frac{t-t_j}{h_t})] \tag{5}$$

In addition, the Gaussian kernel is specified to estimate the point probability. It is suggested by the finding that the spatiotemporal accuracy of Waze reports tends to have a 2D bell shape (*13*). The Gaussian kernel is written as:

$$k(\cdot) = \frac{1}{\sqrt{2\pi}} \exp\,(-\frac{(x_i - x)^2}{2h^2}) \tag{6}$$

Further, we defined pothole hotspots in this study as STKDE density estimation ρ given a location and time that exceeds the average density score μ_ρ , plus 1.96 times the standard deviation of density scores σ_ρ (*46*). That is to say, the hotspots are the areas where pothole complaints at a specific time are significantly higher than the normal ($p<0.05$) density of pothole complaints.

$$\rho \geq \mu_\rho + 1.96\sigma_\rho \tag{7}$$

Spatiotemporal DBSCAN Clustering (ST-DBSCAN)

Clustering is a common method for discovering useful knowledge in large event databases. It is the process of segmenting data into distinct groups, with intra-groups having similar characteristics and inter-groups having distinct characteristics. In this study, the ST-DBSCAN introduced by Derya et.al (*47*) was used to identify the pothole clusters. The main reasons for using this algorithm to cluster Waze reports are: 1) it accounts for the spatial and temporal patterns of potholes, 2) it can discover the clusters with any shape; 3) it can distinguish the noise points (in our case, it could be fake reports; and 4), it does not require prior knowledge of the number of clusters. In Waze-related studies, the ST-DBSCAN has been applied to identify the secondary crash (*48*), end of the queue (*10*), and congestion (*49*). In the following sections, the application of ST-DBSCAN to Waze pothole reports is elaborated.

Figure 3 illustrates the spatiotemporal clustering for Waze pothole reports. Each pothole report has a geotag (i.e., latitude and longitude) and timestamp. The 2D location is projected to the 1D location, which is represented by the log mile marker. This dimensionality reduction could accelerate the clustering efficiency and preferably align the report data with ground truth in traffic direction, yet it assumes that reports are independent between routes. Further, the spatial proximity of the two reports can be defined as the difference between log miles. Regarding the temporal difference, the number of days between reports is used to measure the temporal similarity. That is because the potholes would not disappear in the short term if no repair occurred. Different users may report the same pothole on different days unless the pothole is patched. Turning to the algorithm, ST-DBSCAN requires three essential parameters: spatial threshold ε_s, temporal threshold ε_t, and minimum number of points ($minPts$). These three parameters altogether filter the neighbors to form a cluster. A point *p* is marked as the neighbor of point q if and only if both time and space are within the corresponding neighborhood radius. For instance, points *B* and *C* are the qualified neighbors of point *A*. Besides, $minPts$ is specified to form a dense neighborhood. If a point has more than $minPts$ of neighbors in ε_t and ε_s, then it is viewed as a core point (see blue point *A* in **Figure 3)** that is used to develop a cluster. If a point is not grouped by any clusters, then it is labeled as a noise point (see grey point *N* in **Figure 3**). The noise point is likely to be a false report as suggested by previous studies (*11; 13*).

To implement the ST-DBSCAN, the study referenced the algorithm proposed by Zhang (*48*), Liu (*10*), and Zhang (*50*). Table 2 depicts the pseudocode of ST-DBSCAN. The algorithm begins by enumerating all unvisited reports. Then, for each report *P*, the qualified neighbors are retrieved (i.e., function *ST_neighbors*). If the number of neighbors of the report *P* is less than the $minPts$, then the report is labeled as a noise point. Otherwise, the algorithm steps into searching for neighbors of the identified neighbors of *P* following the same $minPts$ (see ***expandCluster*** in Table 2). The program runs until all points are labeled with cluster id or noise point. A critical procedure of ST-DBSCAN is the selection of the parameters: spatial threshold ε_s, temporal threshold ε_t, and the minimum number of points ($minPts$). The spatial and temporal thresholds control the scope of the searching area. A large spatial or temporal threshold is likely to encompass heterogenous neighbors and smooth out important spatiotemporal variations. Meanwhile, a large proximity threshold downgrades the effect of $minPts$ as the number of neighbors increases. On the other hand, a small spatial or temporal threshold leads to the isolation of points, and it is difficult to form a dense cluster. From prior studies, the authors concluded three typical methods of determining the thresholds. The first one is made by domain knowledge or experience, for instance, Zhang et al. chose one mile and 30 minutes for clustering traffic jams and accidents on the freeway. The second one is the iterative method. This approach usually exhausts the possible combination of parameters and chooses the one that makes the distinct number of clusters at the critical point (*51*). The last one is data driven. It attempts to find the common structure within the dataset. For example, Liu et al. (*10*) proposed a statistical method to update the threshold

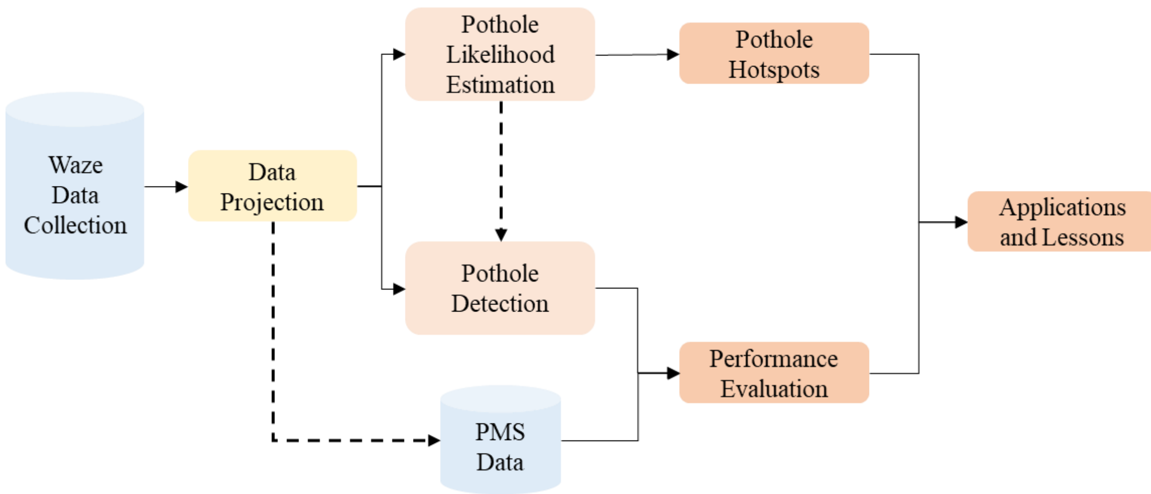

Figure 2. Pipeline of applying pothole reports for pavement management.

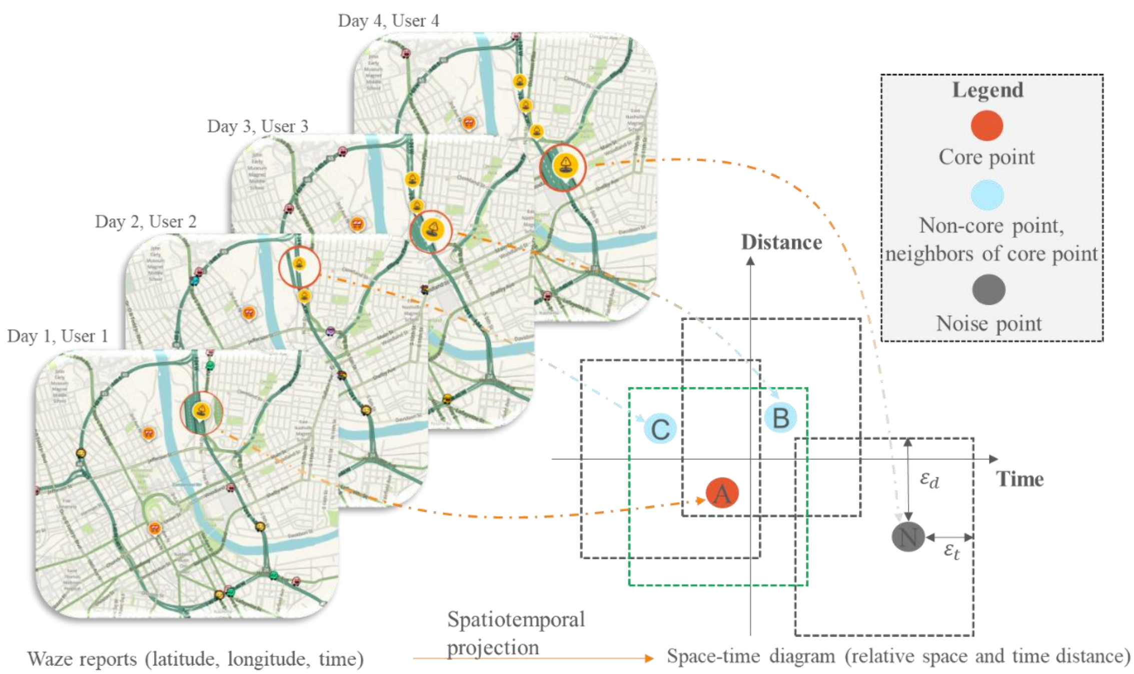

Figure 3. Illustration of spatiotemporal clustering for pothole reports.

Table 2. Pseudo algorithm of modified ST-DBSCAN

Algorithm: ST-DBSCAN

```
ST-DBSCAN (D, ε_t, ε_d, minPts, minDensity)
    cluster_id = 0
    for each pothole report P in dataset D:
        mark P as visited
        // Retrieve spatiotemporal neighbors
        N = ST_neighbors (D, ε_t, ε_d)
        If lenof (N) < minPts
            mark P as Noise
        else
            cluster_id = cluster_id + 1
            expandCluster(P, N, ε_t, ε_d, cluster_id, minPts)
expandCluster (P, N, ε_t, ε_d, cluster_id, minPts, minDensity)
    Assign P to cluster cluster_id
    for each pothole report P' in N:
        mark P' as visited
        N' = ST_neighbors (D, ε_t, ε_d)
        If lenof (N') ≥ minPts
            N= N joined with N'
        If P' is not yet assigned to any cluster
            Assign P' to cluster_id
```

by the observed nearest distance between data points. This study innovatively adopted the spatiotemporal bandwidths estimated from STKDE because the optimal bandwidth captures when and where pothole reports are concentrated. A similar logic was also implied in the DENCLUE clustering algorithm. Under the bandwidth context, the points that are assigned to the same local maximum are put into the same cluster (*52*). The last parameter $minPts$ is set to be 5 as recommended from a previous study that the $minPts$ should be at least twice of the dimensions (*40*).

Data Description

To contribute to pavement management and maintenance, this study makes use of Waze pothole reports and Pavement Management System (PMS) data from TDOT. Waze data are obtained from TDOT through the "Waze for Cities" program[2] with the Waze company, which is free to researchers. Waze data provide information including location (i.e., latitude and longitude), timestamp, street, and reliability of reporters. The PMS data include the pavement work request and daily work request by log mile. PMS data are used as the ground truth to assess pothole detection results. The study primarily focuses on five backbone corridors in Nashville, Tennessee: I-24, I-40, I-65, I-440, and SR-155, as **Figure 4** shows. I-440 and SR-155 are inner and outer city bypasses, respectively. I-40 runs east-west through Nashville city; I-24 runs northwest-southeast through the city; I-65 runs northeast-southwest through the city. They join in the central part of the city. **Figure 4** also illustrates the spatial distribution of annual potholes reports on the study routes. As indicated in the figure, almost everywhere suffered pothole distress. Comparatively speaking, the east of I-24 (log-mm, 13-15), the west of I-40 (log-mm, 0-2,7-12), the east of SR-155 (log-mm, 9-11), and the central urban area had more pothole evidence than other areas. It is worth noting that the highway (near) junction areas such as the junction of I-65 and SR-155, and the junction of I-40 and I-24 have substantial pothole complaints. It makes sense that these areas bear heavy traffic loads all year. On the other hand, to better understand the seasonal characteristics of pothole occurrence, the study spans the entire year 2021. **Figure 5** presents the monthly number of Waze pothole reports per mile of study routes. As we can see, I-40 had the largest amount of pothole complaints, followed by I-24, I-65, SR-155, and I-65. The bypass I-440 produced the least pothole feedback. That makes sense because the entire I-440 was reconstructed in July 2021[3]. In addition, potholes happened considerably more often in the winter and spring. This makes sense because numerous potholes occur after winter storms. Furthermore, with the pavement repair work going on, the number of pothole complaints seemed to decline after March.

Results

STKDE and Hotspot Results

STKDE is carried out for each route using the bandwidths selected by the maximum

[2] "Waze for Cities" program: https://www.waze.com/wazeforcities.

[3] I-440 Reconstruction Nears Completion, https://www.tn.gov/tdot/news/2020/6/23/i-440-reconstruction-nears-completion.html.

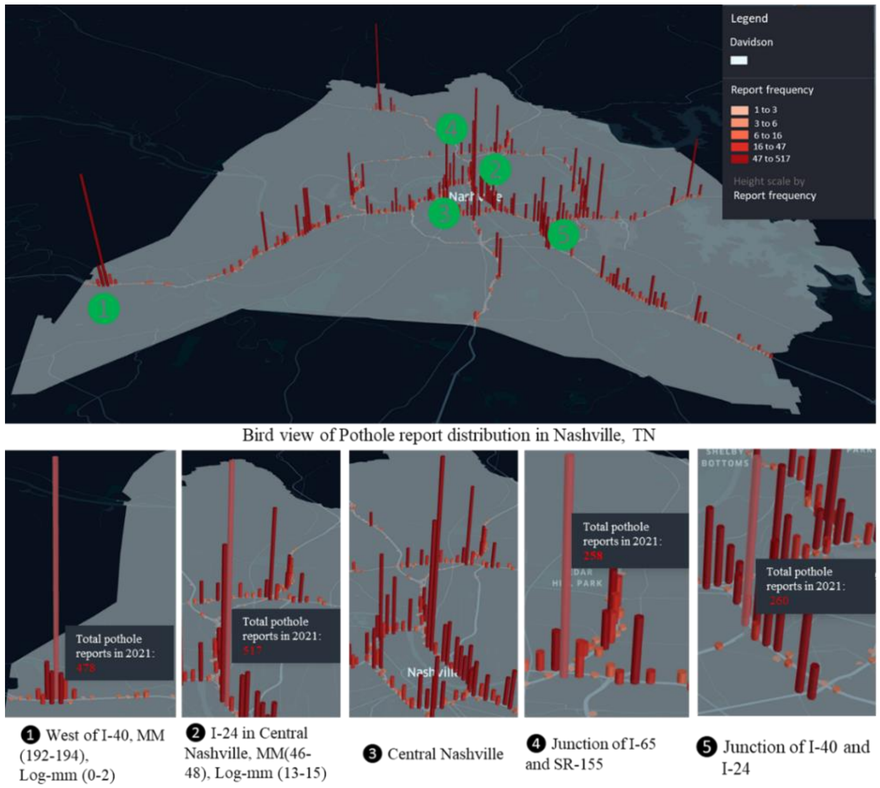

Figure 4. Pothole reports spatial distribution on study routes.

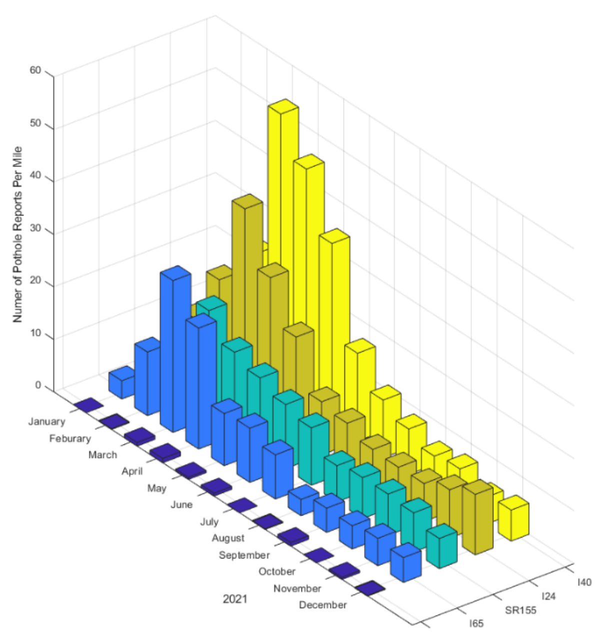

Figure 5. Monthly pothole reports on study routes.

log-likelihood cross-validation method. As an example, **Figure 6** shows the spatiotemporal likelihood of pothole occurrence for I-40 westbound in Nashville. The optimal temporal bandwidth is 24 days, and the optimal spatial bandwidth is 0.04 miles (see optimal parameters in **Table 3**). This implies that Wazers report the potholes frequently in hotspot areas within 48 days (it is twice the bandwidth as the kernel is a symmetric Gaussian kernel). On the other hand, the spatial variation of pothole reports in hotspot areas tends to be narrow, spanning 0.08 miles in two directions. In addition, the STKDE also illustrates the spatiotemporal pattern of pothole occurrence. For instance, in the west of I-40 (from log mile 5 to 10), the pothole probability from February to the end of June is considerably greater than in other areas and other periods. It is worth noting that the STKDE also predicts the probability of pothole occurrence for unobserved areas. This potentially mitigates the bias that users have a different tendency of reporting potholes in different areas and traffic situations. Besides the findings stated above, we should also note the limitations of the proposed method. It can be seen that pothole density is not estimated everywhere (see red points without contours). This is because the bandwidths we estimated are fixed at all locations and times, which is not compatible with long-tailed distributed and spurious noise data (*53*). An adaptive spatiotemporal kernel approach that changes bandwidths locally (*54*) could be a worthwhile study in the future.

Table 3 summarizes the bandwidth and estimation error for the study's routes. It is observed that pothole hotspots exhibit spatial and temporal heterogeneity. For example, a pothole hotspot on I-440 Westbound could be observed by Wazers within about 114 days (about twice 56.87). This suggests the expected time from the request to repair the potholes on I-440 Westbound seems to be much longer than that for other routes. By contrast, the I-24 Westbound had the smallest temporal bandwidth, indicating that pothole reports were concentrated in a short period and the corresponding repair was also prompt. In terms of spatial bandwidth, the I-440 has the largest spatial bandwidth, implying pothole reports are sparsely distributed. In contrast, I-24, I-40, I-65, and SR-155 generated a much smaller spatial bandwidth, suggesting evidence of pothole clusters.

Figure 7 shows the average lifespan of pothole hotspots, aggregated to the mile, as identified by STKDE. The color of the segment indicates the average lifespan of the hotspots in that mile, with red being the longest and green being the shortest. Compared to road segments in the peripheral area, the road segments near the center of the city appear to have denser pothole clusters, but with shorter lifespans. For instance, the east side of the city bypass SR-155, the west of I-40, and the south of I-24 in the peripheral area have longer-lasting pothole clusters of over 160 days. By comparison, pothole hotspots located along I-24, I-65, and I-440 around the downtown area disappear sooner, typically in less than 100 days. Moreover, pothole hotspots tend to cluster near highway junctions such as I-24 and I-65, I-65 and I-440, and I-24 and I-440. These areas have more lanes, more lane changes, and bear heavier traffic than mainline segments elsewhere.

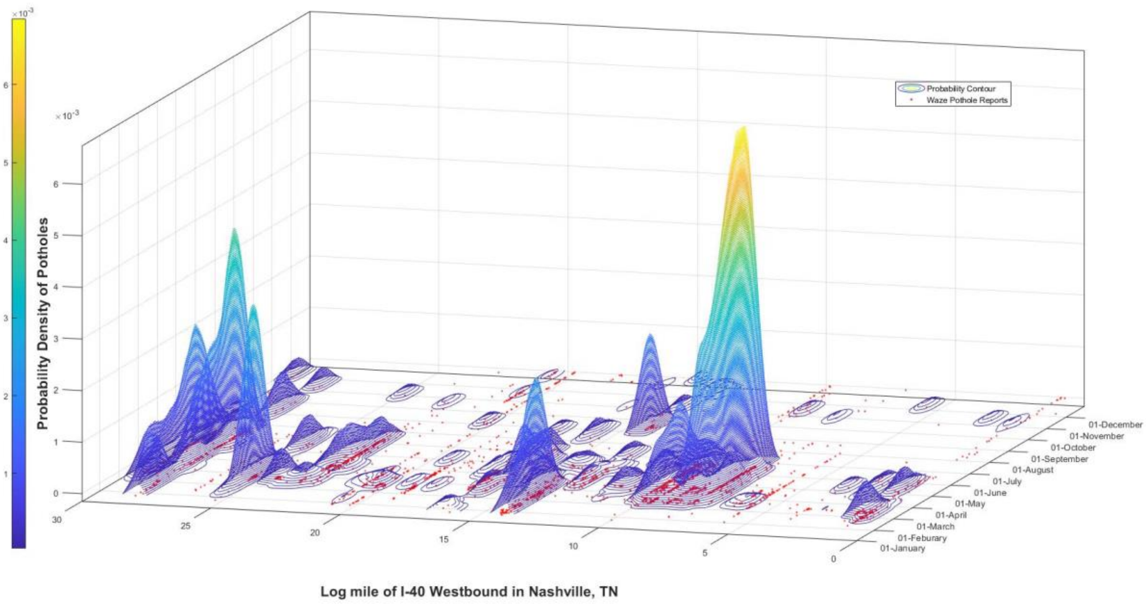

Figure 6. Sample STKDE results (I-40, Nashville, TN).

Table 3. Optimal bandwidth selection and estimation error

Route	Temporal Bandwidth $\boldsymbol{h_t}$	Spatial Bandwidth $\boldsymbol{h_s}$	IMSE
I-24 W	18.90	0.08	0.0017
I-24 E	19.85	0.04	0.0022
I-40 W	23.70	0.04	0.0021
I-40 E	24.46	0.04	0.0022
I-65 S	25.71	0.10	0.0014
I-65 N	24.05	0.05	0.0021
I-440 W	56.87	0.75	0.0003
I-440 E	48.05	1.54	0.0003
SR-155 W	35.79	0.05	0.0018
SR-155 E	31.33	0.05	0.0018

ST-DBSCAN Results

The optimal spatiotemporal bandwidths generated by STKDE were applied for the thresholds of ST-DBSCAN (see **Table 3**). First, we demonstrate the pothole detection results on I-40 westbound as an example. As shown in **Figure 8**, the pink polygons are the identified clusters from the pothole reports (i.e., light blue scatter points). Pothole work requests and work records from the PMS system were added for reference. Each vertical dashed orange line represents a request for manual spot patching, and each vertical solid green line denotes a request for resurfacing. Each dashed purple line represents a manual spot patching repair conducted in the field, and a solid dark blue line marks a pavement resurfacing activity.

As **Figure 8** shows, the shape of pothole report clusters (i.e., pink polygons) reveals two types of potholes in the first left half of 2021: single isolated spots and pothole zones. **Figure 9** exemplifies two types of potholes in the real world. The single isolated spots are short in length, with a certain distance from other potholes. However, they may last for a long time. These potholes tend to show up in the city's peripheral areas. For instance, many slender clusters were detected from the log mm 0 to 8. These clusters cover a prolonged period from early February to the end of June while they are quite concentrated on a short stretch of the road. The pothole zones have comparatively large vertical spans, in the figure, which suggests the potholes are distributed in a longitudinal, and perhaps continual (but not continuous), fashion, along a length of road. These strings of potholes form what we call pothole zones. For this study, a pothole zone is recognized in the case when the longitudinal span of a pothole report cluster is greater than 0.21 miles. This critical value is suggested by the 80th value of all clusters' length, representing the relatively long reporting area. For instance, a pothole zone exists, per WAZE reports, from log mile 13.1 to 14.1 as the red bar to the left of the scatter plot indicates. A pothole zone suggests a cluster of significantly deteriorated pavement conditions that causes uncomfortable, or even unsafe, local driving experience. Therefore, Wazers are more likely to make the effort to report the potholes in such areas. The identification of a pothole zone thus supports, if not triggers, the decision to repair the pavement. According to the state DOT record, pavement resurfacing between log miles 12.5 and 13.5 was requested on March 23, 2021, as the solid green line shows. This request however was trailed by the earliest reports (i.e., February 27, 2022) by concerned Wazers by many days. Two weeks after the request (i.e., April 6, 2021), pavement crews started to resurface the stretch between log mile 7.4 and 13.2 (see solid blue lines) which covers the pothole zone area. The subsequent Waze pothole reports, after the resurfacing effort, indicated persisting potholes near the beginning and the end portions of the newly resurfaced roadway segment. This might be because the resurfacing project was conducted intermittently for two months to resurface the entire region, as we can see that pothole reports drastically reduced starting from June 1, 2021.

Furthermore, when comparing the work request and potholes, it is found that the work request intersects many clusters during pothole seasons, and they fall behind the earliest report (i.e., the left-most point of the pink polygon) in the cluster. Most of the work requests were made in the middle of February, although there have been pothole complaints starting earlier in January. This suggests the superiority of Waze's earlier detection of potholes. The pothole patching work promptly responded to the pothole-dense areas (i.e., log mm 6-20), which are close to the central part of Nashville. By contrast, the boundary areas (e.g., log mm 25-30) seem to get no attention as no work activities were found while multiple work requests have been repeatedly made.

During the pothole off seasons, Waze pothole reports also identified potholes where no work requests or repair records were found for the proximity. Such cases include log mm 0.2 in September and December, log mm 28.1 in August and September, and so on. It should be noted that ST-DBSCAN may also fail to identify a pothole due to insufficient data (e.g., pothole reports) like all clustering techniques. As vividly shown in **Figure 8**, several spot patching works were requested in August from log mm 6 to 14, yet no pothole report clusters were found there, but sparse pothole reports were presented there.

Figure 10 shows the active potholes identified by ST-DBSCAN along the study routes throughout the year 2021. I-40 W consistently has the most potholes with over one pothole per mile active every day in March. I-440 Westbound and Eastbound generate the least number of potholes and have the shortest period of pothole distress within the year (e.g., from March to June). In general, the active potholes have drastically dropped since the end of June, indicating the repair work was close to the end. Nonetheless, it should be noted that there are still a few potholes present in the second half of the year, yet they are not requested for repair.

Figure 11 presents the density plot of the lifespan of identified potholes from pothole reports. Each violin plot shows the lifespan statistics in two directions of travel, i.e., N and S or E and W. The estimated density distribution is truncated at the maximum and minimum values as the pothole lifespan must take on non-negative values. The three dashed horizontal lines from top to bottom represent the 75th, 50th, and 25th percentiles of pothole lifespan values, respectively. The density distribution curves are all right skewed and their median (50th percentile) values suggest that half of the potholes exist for more than two months. Because of the complete reconstruction of the entire I-440 in July 2021 as mentioned in the data description section, there were too few potholes detected on I-440 in 2021 to form a density distribution. With the all-new pavement, it is not likely to come across many potholes in the short term. Except for I-440, the pothole lifespan lasts from a few days (e.g., 10 days) to almost one year (360 days). While some potholes are repaired promptly, a few of them are not for a long time.

Another finding shown in the violin diagram is that pothole lifespans are different for the two travel directions of the same roadway. For example, the median pothole lifespan for the I-24 north direction is about 25 days shorter than that for the south direction. On the one hand, this indicates a prompter response/repair for I-24 north direction than south direction. On the other hand, it suggests potholes distributed concentratedly in the north direction of I-24 so that a pothole patch request and field repair work can cover many potholes at once.

Prior Waze evaluation studies have seen that Waze reports can capture a certain fraction of incidents recorded by official sectors and potentially contribute to the incidents outsides the official database (*12; 13; 55*). Likewise, this study creates five metrics for evaluating the Waze pothole reports based on the ground truth data from PMS

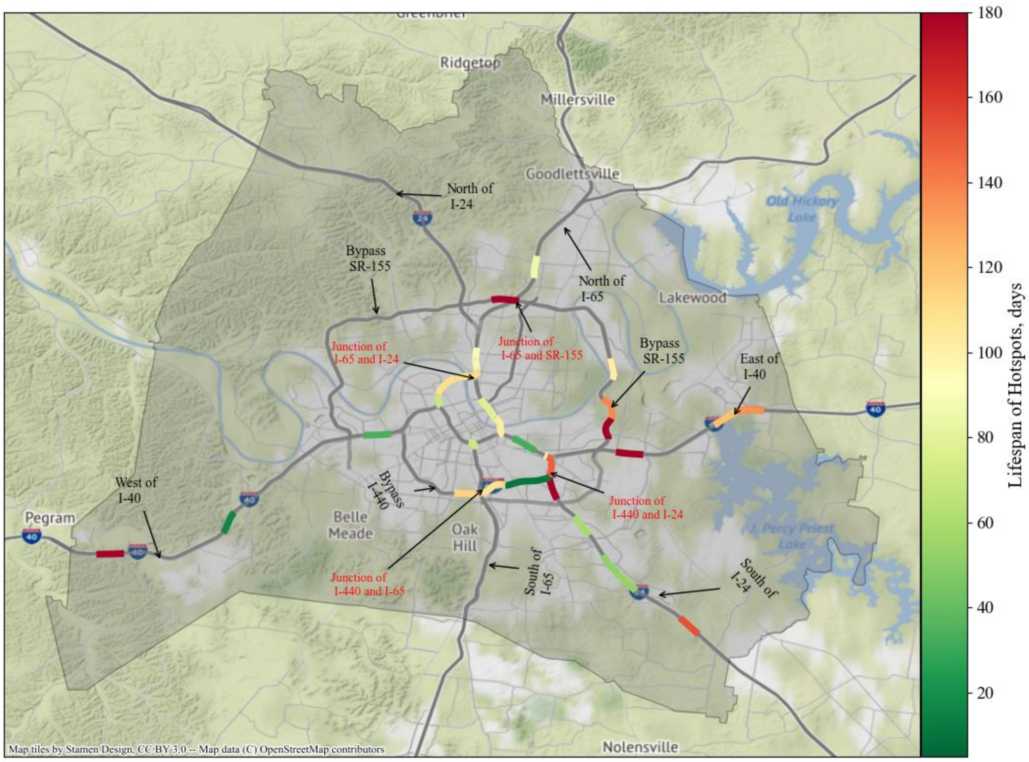

Figure 7. Spatial distribution and lifespan of pothole hotspots.

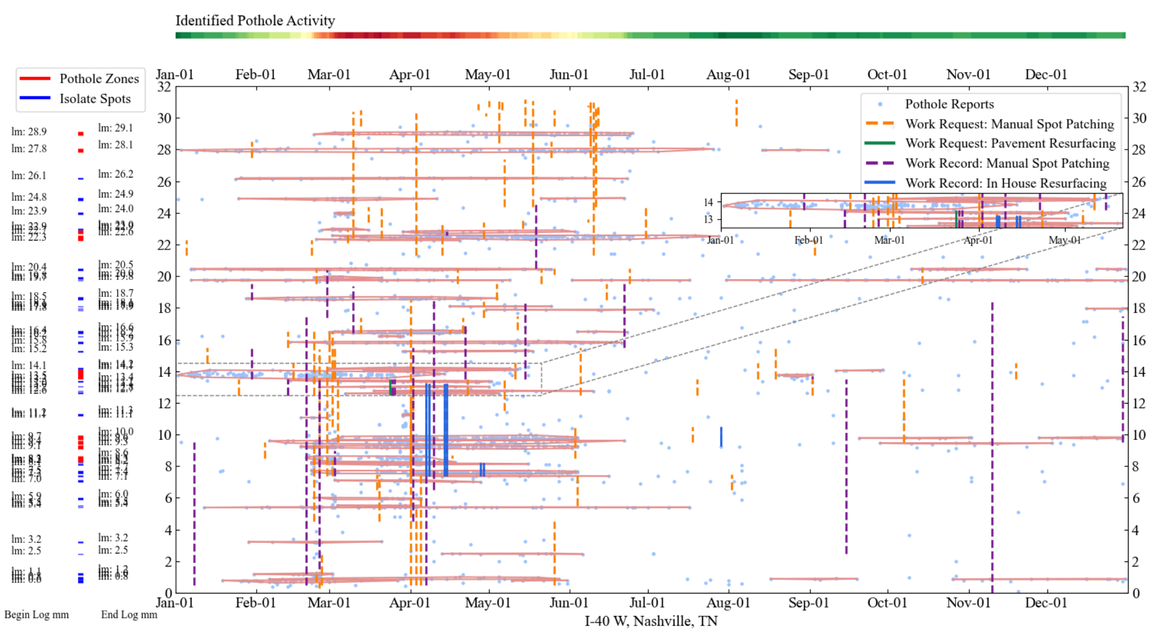

Figure 8. ST-DBSCAN for I-40 W, Nashville, Tennessee.

a. Single spot b. Pothole zone

Figure 9. Example of pothole types.

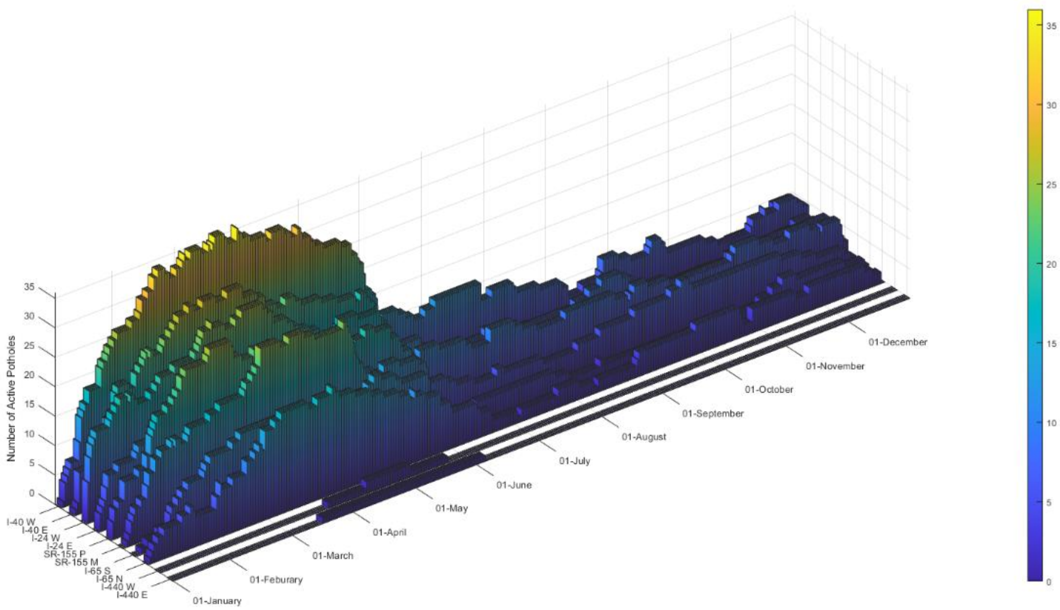

Figure 10. A 3-D Bar chat of number of active potholes detected on study routes.

system:

1. Detection-to-Request (DR): number of Waze pothole report clusters dropping into patching requests.
2. Failure Detection (FD): number of patching requests without proximate Waze pothole report clusters.
3. Complement-to-Request (CR): number of Waze pothole report clusters that are not intersected with any patching requests, which is also known as Wazers' possible contribution (*55*).
4. Detection-to-Request Rate (DRR): rate of DR to total patching requests in the PMS system.
5. Complement-to-Request Rate (CRR): rate of CR to total patching requests in the PMS system.

Notice that pothole patching requests in PMS are made non-directionally. Hence, the total requests represent the number of patching requests for either a single direction or both directions. As shown in **Table 4**, DRR varies across the routes. Over 80% of potholes could be found by Wazers on I-40, followed by I-24 of which DTRR is 66.7%. By comparison, I-65 produced lower DTRR, which is 42.5% and 6.7%, respectively. This might be because Wazers tend to be less likely to report potholes on corridors with sparse potholes where their driving experience is not significantly affected by poor pavement conditions. In addition, it should be noticed that the DTRR of I-440 and SR-155 exceeds 100%. This is because there must be a fraction of requests relating to both directions. In addition, it is found that Waze pothole reports can potentially contribute to extra potholes that are not in the PMS system, these potholes need further confirmation though. Nonetheless, CRR reveals that Waze pothole reports made the highest contribution to discovering unnoticed potholes on SR-155, followed by I-65, I-24, I-40, and I-440.

Discussion

This paper presents a framework of pavement pothole likelihood mapping and pothole detection using crowdsourced pothole data. This work intends to provide pavement crews and decision-makers with a cost-effective way to continually monitor the pavement health and locate the potholes accurately. The convention of hotspot identification is usually applied for confirmed events (*41; 43; 46*) or pavement distresses (*19*). Existing spatiotemporal hotspot identification approaches such as the fuzzy C-means-based method proposed by Martino et al. are subject to the selection of clusters (*56*). Relatively speaking, the STKDE approach applied in this study is more data-driven, without predefining any parameters based on domain knowledge. Unlike conventional studies, this study first conducted the hotspot analysis based on crowdsourced reports. False reports might have effects on the hotspot's location and duration. However, in a density-based framework, the frequency of false reports is not sufficient to make a prominent cluster unless many users make the same mistakes at the same locations, which is not possible in the real world. Although the redundant reports are related to traffic exposure, it is always true that a pothole hotspot would have multiple reports within a period. On the other hand, there is a possibility that pothole hotspots exist in areas with low reporting of potholes and low traffic volume.

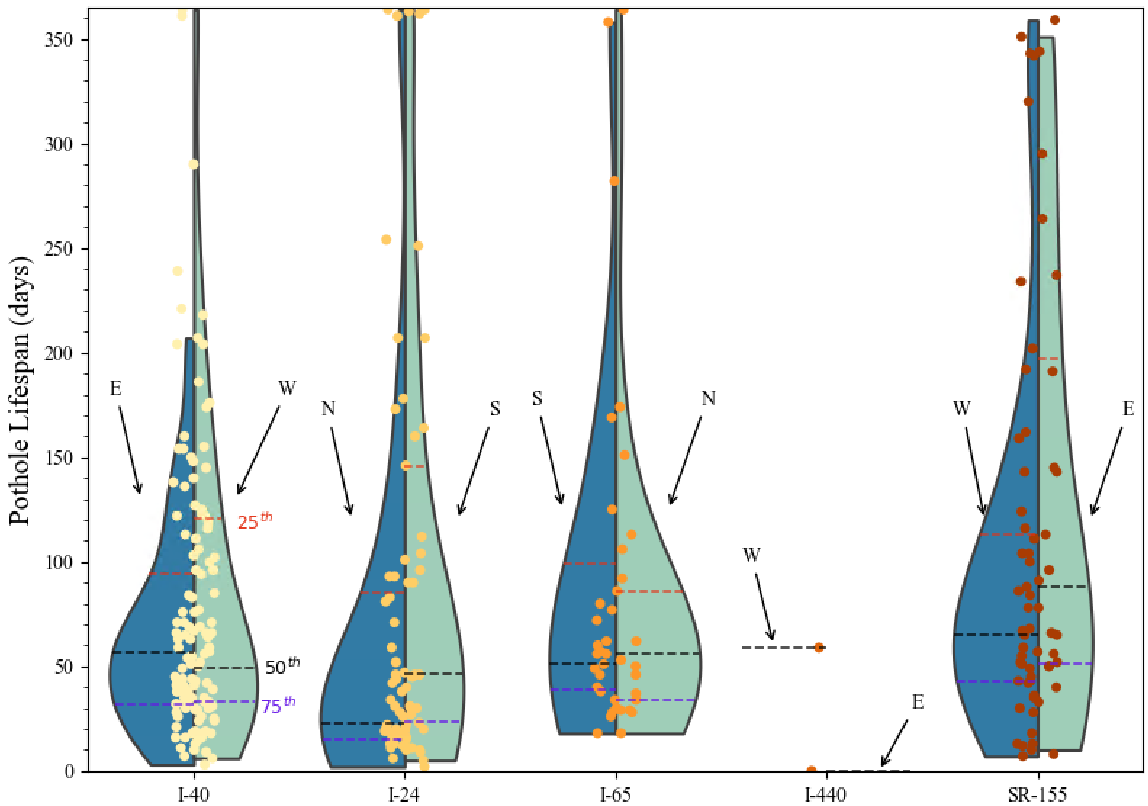

Figure 11. Lifespan distribution of identified potholes.

Table 4. Pothole detection results

Routes	DR	FD	CR	Total Request	DRR	CRR
I-24 W	44	91	19	135	66.7%	20.7%
I-24 E	46	89	9			
I-40 W	75	117	12	192	81.8%	14.6%
I-40 E	82	110	18			
I-65 S	13	60	7	73	42.5%	28.8%
I-65 N	18	55	14			
I-440 W	8	7	1	15	106.7%	6.6%
I-440 E	8	7	0			
SR-155 W	101	10	16	111	182.0%	36.3%
SR-155 E	101	10	24			

Nonetheless, pavement distresses were found to be highly associated with traffic exposure in prior studies (*57-59*). With this said, low-traffic areas (e.g., rural areas) suffer pothole depression less frequently than high-traffic areas (e.g., urban areas). Compared with the study that used the data from Long-Term Pavement Performance (LTPP) program (*19*), the Waze reports might miss the pothole hotspots in these low-traffic areas, yet the Waze-reports-based approach can potentially increase the frequency of pavement monitoring. In addition to traffic exposure, Wazers' reporting behavior is another uncontrollable factor leading to missed potholes, especially single-isolated potholes. Compared to consecutive potholes or pothole zones, Wazers may not experience similar levels of discomfort with isolated potholes, and they are less likely to report them. The non-clustered points that represent sparse or isolated pothole reports in **Figure 8** seem to support this observation. Hence, understanding Wazers' reporting behaviors in future studies may help extract more information from Waze pothole reports.

Likewise, the core of pothole detection is density under the crowdsourcing context. A pothole is recognized only if a designated number of pothole reports are observed within an interval and distance. Therefore, false reports that are distributed sparsely are discarded in the clustering. Like pothole hotspot identification, traffic exposure might affect the quality of pothole detection. However, the difference is that a single isolated pothole cannot form a pothole hotspot. We believe that there is an association between the pothole hotspots and identified potholes whereas this association is not compared in this study, as the goal of this study is to extract useful information from the pothole reports for pavement management and maintenance.

Limitations

There are a few limitations in this study. First, the pothole report is the only option for pavement conditions. Wazers, who are mostly unfamiliar with pavement distress terminologies, might attribute any and all discomforting pavement distresses, such as cracks and ruts, as potholes. In other words, the term "pothole" as reported by Wazers and subsequently employed as the source data in this study, may or may not fit the traditional definition by pavement distress studies. Second, traffic exposure and Waze's market penetration affect the frequency of reports, which implicitly impacts the density of STKDE and the identification of potholes. For instance, rural roadways typically see lower traffic volume per hour per lane than urban roadways, resulting in a much lower number of reports or even non-reports for each pothole.

Conclusion

Compared with the conventional pavement method used for pavement condition and distress identification, Waze's crowdsourced pothole reports vastly expands the means of identifying pothole in a cost-effectively and timely manner. Since potholes occur not only on aging roads but also during the storm seasons, dynamic algorithms are needed to deal with different pothole-occurring patterns. In this study, we demonstrated two density-based approaches in utilizing Waze's potholes reports. One algorithm named STKDE, identifies the pothole hotspots. The other one named ST-DBSCAN focuses on detecting potholes given optimal bandwidths from STKDE. The proposed density-based methods effectively eliminate the common concerns in Waze data application which are redundance and unreliability. In summary, the main implications of this research include:

1. This pothole hotspot study highlights when and where potholes are likely to occur. Decision-makers and crews can plan and prioritize maintenance for these vulnerable areas accordingly.
2. The estimated likelihood of pothole occurrence can be applied to pavement condition evaluation and monitoring. Compared to the annual pavement distress detection approach from TDOT, this crowdsourced Waze data provides a cost-effective way for agencies to monitor pavement conditions more rapidly, frequently, and widely.
3. The early and precise detection of potholes could facilitate pothole repair efficiency, thereby reducing crash risk and property damage to drivers.
4. The clustering results also generate two types of clusters: the single spot and the pothole zone. This information could be used to help pavement crews decide on spot patching or resurfacing.
5. Identified potholes complement the PMS work request and save the labor and cost of inspecting the pavement at regular intervals.

Using Nashville city as an example, this study attempts to mine crowdsourced Waze reports for better pavement management and maintenance. Inevitably, regional differences such as demographics, economics, the density of networks as well as pavement conditions would affect Wazers' reporting willingness and frequency. Hence, future studies could implement the proposed models to compare the effectiveness of pothole detection for different cities. Furthermore, like existing studies that evaluate the impact of environmental factors on incident detection rates (*55; 60*), future studies could also investigate the relationships between the pothole detection rates and environmental factors as aforementioned. Moreover, future studies could compare the effectiveness of the proposed solution of this study with the existing approaches that are based on accelerometers and images, extensive data collection and preparation for existing approaches are needed though.

CHAPTER II. DISCOVER SPATIOTEMPORAL HETEROGENEOUS EFFECT OF POTHOLES ON FLAT TIRE INCIDENTS

A modified version of this chapter was presented by Yangsong Gu at the 2023 TRB annual meeting.

Abstract

Potholes are a nuisance, and they can threaten personal safety and damage property. This study attempts to untangle the association and causality between potholes and flat tire events. To this end, the study collected pothole data from crowdsourced Waze reports and extracted flat tire events from incident operation notes. Considering the spatial and temporal variations of potholes and flat tire incidents, a Geographically and Temporally Weighted Poisson Regression (GTWPR) was developed to investigate the spatiotemporal association between potholes and flat tire frequency. Also, we established a Poisson Fixed Effects Regression model (PFER) to make causal inferences for flat tire frequency. The PFER model fixed the space and time effects to account for unobserved heterogeneity across segments and study periods. The GTWPR model reveals that pothole frequency is positively correlated with flat tire frequency. The potholes in the central city and interchanges of highways are found to have a higher association with flat tire frequency than in other areas. Besides, the flat tire frequency is most strongly correlated with potholes that outbreak during the winter months. Further, the PFER model substantiates that an increment in potholes can significantly cause more flat tire incidents. Despite accounting for spatiotemporal heterogeneity, the PFER and GTWPR models differ in their strengths: the PFER model is better suited for making causal inferences, while the GTWPR model can provide a more comprehensive understanding of covariates and achieve higher predictive performance. The findings of this study recognize tangible connections between how pavement conditions trigger flat tire incidents, and they can pave the way towards prioritizing infrastructural investment decisions related to roadway maintenance.

Introduction

Pavement potholes have always been a nuisance to road users. According to a survey about pothole-related complaints in the past 17 years (before 2022), Tennessee is ranked 8th in states with the worst pothole problems (*3; 4*). Besides, as American Automobile Association data estimated, drivers nationwide spend nearly $3 billion a year fixing damage to punctured tires, bent wheels, and broken-down suspension systems (*5*). Therefore, it is necessary to assess how pavement potholes trigger flat tires so maintenance crews can respond better and reduce the property loss of car owners.

A pothole is a bow-shaped depression in the pavement surface that has a certain depth and width. When a vehicle hits a pothole, the sudden air shift inside the tire can cause the sidewall to blow out (*61*). To make matters worse, potholes may not be visible to drivers when driving fast, exacerbating tire puncturing likelihood (*62*). Hence, a hypothesis can be made that the more potholes on a roadway, the higher chance of tire punctures. While potholes are not a single reason for flat tires, others including sharp objects on the road, heat, wear and tear, and improper inflation can also damage tires (see summary blog (*61*)). Therefore, we cannot exclusively claim that potholes directly cause flat tires, as unobserved environments and unmeasured individual characteristics can implicitly or explicitly cause flat tires.

Currently, the data collection of pavement potholes is largely dependent on advanced laser trucks, accelerometers, or image processing. However, employing these techniques to gather information on pavement potholes frequently and across a wide area can be costly and requires significant labor efforts. In the past decade, the Waze navigation app has come into vogue as it provides crowdsource-based data via collecting and sharing real-time traffic information. When using the Waze app while driving, users can report various traffic incidents such as crashes, traffic jams, and weather conditions, as well as the pothole reports used in this study (*63*). Waze reports are not limited to the location and time since users can report incidents wherever and whenever they are, which enables researchers to monitor pavement conditions widely and frequently. However, previous studies on Waze have identified two limitations of Waze reports, which are redundancy and uncertainty. These limitations arise because multiple users may report the same incident, and some users may submit false reports based on their perception of the incident (*64*). Therefore, Waze reports need to be exploited with caution. As of now, Waze reports such as accident and jam reports have been used to estimate queue length (*10*), identify secondary crashes (*48*), evaluate the level of service (*65*), estimate safety performance (*66*), and so on, yet the application of pothole reports has been not explored.

The distribution of potholes varies both spatially and temporally. For one thing, pavement distress differs across space as traffic volumes vary from place to place (*67*). For another thing, pavement conditions are associated with a seasonal pattern affected by weather, temperature, precipitation and freeze-thaw, and water table depth that varies from different seasons (*68*). The flat tire events caused by potholes have not been well-studied yet. If potholes are linked to flat tire incidents to some extent, then flat tire occurrences are expected to exhibit comparable spatial and temporal features. Hence, to untangle the potential relationship between potholes and flat tire events, both spatial and temporal characteristics should be considered.

This paper aims to examine the association and causality between potholes and flat tire incidents using Waze crowdsourced reports and incident operation notes from the Tennessee Department of Transportation. Specifically, the goals of this study are to:

1. Propose a Geographically and Temporally Weighted Poisson Regression model (hereafter GTWPR) to uncover the correlation between potholes and flat tire frequency.
2. Identify the causal relationship between potholes and flat tire frequency through a Poisson Fixed Effects model.
3. Evaluate the spatial and temporal variation of potholes' correlation with flat tire frequency.
4. Compare the above two-panel data processing techniques in capturing the spatial and temporal effects.

The remainder of this paper is organized as follows. The next section reviews previous related work. Then, the methodology section elaborates on the proposed models for achieving the research goals. The model is evaluated and discussed in the Results section, followed by the limitations and conclusion of this study.

Literature Review

To the best of the researcher's knowledge, this study is among the first to investigate the causal effects of potholes on flat tire events. Previous studies about flat tires emphasized the design of resistant tires (*69; 70*), yet the cause of flat tires from the built environment remains unknown. Therefore, this review section is centered around three topics: summarizing previous studies in examining the impact of potholes in traffic, modeling frequency data (e.g., flat tire frequency) by count model, and causal inference model.

Pothole impact studies

Pavement potholes and other pavement failures are a nuisance to drivers. They can puncture tires or bend wheels and cause accidents. Several researchers have investigated the relationship between pavement surface conditions and vehicle crashes. Anastasopoulos and Mannering found that various factors relating to pavement conditions and quality, such as effects of friction, the international roughness index, pavement rutting, and pavement condition rating, can significantly influence the occurrence of vehicle accidents (*71*). Al-Masaeid studied the impact of pavement conditions on single and multiple-vehicle crash frequencies in rural areas. The results suggest that an increase in the international roughness index (IRI) level or a decrease in the present serviceability rating (PSR) would reduce the single-vehicle accident rate. However, the higher IRI level would increase the multiple-vehicle accident rates (*72*). Some other studies also pointed out the impact of pavement conditions on crash severity. A study conducted by Zeng et al. found that good pavements could reduce fatal and injury crashes by 26% compared with deficient pavements. Deficient pavements are evaluated by pavement cracking, patching, potholes and cutting, and bleeding (*73*). A study by Lee et al. in 2015 showed that poor pavement condition decreases the severity of single-vehicle collisions on low-speed roads while it increases the seriousness on high-speed roads. In their study context, poor pavement condition was categorized as large potholes and deep cracks and discomfort at slow speeds. In summary, previous studies on the relationship between pavement conditions and traffic incidents still look at crash occurrence or severity. However, poor pavement conditions could cause other traffic incidents, such as disabled vehicles and road debris hazards. In these areas, there is no relevant research in the literature.

Modeling Count Data

Normal regression models can be used to discover the association between potholes and flat tires. Considering the outcome (i.e., number of flat tires) is count data, the Poisson Regression (PR) (*74*) is preferred as the baseline model. PR models the logarithm of a count variable (e.g., flat tire frequency) as a linear combination of explanatory variables. Therefore, the model would only generate non-negative prediction values. In transportation studies, PR has been widely used for crash frequency estimation (*75; 76*) and fatalities estimation (*77; 78*). However, recent studies in transportation found that spatial dependence is a crucial element in their factors to explain traffic incidents. Thus, PR has been improved by geographically weighted models, that is, geographically weighted Poisson Regression (GWPR). Studies found that the GWPR model outperforms the standard PR model in terms of model predictive performance and interpretation in spatial heterogeneity (*79-81*). Nonetheless, some built environment factors, like weather and traffic volume, have seasonal patterns. Such temporal change can potentially influence traffic incidents as well. Therefore, some researchers attempted to incorporate the temporal effect into their count model. For instance, Liu et. al. proposed the geographically and temporally weighted ordinal logit regression (GTWOLR) to estimate pedestrian injury severity. Mohammadnazar et. al. applied the Geographically and Temporally Weighted Negative Binomial Regressions (GTWNBR) to estimate the crash frequency on roadway segments and found that the coefficients of explanatory variables vary substantially in space and over time (*82*). They found the model's predictive performance was improved after incorporating the temporal effects as the geographically and temporally weighted model captures both spatial and temporal variation. Hence, it can be employed for panel data[4] analysis to highlight how group level (i.e., spatial unit or location) and temporal (e.g., days, months, years) distinction make a difference in outcomes.

Making Causal Inference

Modeling causal effects is a challenging task. The causal effect, causality for shorthand, means outcome events *y* happened as a consequence of *x*. The causality is beyond the correlation in which the causal inference requires *x* must happen before *y* and the relation between *x* and *y* must not be interpreted by other causes (*84*). Notably, other latent causes could be unidentified or unobserved, while they might be the true cause for change *x* and *y* (*85*). In the literature, there are several approaches widely applied in the transportation field. Glass developed a time series quasi-experiment to investigate the reduction of traffic crash fatalities concerning the police speeding crackdown (*86*). Li et al. applied a Difference in Difference (DID) model to study whether introducing a road congestion charge has an impact on the incidence of road causalities (*87*). Choudhary et al. employed a structural equation model (*88*) to analyze the direct and indirect impact of distracted driving on crash risk. Wagenaar et al. reported on the effects the campaign “Communities Mobilizing for Change on Alcohol” had on arrests and car crash through a randomized control trial method. The essence of the model is that experiments randomly assigned the communities to intervention and control groups so that the environmental characteristics (except for the factor of interest) of groups would be approximately alike between the two groups (*89*). Nevertheless, most approaches require treat-control or before-after comparison groups, which is unsuitable for panel data with more groups and periods. However, Panel data is quite common in the transportation field. For instance, the traffic incidents collected in different states across the years are reported as a form of panel data. To infer the causality of panel data, fixed effects models could be useful as they can remove the effects of confounding variables and unobserved factors by controlling for individual-specific characteristics that are time-invariant. This can isolate the causal effect of the independent variable on the dependent variable(*90*). In an earlier study, Kaplan used a Poisson Fixed Effects Model to investigate the causality between reduction

[4] Panel data refers to the data that are collected across sections and across time. Hence it is possible to use prior and current data to make causal inference (*83*).

of the number of alcohol-related accidents and fatalities and the legal blood alcohol concentration limit policy (*74*).

Identifying Research Gaps

Many researchers have looked for causes that explain or prevent traffic incidents. The traffic incidents data aggregated by geographical unit (e.g., county) and period (e.g., a month) essentially are panel data. The panel data requires the researchers to consider both spatial and temporal variation, which entails a complex modeling process. Of the studies summarized above, most of them focused on the association between pavement distress and crash. Flat tires, as a type of disabled vehicle, have not been given much research attention yet. Besides, the cause of flat tires in previous studies remains unnamed. When confounding factors are present, it can be challenging to explain the causal relationship of flat tire frequency with other factors that may exhibit similar trends. Moreover, the prior studies were conducted in a single direction, taking either correlation or causal inference analysis, whereas the comparison between these two types of panel data analysis is relatively few.

Methodology

This section explains the method used to reveal the correlation and causality between potholes and flat tires. Since flat tire frequency is a count data type, Poisson Regression (PR) is used as a start-up model. After that, two extensions of Poisson Regression, namely, GTWPR and Poisson Fixed Effects Regression (PFER) are developed with panel data.

Poisson Regression

In the Poisson regression model, the probability of occurrence of flat tires $\boldsymbol{n}_i$ at a location, *i* can be formulated as:

$$P(n_i) = \frac{\lambda_i^{n_i} \exp\left(-\lambda_i\right)}{n_i!} \tag{8}$$

where $\lambda_i$is the average flat tire related to a series of exogenous factors at the location $\boldsymbol{i}$. The merit of Poisson Regression is that it transforms the count data regression in a logarithm manner so that the regression can always describe the non-negative response variables. The Poisson Regression is written as:

$$\ln(\lambda_i) = \beta_0 + \beta_k X_i + \varepsilon_i \tag{9}$$

where X_i denotes the explanatory variables, β_o is the intercept and β_k is a vector of the estimated coefficients for explanatory variables. The error term ε_i follows the distribution $N(0, \sigma^2)$ and it is independent of explanatory variables.

The parameters β_0 and β_k are estimated through the maximum log-likelihood method:

$$l(y_i; \beta_o, \beta_k) = -\sum_{i=1}^{n} e^{\beta_0 + \beta_k X_i} + \sum_{i=1}^{n} y_i \cdot (\beta_0 + \beta_k X_i) - \sum_{i=1}^{n} \log\left(y_i!\right) \tag{10}$$

Geographically and Temporally Weighted Poisson Regression

Model fundamentals

The spatiotemporal dependency should be modeled appropriately because both flat tires and potholes could have spatial and temporal variation. To this end, this study employed Geographically and Temporally Weighted Regression to test if the influence of covariates substantially varies across space and time. Essentially, GTWPR is extended from GWPR by incorporating temporal non-stationary. The fundamental GTWPR can be expressed as:

$$\ln(\lambda_i) = \beta_0(u_i, v_i, t_i) + \sum_{k=1}^{k} \beta_k(u_i, v_i, t_i) X_{ik} + \varepsilon_i \tag{11}$$

The parameters $\beta_0(u_i, v_i, t_i), \beta_k(u_i, v_i, t_i)$ can be estimated through weighted maximum log-likelihood as written in **Equation** (12). It is worth noting that GTWPR estimates parameters locally so that they are dependent on the location (u_i, v_i) and time t_i. Therefore, the spatial and temporal effects can be jointly captured.

$$\mathrm{l}(\beta(u_i, v_i, t_i); y_i) = -\sum_{i=1}^{n}\{e^{\beta(u_i,v_i,t_i)X_i} + y_i \cdot (\beta(u_i, v_i, t_i)X_i) - \log(y_i!)\} w(d_{ij}) \tag{12}$$

$w(d_{ij})$ is a function that transforms spatiotemporal distance between individuals into weights. GTWPR gives more importance to the neighboring observations of location *i* than those far away from location *i*. Each observation has a 2D location (i.e., latitude and longitude) tag and a time tag (i.e., month), thus the distance of individual (u_i, v_i, t_i) and (u_j, v_j, t_j) can be quantified by **Equation** (13). A graphical illustration of spatiotemporal distance in the sphere is depicted in **Figure 12**.

$$d_{ij} = d\left((u_i, v_i, t_i), (u_j, v_j, t_j)\right) = \sqrt{\Delta s^2 + \Delta t^2} \tag{13}$$

The shortest path distance between observations Δs is calculated as it measures the reachable distance between observations, which is more practical than the commonly used Euclidean distance in existing studies (*91; 92*). Besides, the temporal difference is elaborated as the month is cyclical regardless of the year. For example, the temporal difference between two flat tire events that happened in January and December should be 1 instead of numeric (i.e., 11). Mathematically, the temporal difference between month t_i and t_j is calculated by:

$$\Delta t = \begin{cases} |t_j - t_i| & if\, |t_j - t_i| \le 6 \\ 12 - |t_j - t_i| & if\, |t_j - t_i| > 6 \end{cases} \tag{14}$$

Previous studies have shown two weighting schemes: fixed bandwidth and adaptive bandwidth. The fixed bandwidth applies a certain distance to query the nearest neighbors while the adaptive bandwidth queries a certain number of nearest neighbors instead of the fixed distance. Considering the radial network shape of study routes, the adaptive bandwidth is employed to ensure the minimum required observation for model inference. As for kernel function, this study employed the Gaussian kernel (see **Equation** (15)), which is the most popular kernel, to compute the decaying weight for neighbors from near end to far end. The weight matrix is a diagonal matrix, with diagonal elements being the weight.

$$W_{ij}(d_{ij}; h_{ST}) = e^{-\frac{d_{ij}^2}{2h_{ST}^2}} \tag{15}$$

where W_{ij}^{ST} with superscript *ST* denotes the spatiotemporal weights, and h_{ST} corresponds to the spatiotemporal bandwidth that covers h_{ST} observations. Notably, the h_{ST} is the conflated bandwidth for space and time. Previous studies have suggested incorporating a scale parameter to balance spatial and temporal distances (*91; 93*), but this approach necessitates additional effort in parameter tuning. In contrast, the current study proposes a simpler method in which both spatial and temporal differences are normalized to a range of 0 to 1, ensuring comparability between the two. Additionally, the spatiotemporal distance corresponds to h_{ST} observations will be scaled down.

Tunning bandwidth and scale parameters

The spatiotemporal bandwidth influences the weights and further affects the model inference and predictive performance. In previous studies, the bandwidth is specified by domain knowledge (*82; 92*), which would not always be justified in different scenarios. To optimize the predictive performance of GTWPR, the spatiotemporal bandwidth should be calibrated from the data itself. This could be accomplished through cross-validation with target performance measurement. In this study, $AICc$ is selected. $AICc$ is modified from the Akaike Information Criterion (AIC) by adding the sample size as a penalty to correct the issue of overfitting of AIC when the sample size is small and unobserved heterogeneity is present (*94*). The objective of cross-validation with $AICc$ can be expressed as:

$$h'_{ST} = \underset{h_{ST} \in [h_l, h_u]}{\operatorname{argmin}} AICc = f(l, n, k, h_{ST}) \tag{16}$$

$$AICc = -2l(h_{ST}) + 2k + \frac{2k(k+1)}{n-k-1} \tag{17}$$

where h_l and h_u denote the lower and upper bound of spatiotemporal bandwidth h_{ST}. l is the abbreviation of the log-likelihood of the fitted model. *n* is the number of observations, and *k* is the number of parameters estimated in the local PR model.

Spatial non-stationary diagnosis

The GTWPR method can uncover local factors that are associated with the frequency of flat tires, but these factors may not exhibit significant spatiotemporal heterogeneity due to the influence of unobserved factors related to space and time. If no spatiotemporal heterogeneous effects are present, the local model is generally on par with the global PR model. In earlier studies, the test was made through the Monte Carlo framework which performs a local model on the data in which the location coordinates are randomly permuted. Thus, the variance of parameter estimates concerning location variation can be estimated. However, this approach is computationally demanding and time-consuming because the model must optimize the parameters every time the locations are shuffled. In recent studies, researchers proposed a simpler approach to compare the statistics of estimated parameters to suggest a significant variance. Referring to their studies (*82; 92*), the non-stationarity test is conducted for each variable by comparing the lower quartile (25^{th} percentile) and upper quartile (75^{th} percentile). For each explanatory variable, the interquartile range (IQR) is computed and compared with 1.96 times of standard error (i.e., $S.E.$) of parameters (see **Equation (18)**).

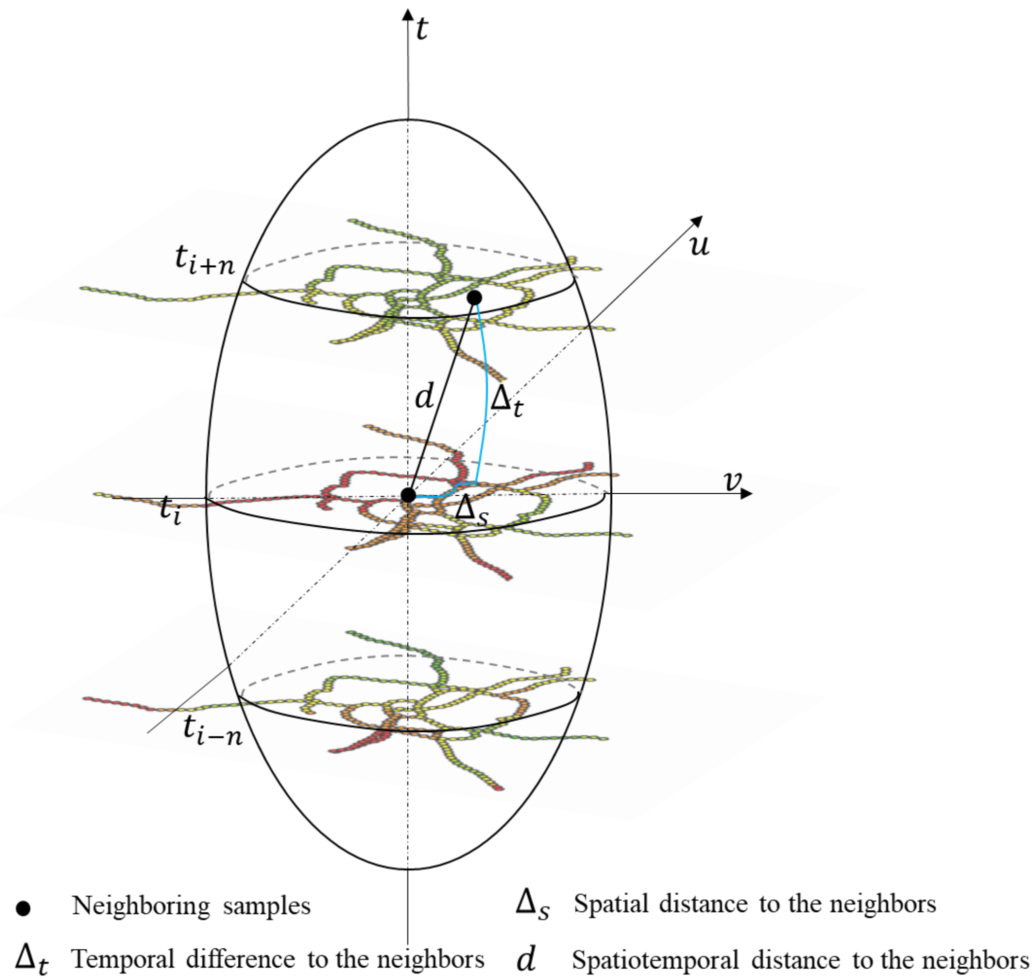

Figure 12. Graphic Spatiotemporal Distance.

$$IQR = \beta_i^{upper} - \beta_i^{lower} \begin{cases} > 1.96\ S.E.\ and\ \max|z| > 1.96, Non-stationary\ test\ is\ passed \\ otherwise, Non-stationary\ test\ is\ failed \end{cases} \quad (18)$$

Poisson Fixed Effects Regression

Although GTWPR can uncover the spatiotemporal correlation between flat tires and potholes, it is not capable of determining the causality between the two. Causality, more specifically, means whether potholes cause flat tire incidents. In the regular PR and GTWPR regression, this causality cannot be justified firmly as other unmeasured covariates such as heat, and road hazards could also contribute to flat tires. In the absence of controlling for or eliminating the influence of these unobserved confounding factors, it is likely to generate misleading conclusions. In the literature, regression discontinuity, quasi-experiment, randomized controlled trial with factorial, and fixed effects models are four major econometric techniques applied in causal inference. The first three approaches typically include two periods or two groups in the experiment such as the before and after the period, or pre-intervention and post-intervention, control group, and treatment group. The fixed-effects model can deal with the panel data when we have multiple observations of the same location over consecutive periods. This study implements the fixed effects model with PR (i.e., Poisson Fixed Effects Regression, PFER), which is derived from the linear fixed-effect model. While PR uses a nonlinear function (i.e., log), it is linear in the exponent. It should be noticed that PFER is used because the number of flat tires is count data, not because of the non-linearity of the causal patterns (*90*). The general two-way Poisson Fixed Effects Model (PFER) [5] for panel data (*95*) assumes that:

$$E(y_{it}|x_{i1} \dots, x_{iT}, c_i) = \mathrm{e}^{\beta_0 + X_{it}\beta_k + \alpha_t + \mu_i + \varepsilon_{it}} = c_i c_t e^{\beta_0 + X_{it}\beta} \quad (19)$$

where the c_i denotes the unobserved effect of individuals which is constant over time, and c_t denotes the time effects. β_k denotes the parameter estimates of time-varying covariates X_{it}. α_t denotes time-fixed effects. μ_i is entity fixed effect that is constant within each entity over time while it varies across the individuals, like pavement feat type and age. ε_{it} is the idiosyncratic, time-varying error term.

The parameters β_0 and β_k can be estimated using the maximum conditional maximum likelihood method (*95*), as shown by **Equation** (20):

$$L(\beta_0, \beta_k) = \sum_{i=1}^{N} \sum_{t=1}^{T} y_{it} \log\left[p_t(x_i, \beta_0, \beta_k)\right] \quad (20)$$

The $y_i = \sum y_{it}$ follows the multinomial distribution conditional on $n_i = \sum y_{it}, \beta_0, x_i, c_i, c_t$, with each probability term being:

$$p_t(x_i, \beta_k) = \frac{c_i c_t e^{\beta_0 + X_{it}\beta_k}}{c_i c_t \sum_{s=1}^{T} e^{\beta_0 + X_{is}\beta_k}} = \frac{e^{\beta_0 + X_{it}\beta_k}}{\sum_{s=1}^{T} e^{\beta_0 + X_{is}\beta_k}} \quad (21)$$

[5] A two-way fixed effects model means both entity effects and time effects are fixed in the model (*88*).

Since the fixed effects of each group are constant over time, they can be canceled out in **Equation** (21). Thus, akin to the differencing out effect in the Linear Fixed Effects model, this approach can alleviate the effects of confounding variables without measuring them directly, and it can even make causal inferences in the absence of random assignment (*90; 96; 97*). The distribution of y_{it} given x_{it} and fixed effects c_i, c_t is unrestricted and allows the overdispersion or under dispersion (*74; 98*). However, the PFER model treats the groups individually so heterogeneity across individuals is allowed (*99*).

Model Assessment Criteria

To evaluate and compare different models, four statistics metrics are employed to measure the goodness of fit.

$\boldsymbol{AICc}$ is a corrected version of AIC beyond which the penalty is added to reduce the issue of the effects of overfitting (*100*) for small-size data. The penalty comprises the sample size and the number of parameters to be estimated. The $AICc$ formula is introduced in above **Equation (17)**.

R-squared for Poisson model ($\boldsymbol{R^2_{poisson}}$) evaluates how well the model fits the data using standardized residuals. A higher $R^2_{poisson}$ (with a maximum of 1) indicates a better fit. It is defined as (*101*):

$$R^2_{Poisson} = 1 - \frac{\sum_{i=1}^{n}(y_i - \widehat{y_i})^2/\widehat{y_i}}{\sum_{i=1}^{n}(y_i - \bar{y})^2/\bar{y}} \tag{22}$$

Where y_i and $\widehat{y_i}$ are the observed and predicted number of flat tire events at location *i*, respectively. $\bar{y}$ is the average number of flat tire events.

Mean Absolute Error (*37*) quantifies the average absolute error between the predicted value and the actual observation. It gives the same weight to the individual difference. A smaller MAE indicates a better model estimation. It is defined by **Equation (23)**.

$$MAE = \frac{\sum_{i=1}^{n}|y_i - \widehat{y_i}|}{n} \tag{23}$$

Root Mean Squared Error (RMSE) represents the square root of the average squared difference between the prediction and actual value. Different from MAE, RMSE is compatible with large errors and large variance of errors. Likewise, a smaller RMSE suggests a better model fit. It takes the form:

$$RMSE = \sqrt{\frac{\sum_{i=1}^{n}(y - \hat{y})^2}{n}} \tag{24}$$

Data Description

Data Source

This study makes use of the operation notes from the Tennessee Department of Transportation Highway Help Truck. The flat tire events are extracted based on keywords such as “flat tires”, “tire change” and ‘ft tire’ on the operation notes. The pothole data is obtained through pothole reports from **Waze** (*63*). Each report contains a unique user ID, location (latitude and longitude), publication date, street description (e.g., I-40 W), and so on. The duplicate reports, that is, with the same user ID and publication date, are dropped before data aggregation.

Besides, the built environment factors are prepared to align with the previous findings, reporting that there are six common causes of flat tires (*102*): sharp objects like construction debris, bad road conditions such as potholes, and heat, which are collectible. In contrast, factors such as wear and tear, tire age, valve stem leakage, and driving habits are linked to individual drivers and are not easily obtainable. Therefore, this study collected road conditions data (e.g., represented potholes), and weather condition data from grid MET (*103*) (e.g., represented by temperature). Besides, serval factors that affect the pavement conditions are also considered, as they would cause flat tire events implicitly. Such factors are known as confounding variables, including pavement maintenance, and pavement feat type (*104*) (see Error! Reference source not found.). T hey are collected from the pavement maintenance system database. Please also note that traffic volume may also be confounded with flat tire events and pothole reports, and therefore, it is considered when normalizing the pothole reports. Traffic volume data is collected from the radar detector system.

The study area includes interstate highways 24, 40, 65, 440, and state routes 6, and 155 which constitute the backbone highway network of Nashville in Tennessee. The study period covers from August 2021 to May 2022.

Data Aggregation

The goal of data aggregation is to segment the spatiotemporal data to create panel observations for regression. The spatial resolution of segments plays a vital role in correlation and causality analysis between flat tires and potholes. If the segment length is too small, many segments will have zero or small flat tire counts, making statistical inference invalid. In addition, Waze pothole reports tend to pop up downstream or upstream of actual potholes due to Waze users' (Wazers) perceptions and the potential delay of reactions (*64*). This kind of spatial lag of pothole reports might cause a cross-dependency on flat tires longitudinally. On the contrary, large segments tend to obscure the correlation and causality as more uncertainties would be included. In view of these perspectives, spatial data resolution is mainly suggested by the spatial accuracy of Waze reports. One mile could encompass over 80% of Waze reports for the same event (*13*), yet a necessary assumption is that other build environment factors are homogeneous within each one-mile segment. The temporal data resolution is determined by the research of interest, as we intended to look at the monthly patterns. Pothole report frequency is associated with active Wazers on the road and is implicitly influenced by the traffic volume. Waze pothole reports at each segment are normalized by the traffic volume calculated by the average daily vehicles per section, which we call Density of Waze Pothole Reports (DWPR) for simplicity[6]. **Figure 13** demonstrates an example of spatiotemporal aggregation of point data (i.e., flat tires, potholes) for I-40. First, the original data with latitude and longitude are projected to a linear referencing system.

[6] Nonetheless, two assumptions still need to be made. One is that Wazers' penetration is homogenous on the network so using traffic volume to normalize reports is appropriate, and the other is that report density is proportional to the frequency of actual potholes, considering the redundancy of reports.

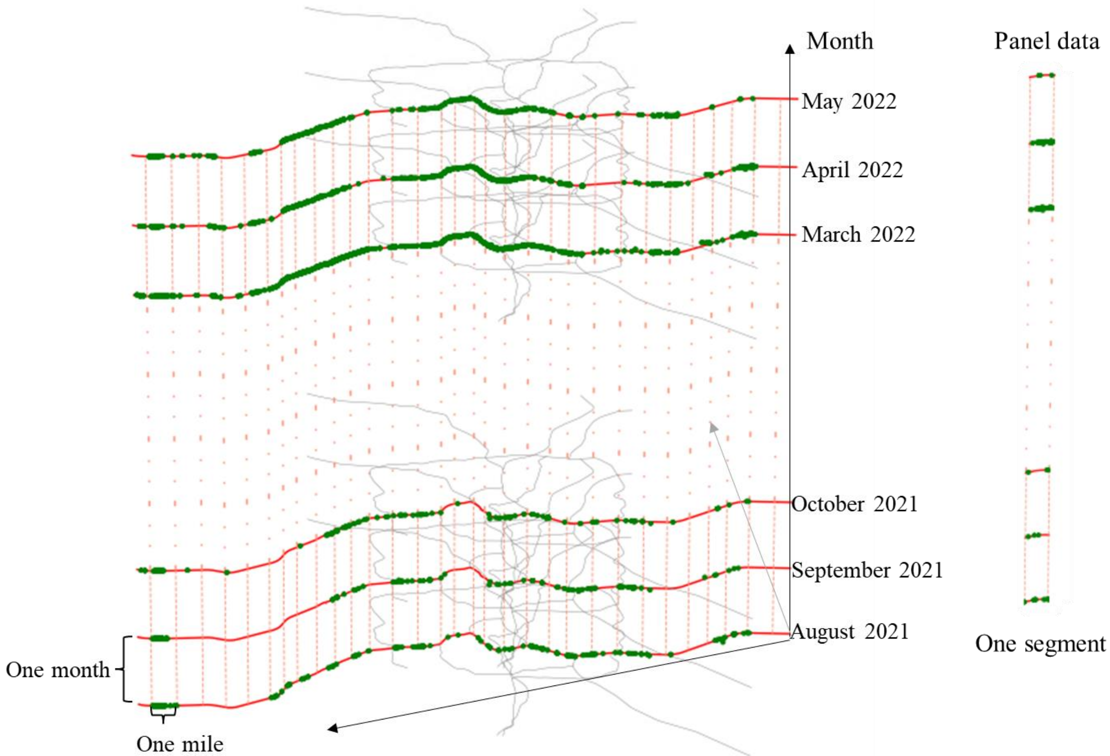

Figure 13. Illustration of spatiotemporal aggregation of point data (example of I-40).

Then the total number of flat tires and pothole reports are aggregated for each spatiotemporal unit (one mile and one month), making up the panel data. After the route segmentation is determined, other explanatory variables (e.g., pavement type) are assigned to the segment based on the spatial conflation using Geographic Information System tools.

Table 5 summarizes the descriptive statistics of dependent and explanatory variables. The total number of segmentations is 1410. As shown in the table, on average, there are 1.8 flat tire events at a one-mile length segment. The severest location is the segment on which 13 flat tire events happened in a month. The average normalized DWPR is 0.55 per vehicle per month. Noticeably, DWPR varies by segment substantially as the standard deviation (i.e., 1.35) is twice as large as the average value. A such large variance may reflect the uneven spatiotemporal distribution of potholes. The average percentage of cars in AADT is 92.8%. The pavement maintenance data document the resurfacing activities before the study period, and they are used as proximate indicators to reflect the pavement repairment history. According to the data, 94.3% of the segments had undergone resurfacing before the study period. Most roadway segments (88.1%) are covered with asphalt pavement, while a smaller percentage is covered with concrete (6.3%) or a combination of concrete and asphalt (5.6%).

Data Explanatory Analysis

As shown in **Figure 14,** the frequency of pothole reports and flat tire events on the study routes varies by month. As expected, there are more pothole complaints during the winter because of the increased frequency of snow and rainstorms. A similar seasonal pattern was observed for flat tire events (i.e., orange bars). The occurrence of flat tire incidents was higher during winter and spring compared to other seasons, suggesting a correlation between potholes and flat tire events. **Figure 15** shows the spatial distribution of flat tire events and pothole reports of study routes. The frequency increases as the point gets redder. The left figure reveals that potholes are frequently reported in the center of Nashville, as well as in the areas south of I-24 and I-64. The north and south parts of SR-6, which are in the city's peripheral area, do not receive any pothole reports during the study period. The figure on the right indicates that a significant number of flat tire events occurred in the central area of the city, as well as to the west of I-40, south of I-24, and east of SR-155. There are certain locations where both high frequencies of pothole reports and flat tires are observed, such as the central city area, as well as the areas to the south of I-24 and west of I-40. This coincidence implies the spatial dependence of flat tire events on the pothole.

Results

The model was prescribed to select the explanatory variables that lead to the minimum $AICc$ in the regular PR model. Then, the VIF (Variance Inflation Factor) was examined for selected explanatory variables, and the results show the maximum VIF value < 5, which indicates that the selected variables do not have strong evidence of correlation (*105*). Thereafter, the GTWPR model was built and solved in a Python environment, and the PR and PFER models were solved through *xtpoisson* function in Stata software

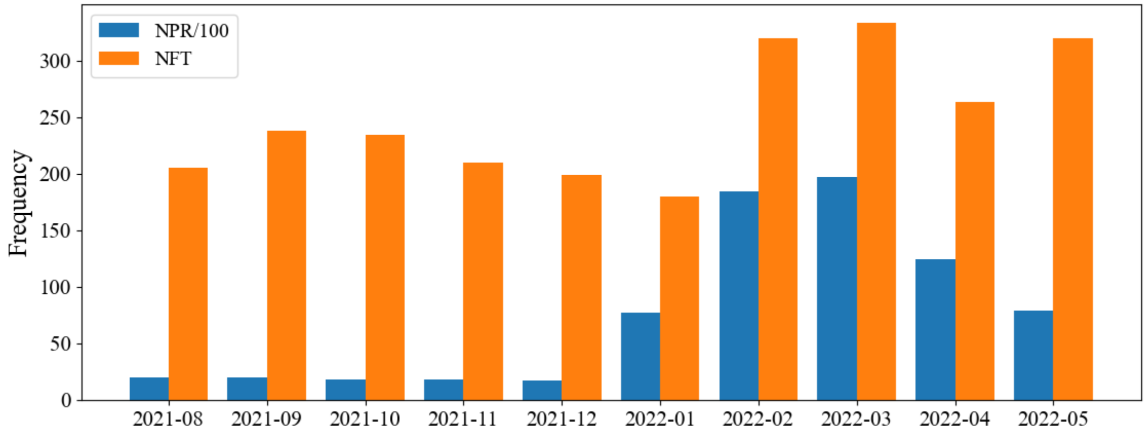

Figure 14. Monthly number of pothole reports (NPR) and flat tires (NFT).

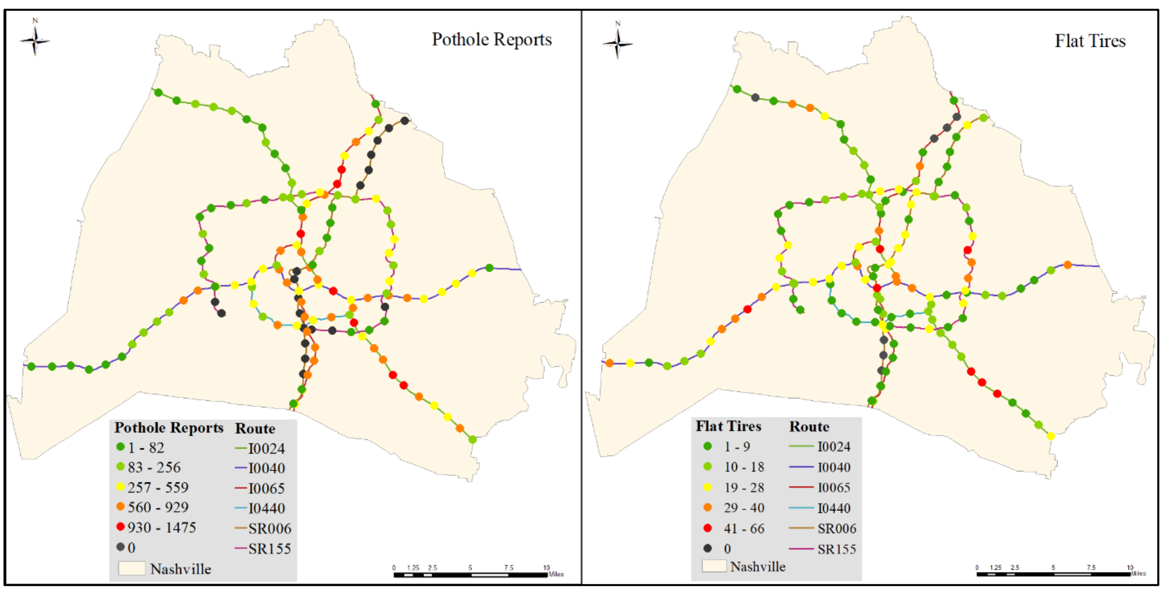

Figure 15. Spatial distribution of pothole reports and flat tires of Nashville, TN.

Table 5. Descriptive statistics of data (total observations:1,410)

Category	**Variables**	**Mean**	**Std.**	**Min**	**Max**	**Time-varying**
Dependent	Number of flat tires	1.8	2.1	0	13	Yes
Continuous Independent Variables						
Time indicator	Month	6.5	3.8	1	12	Yes
Pavement Failure	Density of Waze Pothole Reports (reports/month/volume)	0.55	1.35	0	14.79	Yes
Weather Condition	Minimum daily temperature (°F)	7.6	7.6	-5.7	20.9	Yes
	Maximum daily temperature (°F)	19.9	7.0	6.8	31.3	Yes
	Precipitation (mm)	45.6	20.3	12.5	94.7	Yes
Traffic Exposure	Percent of Car in AADT (%)	92.8	0.6	91	93	No
	Percent of Truck in AADT (%)	7.2	0.6	7	9	No
Categorical Independent Variables						
		Frequency (=1)		**Frequency (=0)**		
Pavement Maintenance	Resurfacing (1 if the pavement is resurfaced at least one time, 0 otherwise)	1329		81		No
	Reconstruction (1 if the pavement is reconstructed at least one time, 0 otherwise)	419		991		No
Pavement Feat Type	Asphalt (1 f yes, 0 otherwise)	1242		168		No
	Concrete (1 f yes, 0 otherwise)	89		1321		No
	Composite (1 f yes, 0 otherwise)	79		1331		No

(https://www.stata.com/). The spatiotemporal bandwidth is 60 after parameter tuning. **Table 6** presents the estimation results for global PR, PFER, and GTWPR of which the global PR is viewed as a baseline model. In the following sections, the modeling results are described and discussed.

Global PR

The PR estimate results in **Table 6** indicate that all involved explanatory variables - except the "composite pavement type" - are statistically significant in explaining the relationship to flat tire frequency. Several factors have a positive effect on the occurrence of flat tires. For instance, one-unit additional DWPR contributes to a 9.5% increase in flat tire frequency. High temperatures also appear to have a non-negligible impact on flat tire occurrence. With the maximum temperature increasing by 10° **F**, the flat tire frequency could increase by 9%. It should be highlighted that flat tires are more likely to happen to passenger cars than trucks, as the coefficient is significantly greater than 0 (i.e., 2.364). Moreover, it has been observed that flat tires are more frequent on concrete pavement, resulting in a 32.4% higher incidence rate compared to asphalt pavement. By comparison, composite pavement does not have an evident association with flat tire events (i.e., p-value >0.1). The correlation between concrete and composite-type pavement supports the existing opinion that asphalt pavement could create soft contact with tires and grip tires better than concrete or composite pavement and a part of the cracked concrete pavement of the road are more rigid and sharper than asphalt pavement (*18*). Roadway resurfacing also correlates with flat tire incidents: a flat tire incident is 31.5% less likely to happen in resurfaced areas than in un-resurfaced areas. It makes sense that resurfaced pavement is more resistant to pavement distress.

PFER

The PFER model contains only two time-varying factors as other time-invariant factors are constant and controlled within the individual segments to allow heterogeneity of flat tire occurrences. The results suggest a significant causal relationship between potholes and flat tire frequency, and a higher number of potholes significantly results in a larger number of flat tire incidents. We also should note that the estimates of potholes in the PFER are larger than the global PR model, which not only corroborates the association between potholes and flat tire frequency but also indicates a more intensive causal effect. The result shows that flat tire events will increase by 19.2% for one unit increase of DWPR reports. Besides, higher maximum daily temperature could also cause an increase in flat tire frequency, with a 10 °F increase in temperature associated with a 9% increase in flat tire frequency. The temperature effect is consistent with the estimate generated by the PR model.

GTWPR

For each factor, the mean, 25th percentile, and 75th percentile values are summarized, and a spatial non-stationary test is performed. The results show that all factors except for the composite pavement passed the test, indicating that the influence of covariates exhibits significant spatial and temporal variability. The GTWPR model produces a lower mean correlation of DWPR compared to both the PR and FEPR models, with one unit increase in DWPR associating with 7.2% more flat tire incidents. The DWPR estimate at the 75th percentile is slightly higher than the estimate obtained from the PR model, but still significantly smaller than that of the FEPR model. By contrast, the average effect of maximum daily temperature is slightly overestimated in GTWPR compared to PR and FEPR models. Although the average effects of other factors such as car proportion, concrete pavement, and pavement resurface are close to the estimate from the PR model, the 25th and 75th in GTWPR can reveal a smaller or larger correlation.

Figure 16 illustrates the spatial distribution of the coefficients that are statistically significant at a 90% confidence interval. Each point represents the centroid of the segment, and the color highlights the average effects: the redder dots, the higher correlation, which is as opposed to greener points. Focusing on DWPR reports (**Figure 16. a),** it is observed that the coefficients are positive everywhere, which naturally reflects that driving over pothole areas is exposed to a higher chance of puncturing vehicle tires. Intuitively, the correlation of Nashville's central areas, as well as highway interchange areas (e.g., I-40 and I-65, I-40 and I-24, SR-155 and I-40) are much higher than other areas. One possible reason for this is that these areas experience a high volume of daily traffic, which in turn increases the number of vehicles that are susceptible to damage from potholes. As a result, it is crucial to carry out prompt repairs of potholes that occur in these areas to reduce the harm caused to vehicles. Likewise, the temperature is observed to have a significantly positive correlation with flat tires almost everywhere except for the west of I-40. It is worth noting that temperature has the highest correlation with flat tire incidents on the northeast interchange area of bypass SR-155 and SR6, SR-155, and I-65, followed by the Nashville central area (**Figure 16. b**). Although the temperature may not vary considerably across a city, the contemporaneous effect of traffic load may amplify the association of temperature with flat tire events. A similar spatial correlation pattern was observed for passenger car proportion, as **Figure 16. c** shows. The coefficient takes the greatest around central Nashville, decaying towards the city's peripheral area, which conforms to the fact that there are mainly commercial areas in the central city. On the other hand, trucks are less likely to encounter flat tires than passenger cars. Trucks are designed with heavy bodies and long travel suspensions that can provide a smoother ride and more stability, which is likely why they are better equipped to handle rough pavement than passenger cars. **Figure 16.d** shows the distribution of the coefficients for pavement resurfacing. It is expected that resurfaced pavement is associated with lower flat tire events for all significant estimates. The coefficients reach the minimum in the interchange area of SR-155 and SR-6 and SR-155 and I-65, indicating resurfacing pavement in these areas can comparatively gain a larger benefit than other areas. It turns out that these interchange areas tend to be a sensitive location for flat tires as we also notice that the design of concrete pavement in this area has the largest positive association with flat tire incidents as compared to asphalt pavement (**Figure 16. e**). Lastly, the composite pavement has a significantly negative effect on flat tire incidents only at the interchanges of I-440 and I-65, and I-440 and I-24 which conforms to the fact that composite pavement is relatively employed in Nashville highways as **Table 5** shows. Hence, applying composite pavement in interchange areas that carry heavy traffic may provide a more tire-friendly surface for passenger cars.

Figure 17 shows the monthly variation of coefficients that are statistically significant at a 90% confidence interval. The height of a rectangle box represents the interquartile range of coefficients at a month. It is observed that many factors, such as potholes, maximum daily temperature, and so forth, have a longish box, which further corroborates their varying spatial effects on flat tire frequency. The median value of coefficients, highlighted by the notch of each box, fluctuates across the month, reflecting varying temporal dependency of factors. Potholes, car proportion, and pavement resurfacing are associated with flat tire incidents every month, while temperatures and pavement types are only found to be correlated with flat tire frequencies in specific months. During winter seasons, freeze-thaw cycles coming aftermath of heavy snow or rain can create many potholes, increasing the chance of hitting potholes. Therefore, **Figure 17. a** reveals that pothole has a comparatively large association with flat tire incidents during winter months (e.g., December, January, and February). It should be noted that there is a significant correlation between pothole incidents and flat tire occurrences during August. One possible explanation is that potholes that are not repaired by pavement crews during winter may continue to grow and deteriorate over time, which can cause greater damage to vehicle tires during the summer period. High temperature, on the one hand, particularly during summer, can impact the air pressure inside a tire, resulting in a potential blowout or leakage. On the other hand, high temperatures during winter and spring can accelerate the melting of ice on the roads, which can cause the road surface to heave and crack, thereby expediting the formation of potholes and increasing the risk of flat tires. However, the study found that maximum daily temperatures had a significant correlation only during the winter and spring seasons (see **Figure 17. b**), supporting the latter point. **Figure 17. c** gives the monthly variation of the coefficient for car proportions. The correlation stays large before December and gradually decreases since January. The reason is likely to be related to the fact that TDOT started resurfacing and patching potholes at the beginning of January (*106*), which undoubtedly reduced the pothole exposure to passenger cars. Following **Figure 17.**d, the coefficient for resurfacing displays a monthly pattern that suggests that resurfaced pavement can offer advantages in preventing flat tires, particularly during the winter season. This makes sense as the resurfaced pavement is less likely to cause potholes again in the short term and can provide an even and smooth surface for vehicle tires. **Figure 17. e** indicates that the coefficient for concrete pavement suggests a higher risk of flat tires on concrete pavement compared to asphalt pavement, except for the winter months in which fewer significant coefficients are observed. On the contrary, composite pavement is related to fewer flat tire incidents during February and March compared to asphalt pavement, as **Figure 17. f** shows.

Limitations

This study examined the association and causality between potholes and flat tire frequencies. Nonetheless, there are several limitations. First, the segmentation of potholes and flat tires eliminated the direction. This might affect the model's interpretation if the flat tires and potholes have directional distribution. Second, Wazers who are not familiar with pavement distress terminology may mistakenly identify any kind of discomforting pavement damage, such as cracks and ruts, as potholes. Thereby, other types of pavement damage may also be implicated in the occurrence of flat tire incidents. Although previous studies claim that spatiotemporal accuracy could be acceptable for statistical modeling for transportation analysis (*12; 55; 64*), the false pothole reports (*13*) might distract the parameter estimation. Due to the difficulty of collecting unique potholes over time, we use aggregated and normalized Waze pothole reports to serve as a surrogate measure of pothole severity. Hence, all the findings are concluded based on such pothole severity instead of individual potholes. Third, the basic model we used is Poisson Regression, which cannot accommodate excessive zeros counts. Alternatively, a zero-inflated Poisson model could be considered to improve the model estimation (*107*).

Conclusion

Potholes can puncture tires and even lead to crash hazards. This study attempts to examine the association and causality between them by using incident operation notes and crowdsourced Waze data. Because both flat tire events and pothole occurrences entail spatial and temporal variation. GTWPR and PFER models were employed together to deal with the panel data effectively in addition to the baseline PR model.

The first model geographically and temporally weighted Poisson regression model, fits the panel data locally and outperforms the baseline PR model by accounting for effects of unobserved factors related to space and time. The GTWPR model reveals that pothole is positively correlated with flat tire incidents and one unit increase of DWPR is associated with 7.2% more flat tire incidents on average. The average effect of potholes in the GTWPR model is close to the global PR model's estimate, yet the GTWPR gives a more comprehensive understanding of the impact of potholes across space and over time. From the spatial perspective, the correlation of Nashville's central areas, as well as highway interchange areas (e.g., I-40 and I-65, I-40 and I-24, SR-155 and I-40) are much higher than other areas. From the temporal perspective, GTWPR reveals that pothole has a larger positive association with flat tire incidents during winter months, which naturally reflects the pothole outbreak period. In addition to potholes, the increment in the daily maximum temperature is revealed to be positively correlated with the flat tire frequencies. Besides, it is found flat tire incidents are less likely to occur on resurfaced pavement and asphalt pavement. These findings are valuable for practitioners to intentionally fix potholes to reduce the property loss caused by flat tires. In addition, other vital factors show a strong spatial correlation with flat tire events, such as pavement type, resurfacing, reconstruction, and so on. The findings of this study recognize tangible connections of how pavement conditions influence flat tire events, and they can pave the way towards prioritizing infrastructural investment decisions related to roadway maintenance.

Potholes are not the sole reason for flat tires. Both the PR and GTWPR models cannot rule out the impact of other unobserved confounding factors, such as the pavement type in the GTWPR model. Thus, Poisson Fixed Effects Regression is employed to infer the causal relationship between potholes and flat tire incidents. PFER eliminated the segments with zero counts throughout the study area and controlled the group effects and time effects. FEPR produced a higher correlation between potholes and flat tire frequency compared to PR and GTWPR models. The small p-value suggests that more potholes can cause more flat tire incidents.

It is worth noting that GTWPR and PFER treat the spatial and temporal effects differently. In GTWPR, the spatial and temporal effects are reflected by the local regression. The smaller the proximity in the time-space 3D sphere, the higher weight of the observations. Thus, both spatial and temporal dependency heterogeneity is allowed. In comparison, the PFER model controlled the time and group effects by relying on the variation of observations within the group. The time and group effects cannot be estimated, yet they are allowed to vary across space. More importantly, the fixed time and group effects represent the unobserved factors. Thus, PFER can account for the spatial and temporal unobserved heterogeneity.

In addition to empirical contributions, this study also makes methodological contributions. This study is among the first to compare the geographically and temporally weighted and fixed effects models. Both models take spatial and temporal variation into account. By contrast, the former model is only able to capture the correlation, and the latter model can claim the causality. The findings from the two models could provide rigorous reasoning for making countermeasures for practice. Future research could consider more performant machine learning methods such as the geographical random forest model (*108*) to tackle the potential non-linear relationship as the method utilized in this paper only produce a linear relationship for explaining flat tire frequency.

Table 6. Model regression results

Predictors	PR	PFER	GTWPR				Non-stationarity
			Mean	25^{th}	75^{th}	Max |Z|	
Pothole Severity	0.090***	0.176***	0.070	0.068	0.094	5.675	Yes
Marginal Effects	9.5%	19.2%	7.2%	7.0%	9.9%		
Maximum Daily Temperature (°F)	0.009***	0.009**	0.011	0.004	0.018	3.598	Yes
Marginal Effects	0.9%	0.9%	1.1%	0.4%	1.8%		
Percent of Car in AADT (%)	2.364***		2.755	2.35	3.119	5.242	Yes
Marginal Effects	963.3%		1472.1%	954.6%	2163.1%		
Pavement Type (base: asphalt)							
Concrete	0.281***		0.230	0.079	0.341	3.594	Yes
Marginal Effects	32.4%		25.9%	8.2%	40.6%		
Composite	0.058		-0.041	-0.158	0.087	1.591	No
Marginal Effects	6.0%		-4.0%	-14.6%	9.1%		
Pavement Resurface (Yes)	-0.378 ***		-0.371	-0.508	-0.237	0.075	No
Marginal Effects	-31.5%		-31.0%	-39.9%	-21.2%		
Summary Statistics							
R-squared	0.18	*NA*	0.36				
AICc	5150	3320.0	4834				
MAE	1.41	1.55	1.31				
RMSE	1.92	2.16	1.79				
Loglikelihood of model	-2567	-1657.3	-2404				
Loglikelihood at constant	-2896	*NA*	-2798				

*Note, the superscript of coefficients denotes the significance at *** 1%, ** 5%, and * 10%

*The number under the coefficient denotes the z Statistics.

* The effective number of observations in Poisson Fixed Effects model is 1220 after dropping the 190 all zero outcomes from 19 groups.

* The fixed effects model treats each spatial unit individually; therefore, the time-invariant factors are dropped in regression.

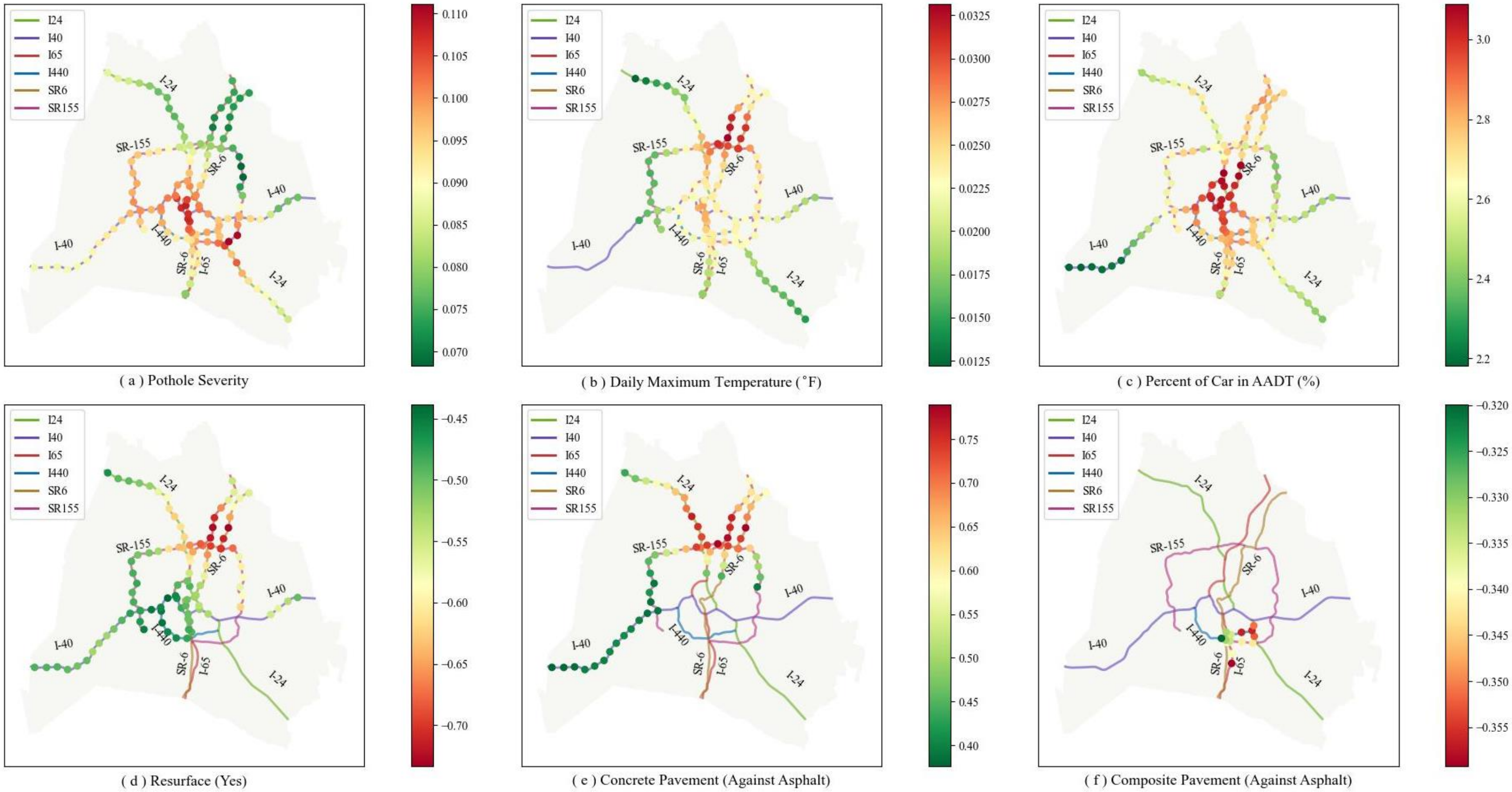

Figure 16. Spatial varying relationships between flat tires and explanatory variables.

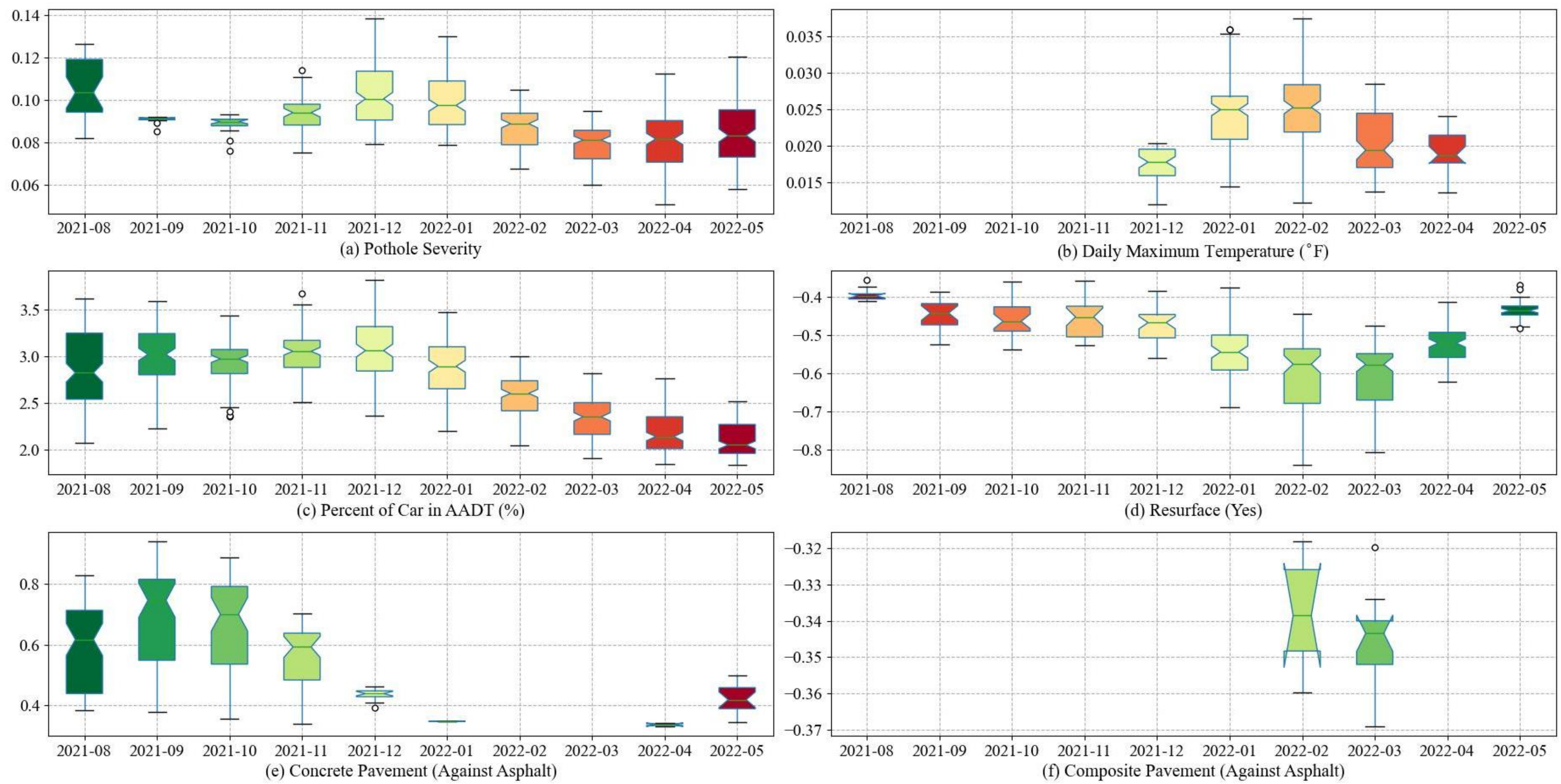

Figure 17. Temporal varying relationships between flat tires and explanatory variables.

CHAPTER III. MODELING SPATIOTEMPORAL NON-STATIONARY AND UNOBSERVED HETEROGENEITY IN INTERVAL-CENSORED TRAFFIC INCIDENT TIME TO NORMAL FLOW: A GEOGRAPHICALLY AND TEMPORALLY WEIGHTED PROPORTIONAL HAZARD ANALYSIS

Abstract

Non-recurrent traffic congestion arising from traffic incidents is unpredictable but should be dealt with efficiently to mitigate its impact on safety and travel time reliability. While numerous studies and practices have been done about incident clearance time, the recovery time (i.e., the time between mainline reopening and traffic returning to normal) is barely considered in the analysis of overall incident impact duration (i.e., time to return to the normal flow of traffic, NFT). Overlooking the recovery time would undoubtedly underestimate the total incident-induced impact. Furthermore, the spatiotemporal heterogeneity of observed factors is not adequately emphasized when modeling incident duration. This study addresses these gaps by proposing a novel approach to estimate recovery time using crowdsourced user reports and developing a geographically and temporally weighted proportional hazard (GWTPH) model to investigate factors associated with the crash NFT duration. The results show that the GWTPH model outperforms the global proportional hazard model in goodness of fit. The non-stationary test indicates that crash NFT duration is spatiotemporally correlated with factors such as the presence of HELP trucks, disseminating information about the traffic incident, e.g., through dynamic message signs, in-transit time of first responders, and traffic demand. The GWTPH model further highlights that information dissemination on certain interstates (e.g., I-24 smart corridor) is particularly effective in reducing the return to normal times during morning peaks. The study's findings and application of new spatiotemporal techniques can be valuable for researchers and practitioners to localize improvement solutions for incident management.

Introduction

Traffic incidents refer to events or situations that reduce roadway capacity or increase abnormal travel demands. Common traffic incidents include crashes, stalls, and road debris. They can cause nonrecurring traffic congestion and decrease travel time reliability (*109*). As estimated by FHWA, 60% of delays caused by traffic congestion are results of traffic incidents (*110*). Besides, traffic incidents, especially vehicle crashes, can pose a great threat to people's property and life. According to a technical report published by the National Highway Safety Administration, the total economic costs of crashes and resulting congestion reached $340 billion in 2019 in the US (*111*). Hence, transportation agencies and emergency responders have been seeking effective solutions to reduce the incident duration thereby minimizing incident impact on travel time reliability and safety.

As defined in many previous studies (*112-115*), a typical progression of a traffic incident can be broken down into four distinct phases: detection, response, clearance, and recovery time (see **Figure 18**). Specifically, detection time refers to the time between incident occurrence and the incident reported; response time is the time between incident notifications by officials and the time the first responder arrives at the scene; clearance time is the time from the arrival of the first responder to the moment when the incident is cleared and service vehicles no longer directly affect roadway traffic; and recovery time is the time taken for traffic flow to return to normal after the incident is cleared. The detection time is short yet often unknown because the actual time of occurrence is usually uncertain (*116*).

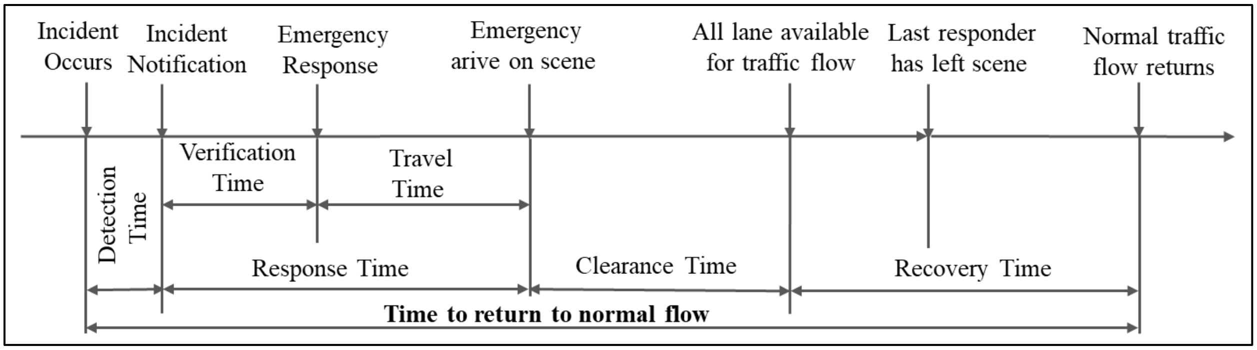

Figure 18. Four components of an incident timeline.

The response time and clearance time are usually available through operation logs noted by responders. In contrast, the recovery time is mostly not available as it is difficult to pinpoint the exact moment when traffic returns to normal. In studies analyzing the impact of traffic incidents, researchers typically quantify the additional delays and queues resulting from incidents. However, these delays and queues often remain after the clearance of the incident, especially when it occurs during periods of heavy traffic congestion. Research also found that secondary crashes are likely to happen during the traffic recovery period (*117; 118*). Despite the importance of estimating recovery time in queueing and safety management, relatively few studies hitherto have focused on resolving recovery time (*119; 120*).

Crowdsourcing provides a new solution to estimate the incident recovery time. Under the crowdsourcing context, road users serve as moving sensors and can report traffic congestion as and when they encounter it. The crowdsourced data breaks through the limitations of conventional fixed location data (e.g., traffic detectors) in many ways. One noteworthy example of transportation is the Waze app. Via the Waze app, Waze users (Wazers) can share perceptions of traffic conditions in areas where fixed traffic detectors are not installed. Many previous studies have explored the potential of Waze traffic jam reports in traffic congestion-related studies, such as travel time reliability evaluation (*65*), dynamic queueing estimation (*10*), and secondary crash identification (*48*). As traffic congestion may present throughout the incident timeline, Wazers can collect the congestion information post-incident clearance.

On the other hand, many statistical models have been employed to model the incident duration as a function of multiple factors. However, most of them assume that the effect of factors is constant across space and time. This assumption reduces the model's explanatory power due to overlooking the heterogeneous effect of factors, such as urban area traffic is usually heavier than the rural area, and peak hour traffic is usually heavier than off-peak hours. To capture the heterogeneity, some studies employed a random-parameter modeling technique to allow the estimates to vary following a specific distribution, and the model predictive capabilities are improved compared to regular models (*92; 121; 122*). However, the specified parameter distribution is usually subjective and cannot explain any spatiotemporal heterogeneity. To localize the countermeasures for improving incident management, it is necessary to improve the model explanatory power in addition to the goodness of fit.

In this study, we extend the incident duration by adding recovery time to incident response and clearance time and explore the spatiotemporal variation of determinants that are associated with incident duration. It should be noticed that the incident investigated in this study, specifically, refers to crash, as the crash has a significant impact on travel delay, property damage, and even life loss (*123; 124*).

Literature Review

The subsequent section first outlines the research and methods utilized for estimating recovery time and modeling incident duration, followed by a review of the state-of-the-art techniques for addressing unobserved heterogeneity in estimating incident duration.

Definition of incident duration

Transportation agencies and researchers have investigated different incident duration in the past several decades. For example, the Federal Highway Administration (FHWA) uses the roadway clearance time and incident clearance time as metrics for evaluating Traffic Incident Management (*46*) performance. The roadway clearance time was defined as the time between the first record of an incident by a responder and the first confirmation that all traffic lanes returned to fully operational status (*125*). By contrast, the incident clearance time is defined as the time between the first record of the incident by a responder and the first confirmation that all evidence of the incident was removed or the last responder left the incident scene. Likewise, the Highway Capacity Manual published in 2010 (*126*) defines the incident duration as the sum of incident detection, response, and clearance time for general travel time reliability analysis. However, researchers define incident duration differently for their study purpose. Several studies have defined the start of incident duration from the moment the incident occurred (*121; 127; 128*). While most of the studies count the incident duration starting from the incident reported (*116; 129-131*) because detection time is not typically reported because the actual time the incident occurred is often unknown (*116*). With the aid of intelligent incident detection tools, the crash can be quickly detected and reported to the operator or emergency services, leading to a short detection time. On the other hand, the end of incident duration is not in agreement among the existing studies. Some studies consider the end of incident duration to be the moment when the last responder departs the scene, disregarding the recovery time (*114; 132; 133*) while only a few studies considered the recovery time as the last component of incident duration (*113; 121*). The recovery time, as the consequence of the incident, is a crucial component of incident-induced delay. Without measuring the recovery time, the incident impact might be largely underestimated. However, as opposed to the clearance time, the end of recovery time is often uncertain and can be followed up by responders. Hence, measuring recovery time is quite challenging, making it difficult to determine the complete duration of the incident's impact.

Estimate Recovery Time

As an essential component of incident duration, recovery time gets little attention. Estimating recovery time requires determining when the incident has been cleared and when traffic has returned to normal. The former information can be obtained through notes from emergency responders. In contrast, the latter is more difficult to determine as the boundary between abnormal and normal traffic conditions is not clear. Moreover, using travel speed as the indicator of traffic status is limited by the fixed detector locations. Conventionally, a queuing model can estimate the gross time needed to dissipate the accumulated vehicles (*120*). However, such a deterministic model assumes that the arrival and departure rates are constant, which is not realistic since the arrival flow may vary due to the traffic diversion upstream. Zeng (*119*) developed a method to estimate incident recovery time by differencing a segment of travel time under incident conditions and travel time without an incident. Likewise, Hojati et al. (*121*) applied a similar difference-in-travel-time approach to estimate incident recovery time using speed data from loop detectors. However, the accuracy of estimates depends on the size and quality of the sample speed data and the baseline travel time. It is barely possible to obtain a robust baseline travel time as various factors can affect travel time.

Incident Duration Model

In the past decades, many models have been used to model incident duration. Methodologically, they can be divided into statistical methods and machine learning methods.

Table 7 summarizes the representative studies of each approach. The first type is Hazard-based duration models, including the accelerated failure time model (*121; 128; 134*) and proportional hazard model (*122; 127; 130; 135; 136*); The second type is normal regression such as quantile regression (*116; 137; 138*); The last approach is machine learning models like random forest and support vector machine (*139-142*). Although machine learning models tend to have a higher prediction accuracy than rigorous statistical models, they are inferior to statistical models in terms of interpreting incident duration (*142*). For this reason, many studies have focused on statistical models, especially the hazard-based duration model.

Unobserved Heterogeneity

Unobserved heterogeneity refers to the individual difference caused by unobserved factors. Unobserved heterogeneity such as the distribution of emergency resources affects the incident duration, whereas they are hardly measured in practice. For instance, the spatial distribution and number of emergency responders to the crash locale could influence the incident response time. Their service characteristics data are rarely available in most situations. On the other hand, ignoring primary heterogeneity would result in erroneous inferences on the coefficient estimates (*143*). Existing studies have established two techniques to account for unobserved heterogeneity when estimating incident duration. The first approach is to include a term for heterogeneity in the duration density function and specify a particular distribution for it. Such distribution includes the gamma distribution, inverse Gaussian distribution, and frailty distribution as shown in **Table 7.** With a heterogeneity term embedded, the duration density becomes a function of unobserved heterogeneity and can account for variation across individuals. The second method allows the parameters to vary across observations according to pre-specified distribution, namely, the random parameter model. See studies conducted by Islam et al. (*122*), Wali et al. (*137*), Tirtha et al. (*135*), and Zeng et al. (*136*) in **Table** 7. The idea of the approach is that the effect of unobserved factors can be accounted for by allowing parameters to vary within a specific distribution or group. Thus, the modeling process for the above-described techniques needs random sampling and simulation of parameters. Additionally, either the distribution of heterogeneity terms or the parameters must be predetermined subjectively. Hence, a more data-driven method is needed. Recent studies from other fields have seen that disaggregating models into geographical space in the form of local sub-models could also explain the unobserved heterogeneity. A local model can mitigate the influence of unobserved heterogeneity in a relatively homogeneous region. For instance, it was found that geographically weighted models can account satisfactorily for the unobserved heterogeneity in crash rate analysis (*79; 108; 144*), traffic volume estimation (*145*), traffic states prediction (*146*), and so on. Compared to existing techniques for addressing heterogeneity, the geographic model is more straightforward and potentially can uncover the spatiotemporal heterogeneity of certain observed factors.

Research Gaps

Through the literature review, two limitations in prior incident duration studies have been identified. First, despite the importance of recovery time in quantifying incident delay, few studies consider it. Although several studies have attempted to estimate the recovery time via the difference-in-travel-time approach, the calculated results are subject to the location of detectors, speed sample size, and qualification of background travel time. Second, unobserved heterogeneity was previously handled by either incorporating a heterogeneity term with a specified distribution or allowing parameters to vary across observations, which cannot account for the nature of spatiotemporal heterogeneity of incident covariates. Failing to capture the spatiotemporal variation of incident covariates will certainly decrease the estimation accuracy and limit the understanding of incident duration. To address these limitations, this study focused on crash incidents and exploited Waze Jam reports to estimate crash recovery time. Then, a rigorous statistical model, namely, a geographically and temporally weighted hazard-based model, is developed to untangle the spatiotemporal heterogeneity of contributing factors.

Methodology

Estimate Recovery time from Waze Report

Depending on the definition of clearance time in practice, there are two types of recovery time, respectively, which are referenced to the time when traffic lanes open and the left responder has left the scene, respectively (7). However, in some cases, shoulder lanes might remain occupied as incident vehicles are moved to shoulder lanes to wait for towing, emergency, or police help. Once all travel lanes open, the accumulated vehicles are released at a rate close to capacity. Congestion continues to persist until all vehicles in the queue have been discharged. By contrast, the incident clearance time contains roadway clearance time but also the treatment time elapsed in dealing with stopped vehicles on shoulder lanes. The treatment time varies depending on the severity of the crash and in transit time of other responders. This leads to the often case that main lanes traffic had returned to the normal status before all responders left the scene. Therefore, the recovery time of this study is determined based on the end of roadway clearance time, as depicted in **Figure 18**.

As a result, Waze traffic jam reports associated with post-crashes were searched based on this time when travel lanes are no longer blocked. It should be noted that noisy reports are often the case. As an example, reports of traffic jams related to an incident downstream may be mistaken for the crash that occurred upstream. Therefore, the researchers set up a criterion to separate close yet not associated incidents. Analogous to the concept of vehicle headway, the researchers define report headway as the time interval between two sequential jam reports to the same event. Notably, if a large headway is applied to cut off the sequential reports, the noisy jam reports from other incidents might exaggerate the crash duration of interest. On the other hand, if a small headway is applied, the crash duration might be shorter than the actual recovery time due to the early cut. Therefore, appropriately cutting off sequential reports is the critical point in estimating recovery time. To this end, the researchers conducted a spatiotemporal clustering on the crash and jam reports. As clustering is not the focus of this paper, readers can refer to the Liu et al. paper for detailed information (*10*). Then for each matched crash, the researchers computed all headway between two sequential reports within a cluster. The headway value corresponding to the 90th percentile (16 minutes) is used for the general cut-off criterion.

Table 7. Summary of representative studies for incident duration estimation

Category	No.	Authors	Methods	Duration	Heterogeneity
Hazard-based models	1	Li et al. (*128)*	Accelerated failure time (AFT) model and its extensions	Incident detection + response + clearance time	Inverse Gaussian distribution with frailty distribution, mixed effects
	2	Hojati et al. (*134)*	AFT model	Incident detection + response + clearance time	Weibull with gamma heterogeneity distribution
	3	Hojati et al. (*121)*	AFT model	Incident detection + response + clearance + recovery time	Random Parameter and Weibull with Gamma heterogeneity
	4	Nam and Mannering (*127)*	Proportional Hazard (PH) model	Incident detection + response + clearance time	Weibull with gamma heterogeneity distribution
	5	Islam et al. (*122)*	PH model	Incident clearance time	Weibull with gamma heterogeneity distribution and latent class categorization
Normal Regression	6	Khattak, Schofer and Wang (*116)*	Truncated Linear regression	Incident detection + response + clearance time	Not applicable
	7	Khattak et al. (*137)*	Quantile Regression and Ordinary least square model	Incident detection + response + clearance time	Not applicable
	9	Wali, Khattak and Liu (*138)*	Quantile Regression	Incident detection + response + clearance time	Random Parameter
Machine Learning	10	Hamad et al. (*139)*	Random Forest	Incident detection + response + clearance time	Not applicable
	11	Wu, Chen and Zheng (*140)*	Support Vector Machine	Incident detection + response + clearance time	Not applicable
	12	Tang et al. (*141)*	Extreme gradient boosting model	Incident clearance time	Not applicable
	13	Tang et al. (*142)*	Back Propagation Neural Network	Incident clearance time	Not applicable

The remaining 10 percent of headway values exceed 16 minutes among all crash events, possibly representing the extreme situation when a longstanding crash presents itself. Therefore, as **Figure 19** illustrates, the search algorithm starts with looking for jam reports happening after all lanes are available for traffic flow. Wazers A, B, C, and D reported congestion sequentially within a headway time. On the other hand, Wazers might not report congestion anymore when traffic returns to normal, indicated by the condition when no follow-up jam report occurs in 16 minutes, as shown by Wazers' reports **D** and **E** in **Figure 19**. Therefore, the traffic status is likely to restore within this 16-minute interval, leading the final recovery time to be interval censored[7]. Please also notice that the end of recovery time estimated by Waze reports indicates the approximate time when traffic congestion disappeared, which is consistent with the definition in several prior studies (*114-116; 120*).

General parametric proportional hazard model (GPH)

Hazard-based duration models have been widely applied to investigate the survival time of a subject in a manner of explaining causality in duration data, especially in clinical trials and biometrics. The incident duration is typically not censored in previous studies that have primarily examined deterministic durations such as response and clearance time. However, turning to this study, the crash duration is interval censored as the end of recovery time is only known within an interval, which makes the model estimation different from existing models. In a general hazard-based duration model, the interest is not only in the duration itself but also in the probability of an incident ending in the following short period. Hence, the conditional probability of an incident duration ending at some time *t* given that the duration has continued until time *t* can be formulated by:

$$h(t) = \frac{f(t)}{S(t)} = \frac{f(t)}{1 - F(t)} \tag{25}$$

Where $f(t)$ and $F(t)$ represent the density distribution and cumulative distribution of crash duration, respectively. It is not difficult to find that hazard risk is inversely related to survival probability. That means, for instance, it is more likely to reach the end of crash duration (i.e., survival probability decreases) if the hazard risk increases, and vice versa.

The most widely used survival analysis model is probably the proportional hazards model. It assumes that the hazard function $h(t|X_i)$ conditional on X_i is proportional to an arbitrary baseline hazard $h_0(t)$, which takes the form:

$$h(t|X_i) = h_0(t)\exp(\beta X_i) \tag{26}$$

Where $\exp(\beta X_i)$ is also noted as the relative risk which allows researchers to connect crash duration with explanatory factors.

When modeling the left- or right-only censored data, the parameters β can be estimated through the partial maximum log-likelihood (*148*) at the point level. However, the log-likelihood function must distinctly treat interval-censored observations as the actual

[7] By interval censored, it means that the moment when traffic status return to normal is known only to lie within an interval instead of being observed exactly (*147*).

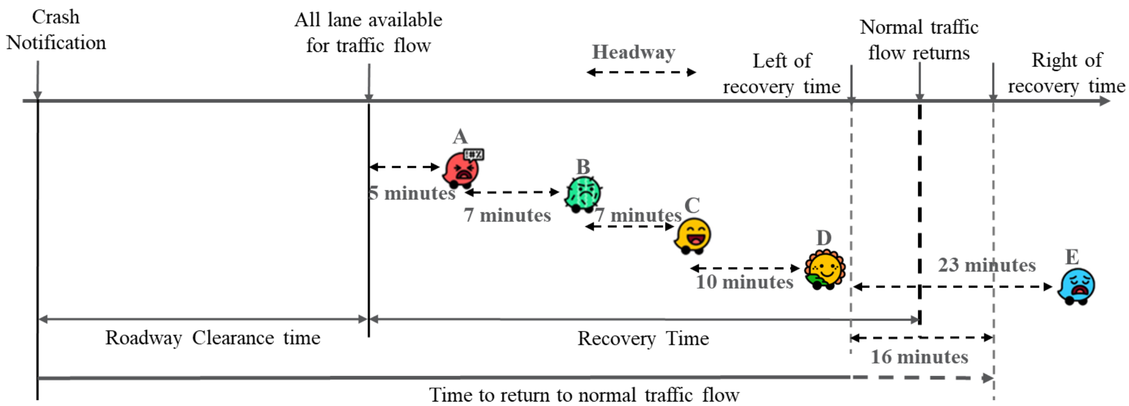

Figure 19. Illustration of recovery time based on Waze Jam reports.

failure occurs between a short interval, which is the case of this study. Therefore, cumulative hazard probability is considered to quantify the risk of event failure at that period. By integrating two sides of the above **Equation (26)**, we can get:

$$H(t) = \int \frac{f(t)}{1 - F(t)} dt = \int \frac{f_0(t)}{1 - F_0(t)} \exp\,(\beta X_i) dt \tag{27}$$

Calculating the integral, the cumulative hazard function is now converted to a cumulative density distribution of survival time t.

$$-\ln\,(1 - F(t)) = -\ln\,(1 - F_0(t)) \exp\,(\beta X_i) \tag{28}$$

Since survival probability $S(t) = \Pr\,(T > t) = 1 - F(t)$, equation (28) can be alternatively represented by:

$$S(t) = S_0(t)^{\exp(\beta X_i)} \tag{29}$$

Let $(l_i, r_i]$ denotes the time interval that contains the true incident duration t. Assuming that the censoring mechanism is independent of both crash duration and covariates, the joint log-likelihood (*149*) can is proportional to:

$$LLK = \sum_{i=1}^{n} \log[H(l_i|\alpha) - H(r_i|\alpha)] = \sum_{i=1}^{n} \log\,[S_0(l_i|\alpha)^{e^{X_i\beta}} - S_0(r_i|\alpha)^{e^{X_i\beta}}] \tag{30}$$

Where α is a vector of parameters of parametric baseline hazard. This study applied the Weibull distribution, a generalized exponential distribution, to estimate baseline crash duration. The basic survival probability of the Weibull distribution is given by **Equation (31)**, with shape parameter $\lambda > 0$ and scale parameter $P > 0$. $S_0(t_i|\alpha)$ is a baseline survival function that describes the survival probability without the effect of exogenous factors. $S_0(t_i|\alpha) = \Pr\,(T > t_i|X_i = 0)$. Intuitively, the model estimates unknown parameters by maximizing the cumulative survival probability in between an interval.

$$S(t) = \exp(-(\lambda t)^p) \tag{31}$$

Geographically and Temporally Weighted Proportional Hazard model (GTWPH)

A modified local log-likelihood function at a spatial unit s (i.e., latitude, longitude) and time *t* (in this study, *t* is the hour of the day) is given by:

$$LLK(\beta(s,t)) \sum_{i=1}^{n} \log\,[w_i(s,t) S_0(l_i|\alpha)^{e^{X_i\beta(s,t)}} - w_i(s,t) S_0(r_i|\alpha)^{e^{X_i\beta(s,t)}}] \tag{32}$$

where $w_i(s,t)$ is spatiotemporal integrated weight calculated by the distance in space-time dimension. Spatiotemporal weighted proportional hazard allows parameters $\beta_k(s,t)$ to vary across observations and time, which accounts for the spatiotemporal heterogeneity of certain observed factors.

Weight scheme

Geographically and temporally weighted regression can be viewed as a disaggregation of global regression into spatiotemporal space in the form of local sub-models. The local model takes in neighboring data points by assigning them weights strategically. The weights are typically characterized by the proximity (i.e., spatiotemporal distance) between data points. The scale of distance could vary a lot depending on the value of attributes. Therefore, a Gaussian kernel function can be applied to transform the spatiotemporal proximity to weight, with the distance effect being scaled down by bandwidth. The spatiotemporal compound weights W_{ij}^{ST} can be expressed as:

$$W_{ij}^{ST} = e^{-\frac{d\left((u_i,v_i,t_i),(u_j,v_j,t_j)\right)}{2h_{ST}^2}} \tag{33}$$

where h_{ST} represents the spatiotemporal bandwidth. It can be either fixed bandwidth that represents the distance or adaptive bandwidth that denotes the number of nearest neighboring samples. In this study, the crash happens only on routes, which may distribute sparsely or densely due to the network geometry. Using fixed bandwidth may not be able to include the minimum required observations for model inference especially for rural areas where crashes are fewer than in urban areas. To ensure the quality of model inference, this study adopted adaptive kernel bandwidth. $d\left((u_i, v_i, t_i), (u_j, v_j, t_j)\right)$ represents the spatiotemporal distance between two observations *i* and j. (u_i, v_i, t_i) marks longitude, latitude, and time of sample *i* separately. As shown in **Figure 20,** the spatiotemporal distance can be composed of the geometry distance of spatial difference Δs and temporal difference Δt. To mitigate the impact of route geometry (e.g., the radial road network of this study) on spatial distance, the shortest path distance between all paired crash observations is calculated. On the other hand, the temporal difference is measured at the hour level and the hour is cyclical every 24 hours. For instance, the temporal difference between two crashes that happened at 23:00 and 1:00 respectively should be two hours as opposed to the numeric difference (i.e., 22 hours). Hence, the temporal proximity is formulated as **Equation (34)**. Notably, the temporal difference would belong to [0,12].

$$\Delta t = \begin{cases} |t_j - t_i| & if\ |t_j - t_i| \leq 12 \\ 24 - |t_j - t_i| & if\ |t_j - t_i| > 12 \end{cases} \tag{34}$$

Lastly, the spatiotemporal integrated distance takes the following form:

$$d\left((u_i, v_i, t_i), (u_j, v_j, t_j)\right) = \sqrt{\Delta s^2 + \tau \Delta t^2} \tag{35}$$

Where τ is a scale parameter that balances the temporal distance effect with spatial distance.

Tunning bandwidth and scale parameter

Two parameters, the bandwidth and scale parameters, can be determined through cross-validation using a target performance measurement. The proposed model applied the Akaike Information Criterion corrected (i.e., $AICc$) (**Equation (37)**) to choose the suitable values for bandwidth and scale parameters. $AICc$ is extended from the Akaike Information Criterion (AIC) by adding the sample size as a penalty. Thus, $AICc$ is more suitable than AIC in model selection in case the sample size is small. Besides, the prior study found that $AICc$ can also perform well due to the penalty afforded when unobserved heterogeneity is present (*94*). The objective of cross-validation is to minimize the $AICc$ by tunning bandwidth and scale parameters, which can be expressed as:

$$h, \tau = \underset{h_i \in [h_l, h_u], \tau_i \in [\tau_l, \tau_u]}{\operatorname{argmin}} \boldsymbol{AICc} = f(\boldsymbol{L}, n, k, h_i, \tau_i) \tag{36}$$

Where $AICc$ is defined by:

$$AICc = -2\boldsymbol{L}(\boldsymbol{h_i}, \tau_i) + 2k + \frac{2k(k+1)}{n-k-1} \tag{37}$$

Model assessment

To examine whether the spatiotemporal weighted local model can outperform the global model, McFadden's Pseudo R-square, which is commonly used in log-transformed statistical models, is computed in addition to log likelihood defined by **Equation** (32) and $AICc$ defined by **Equation (37)**. McFadden's Pseudo R-square measures the improvement of a fitted model from a null model (i.e., constant-only model). It takes the form:

$$McFadden's\ R^2 = 1 - \frac{\ln(L)}{\ln(L_{null})} \tag{38}$$

Where $\ln(L)$ is log-likelihood from the fitted model and $\ln(L_{null})$ is log-likelihood from a null model. A larger Pseudo R-square indicates better goodness of fit.

Spatiotemporal non-stationary test

The geographically and temporally weighted model places higher importance on neighboring samples than distant samples. The model can outperform the standard model if there is significant evidence showing spatiotemporal dependence. Therefore, inter quantile range (IQR) is computed and compared with 1.96 (95% confidence interval) times of standard error (i.e., S. E.) of the global model for each predictor (*92*). As **Equation (39)** shows, IQR measures the spread of the middle half of one parameter estimate that lies in the upper bound (i.e., 75th) and the lower bound (i.e., 25th) of parameters. The higher IQR value indicates the more substantial volatility of parameter estimates. Besides this, maximum z-value $|z_i|$ from each local model is used to test if an IQR is significantly greater than 1.96 standard error. The test for spatiotemporal non-stationary passes only if both conditions are satisfied.

$$IQR = \beta_i^{upper} - \beta_i^{lower} \begin{cases} > 1.96\ S.E.\ and\ \max|z_i| > 1.96, Non-stationary\ test\ is\ passed \\ otherwise, Non-stationary\ test\ is\ failed \end{cases} \tag{39}$$

Data Description

Multiple datasets were used in this study, including traffic volume data from Radar Detection System, jam reports from Waze, incidents operation notes data from TDOT, and weather data from underground. The study area focuses on five backbone corridors in Nashville, Tennessee: Interstate 24, 40, 65, 440, and State Route 155, as shown in **Figure 22**. The study covers the period from August 2021 to July 2022.

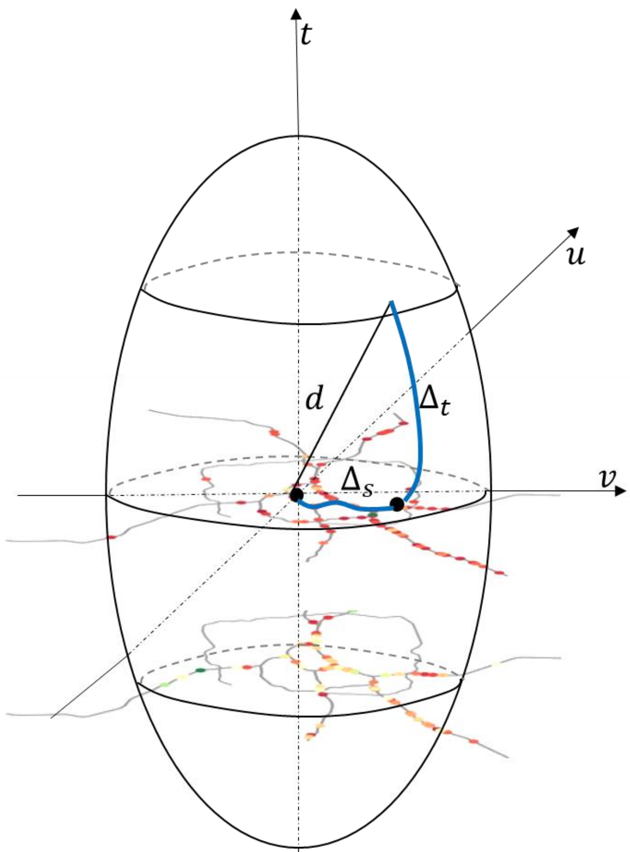

● Neighboring samples Δ_s Spatial distance to the neighbors

Δ_t Temporal difference to the neighbors d Spatiotemporal distance to the neighbors

Figure 20. Illustration of spatiotemporal distance.

Around 40% of all crashes recorded during the study period were detected by Waze Jam reports in the recovery phase, amounting to a total of 1268 crashes. Crash duration comprises the response time, roadway clearance time, and recovery time. The first two are retrieved from the incident operation log, and the recovery time is estimated from Waze jam reports. As shown in **Table 8**, the average crash duration is 57.69 minutes. The fact that the standard deviation is 47.64 minutes close to the mean value suggests a wide range of crash durations, indicating significant variability.

To model the crash duration, this study preferentially collected explanatory data that have a significant impact on crash duration in prior studies (*122; 127; 134; 150*). They are listed in **Table 8.** Arrival traffic not only affects the crash clearance but also the recovery, depending on the number of vehicles accumulated during crash response and clearance. To characterize the traffic demand, this study extracted the traffic volume from the nearest traffic detector upstream of the crash location and aggregated them by volume per lane per hour per direction. The 80th average lane volume (*119*) by the hour of day and day of the week in the crash month is further applied to reflect the regular travel pattern at the crash locale. The average hourly traffic demand during crash clearance is 940 vehicles per lane (see environmental conditions in **Table 8**).

In addition to traffic demand, many other operational factors were also collected, such as deploying dynamic message signs, the presence of a HELP truck, emergency medical services (i.e., EMS), fire, police, tow truck, and the in-transit time of the first responder. Their presence affects the crash clearance time. Notably, the HELP truck is a freeway service patrol carried out by TDOT, which initially aims to provide a fast response to freeway incidents (*151; 152*). HELP truck patrols the most heavily traveled freeways in four major cities in Tennessee (i.e., Nashville, Knoxville, Chattanooga, and Memphis). The HELP truck patrol area covers the study area, whereas the HELP truck may not respond to every incident. For instance, shows that 1235 out of 1268 crashes were responded to by Help trucks (i.e., 33 crashes were missed by HELP trucks). The impact of freeway patrol services on crash duration has also been investigated in prior studies. For example, it was found that crashes that occurred in Alabama service and assistance patrol areas were associated with 21.9% lower clearance times (*122*). In a native study, the HELP program was established as the most efficient responder compared with the Traffic Management Center (TMC) operator in decreasing the clearance time of disabled vehicles in Tennessee (*114*).

Besides, crash characteristics including lane block rate, ramp closure, and number of vehicles involved are considered. As **Table 8** shows**,** the average lane blockage is 31%. Among all crashes, 283 crashes caused the ramp closure. 1128 crashes involved more than 2 vehicles.

Data Explanatory Analysis

Figure 21 demonstrates the hourly pattern of crash duration. From left to right, the green box illustrates the clearance time, the orange box depicts the recovery time, and the red box represents the total duration of the crash. There are few observations between

Table 8. Descriptive statistics of collected variables.

Variable	Description of variables	observations	Mean	Standard Deviation
Dependent				
Crash Duration	Duration from crash reported to normal traffic status (minutes)	1268	57.69	47.64
Duration from crash reported to normal traffic status (minutes)				
Operational/Response Factors				
HELP Truck	Freeway service patrol response present (1 if yes, 0 otherwise)	1235	0.97	0.16
Police	Police response present (1 if yes, 0 otherwise)	902	0.71	0.45
Fire	Fire response present (1 if yes, 0 otherwise)	373	0.29	0.46
EMS	EMS response present (1 if yes, 0 otherwise)	402	0.32	0.47
Tow Turck	Tow truck response present (1 if yes, 0 otherwise)	252	0.20	0.40
In-transit Time	Response time of first arrival operator (minutes)	1268	7.19	10.03
Dynamic Message Sign (DMS)	Crash information was disseminated via upstream Dynamic Message Sign (1 if yes, 0 otherwise)	1055	0.83	0.37
Crash Characteristics				
Lane block rate	The ratio of lane(s) blocked to all lanes	1268	0.31	0.15
Ramp	Ramp Closure (1 if yes, 0 otherwise)	283	0.22	0.42
Vehicles involved	More than 2 vehicles involved in a crash (1 if yes, 0 otherwise)	1128	0.89	0.31
Environmental conditions				
Day of week	Weekday (1 if yes, 0 otherwise)	1083	0.85	0.35
Traffic demand	Average hourly traffic volume per lane during crash clearance period (vehicles/lane/hour/1000)	1268	0.94	0.16

1 AM and 3 AM, and crashes occurred in this period and lasted longer than other periods of the day. Perhaps this is because of a delayed emergency response. During the daytime (before 6 PM), the clearance time tends to be considerably longer than at night, except for the early morning hours (between 1-3 AM). Morning hours (4-8 AM) and afternoon hours (1-4 PM) tend to have longer crash durations than other hours. Besides, the peak recovery time appears at 5-7 AM and 2-4 PM. Theoretically, a shorter clearance time can result in fewer vehicles piling up, leading to a shorter recovery time. However, it is important to acknowledge that even though the clearance time may be short during peak hours, the recovery time could be considerably longer because of the regular traffic demand. **Figure 22** illustrates the spatial pattern of crash duration at route mile markers. The bar's height denotes the average crash duration by that mile marker. Spatial non-stationary crash duration is observed as the city's inner areas generally have longer crash duration than the city's peripheral area. It is worth highlighting that certain locations have notably large crash durations such as eastbound and westbound of I-40.

Results

To optimize the model goodness of fit and enhance the model interpretation, the model selected the explanatory variables that lead to the minimum $AICc$ in the global proportional hazard model. Thereafter, the GTWPH model was built based on the same explanatory variables and additional weights quantified from space and time dimensions. Both the global PPH model and GTWPH model are solved in R environments. The tuned spatiotemporal adaptive bandwidth is 237 nearest neighbors, and the scale parameter is 6.3. **Table 9** shows the estimation results for the global PPH and GTWPH models. In the following sections, the modeling results are summarized and discussed.

Global PPH model

Turning to the global model in **Table 9**, all parameters in the final global model are statistically significant at a 90% confidence interval. A negative parameter estimate implies an increasing hazard risk, that is, a shorter crash duration when such a factor is present or increased. This is because proportional hazard models the conditional probability of crash duration ending at time t. For instance, HELP trucks and Tow trucks were found to have a significantly positive association with crash duration. According to the marginal effects, the duration of a crash is 36.5% longer when a HELP truck is present and 28.9% longer when a Tow truck is present while holding other factors constant. However, some prior practices and studies have shown that highway freeway services patrol can reduce the crash duration and mitigate traffic congestion to a different extent in New York (*153*), Florida (*154*), and Alabama (*122*). The reason behind the seemingly "counterintuitive" outcome of this study may be that HELP trucks prioritize responding to major crashes instead of minor crashes due to limited HELP resources in peak hours. In addition, the other characteristics of crash observations are not strictly matched when comparing crash duration with and without HELP presence. Hence, using this regression method, the parameter estimates can solely demonstrate the correlation between the HELP truck and the duration of the crash

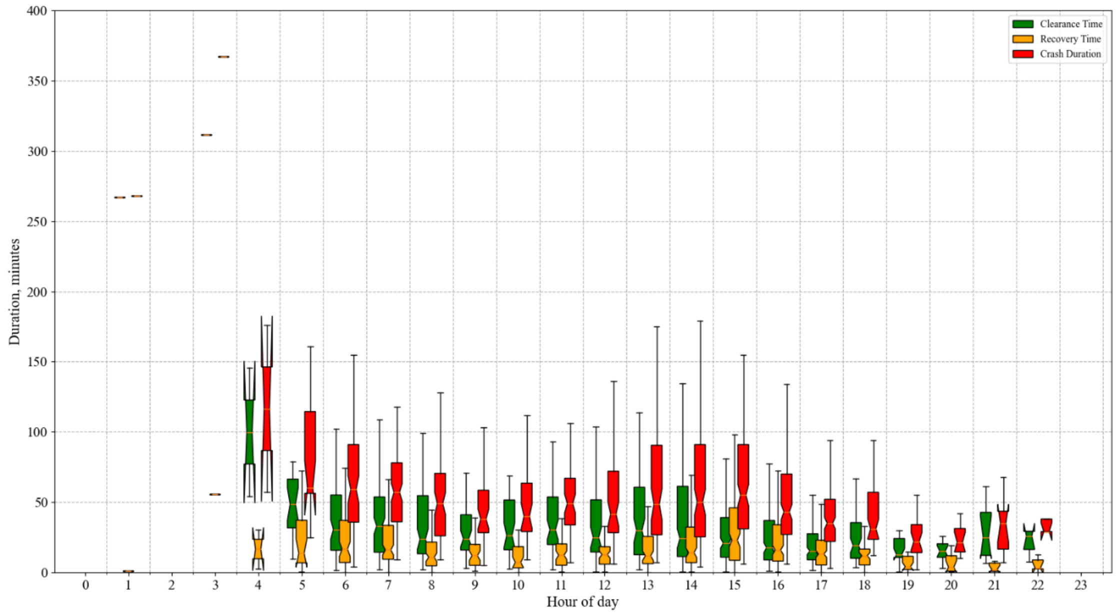

Figure 21. Hourly distribution of crash duration.

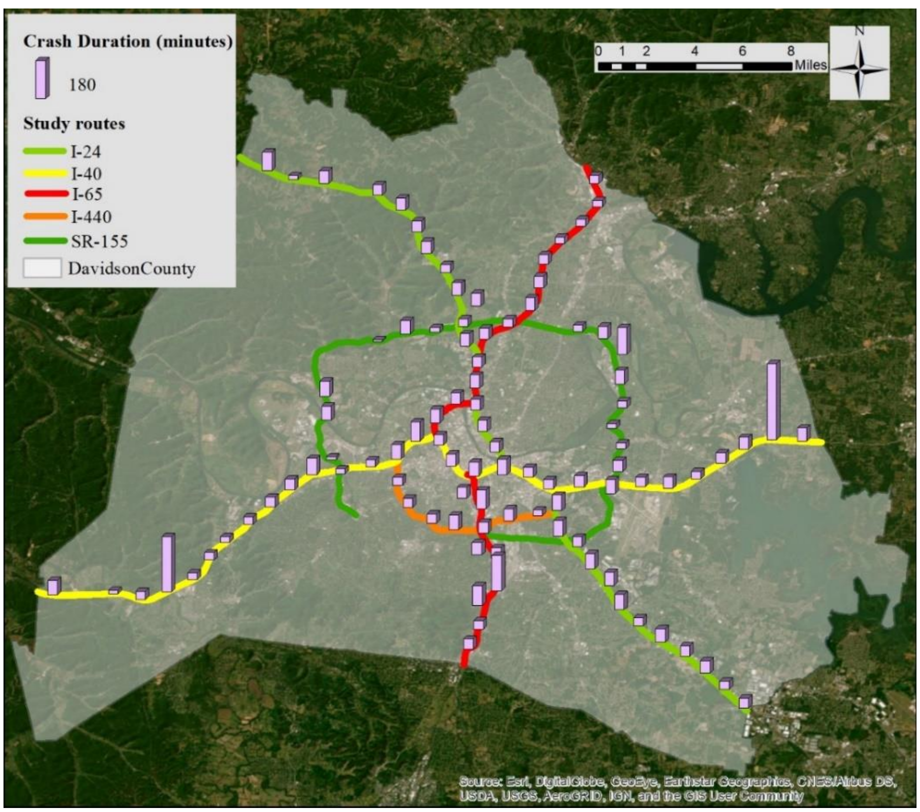

Figure 22. Spatial distribution of crash duration (aggregated by mile marker).

Furthermore, the in-transit time of the first responder is found to have a significant positive impact on crash duration. When controlling for other variables, a one-minute delay in response time is linked to a 2% increase in crash duration. Therefore, it is important to deploy patrol resources efficiently. Besides, it is found that usage of DMS was associated with shorter crash duration based on this global model. The use of DMS to distribute information about crashes is associated with a 32.8% reduction in crash duration when compared to situations where DMS is not used. This makes sense since the usage of DMS could potentially induce a fraction of traffic to divert thereby reducing crash duration. This finding also corroborates Khattak's study (*116*). Turning to traffic impact, traffic demand upstream of the crash locale shows a positive impact on the crash duration. The crash duration is 35.2% longer when traffic demand increases by 1,000 vehicles per lane while holding other factors constant. It makes sense that the more vehicles that arrive from upstream during the response and clearance phases, the longer time the recovery period is needed. Regarding the impact of crash characteristics, it is observed that the larger lane block ratio is associated with longer crash duration. Especially, when the ramp is closed, the crash duration is **28.7%** longer.

GTWPH model

The spatiotemporal non-stationary test was first conducted for GTWPH estimates. The last column of **Table 9** indicates that, except for Tow truck, lane block ratio, and ramp closure, all explanatory factors passed the spatiotemporal non-stationary test. This suggests that crash duration has a spatiotemporal dependency on HELP truck, DMS, Traffic Demand, and in-transit time of first responders have spatiotemporal. Please note that the parameter estimates of GTWPH presented in **Table 9** include both statistically significant and non-significant estimates generated from the local model. By comparison, the mean values of GTWPH estimates are smaller than the global model's estimates, except for the traffic demand. For example, the presence of a HELP truck is associated with a 32.1% longer crash duration, which is about 4.4% lower than the global model. Setting dynamic message signs can bring about a 24.3% shorter crash duration, which is about 8.5% lower than the global model. It is worth noting that traffic demand has a much larger impact on the crash duration in the GTWPH model. A one-unit increase in traffic demand is associated with a 50.8% increase in crash duration, which is about 21.8% larger than the global model estimate. It reveals that the spatiotemporal heterogeneity of traffic demand can significantly affect the crash duration.

Tuning to model performance, the GTWPH model outperforms the global PPH model as indicated by the McFadden R^2, log-likelihood, and $AICc$. After applying spatiotemporal weights to the parametric model, the pseudo-R-square increased from 0.0264 to 0.0507, indicating that accounting for spatiotemporal heterogeneity of factors can improve the model's performance.

In contrast to the global PPH model, the GTWPH model can reveal the spatiotemporal heterogeneity of factors. **Figure 23** showcases the spatial dependency of crash duration. Each dot represents the average value of estimates that are statistically

Table 9. Weibull distribution with global and geographically and temporally weighted proportional hazard model

	Global PPH		GTWPH							
Variables	Global β	t-statistics	Mean β	1^{st} q. β	3^{rd} q. β	Std.	Δ	1.96 Se.	Max $\|Z\|$	Test
HELP Truck	-0.454**[a]	-2.529	-0.388	-0.621	-0.201	0.269	0.419	0.352	2.027	Yes
Marginal Effect [b]	**36.5%**		**32.1%**			**20.0%**				
Tow Truck	-0.341***	-4.589	-0.239	-0.287	-0.194	0.062	0.093	0.146	3.293	No
Marginal Effect	**28.9%**		**21.2%**			**4.9%**				
DMS	0.284***	3.605	0.218	0.034	0.464	0.228	0.430	0.154	3.788	Yes
Marginal Effect	**-32.8%**		**-24.3%**			**31.0%**				
Lane block rate	-0.895***	-4.973	-0.687	-0.814	-0.535	0.187	0.279	0.353	3.649	No
Marginal Effect	**59.1%**		**49.7%**			**9.5%**				
Ramp	-0.338***	-4.941	-0.282	-0.314	-0.236	0.063	0.078	0.134	3.625	No
Marginal Effect	**28.7%**		**24.6%**			**4.6%**				
Traffic Demand	-0.358**	-2.038	-0.730	-1.297	-0.409	0.717	0.888	0.345	4.303	Yes
Marginal Effect	**30.1%**		**51.8%**			**51.5%**				
In-transit time	-0.020***	-7.135	-0.016	-0.019	-0.013	0.003	0.006	0.005	4.925	Yes
Marginal Effect	**2.0%**		**1.6%**			**3.3%**				
McFadden R^2	0.0264					0.0507				
Log-Likelihood	-2784					-2714				
$AICc$	5588					5448				

Note. a. *** p<1%, ** p<5%, * p<10%. b. The marginal Effect is the percent change of crash NFT duration in response to one unit change of an independent variable while keeping other variables constant.

significant at a 90% level (i.e., p-value < 0.1) at each mile marker. The color highlights the magnitude of the estimates, with greener color indicating a larger value and redder color representing a smaller value. According to the map, it is found that the presence of HELP trucks (**Figure 23. a**) in the center part of Nashville city is associated with longer crash duration than the city's peripheral areas. The same phenomenon is observed on the Tow truck (**Figure 23. b**). It might be because the city's inner area experiences heavier traffic than rural areas and emergency response resources are more concentrated in the city's inner area. Crash duration reduction was observed in all study routes when DMS was used, as indicated in **Figure 23. c**. Especially, compared to other routes, the south portion of I-24, also known as the smart corridor, experienced a greater reduction in crash duration when DMS was deployed. Traffic demand of south I-24, east I-40, and south 65 produced a larger impact on crash duration than in other areas, as **Figure 23. d** indicates. The impact of lane closure ratio on crash duration is not uniform, neither across a route nor within a region (see **Figure 23. e**). Besides, it is found that ramp closure, especially on the west stretch of I-40, and central city areas cause a larger impact on crash duration than other areas (see **Figure 23. f**). This could be due to a higher traffic demand entering and exiting the ramps in the downtown area compared to other regions. Lastly, the In-transit time of the first responder is essential to prevent the deterioration of traffic conditions, so it is often the focus of the freeway service program. According to **Figure 23. h**, it turned out that delayed in-transit time could cause longer crash duration in the peripheral areas than in the central city. The unequal distribution of emergency response resources across different locations could be a contributing factor to this phenomenon.

Traffic demand varies by the hour of the day, and the available responder resources are also different during the daytime and nighttime. Therefore, it is essential to look into the hourly effect of explanatory variables. **Figure 24** box plots illustrate the temporal variation of estimated parameters that are statistically significant in local sub-models. Red boxes highlight the peak hours and cyan boxes depict the off-peak hours. Notice that the magnitude of factors differs to a high degree. Compared to off-peak hours, the presence of HELP trucks in peak hours is associated with longer crash duration (**Figure 24. a**). By contrast, the presence of tow trucks during peak hours involved shorter crash duration compared to off-peak hours (**Figure 24. b**). The impact of traffic demand on crash duration is more volatile in the morning peak as indicated by relatively long boxes. The positive impact keeps decreasing until the afternoon peak (**Figure 24. c**). Traffic demand during the evening period (7-10 PM) tends to have the largest impact in increasing crash duration throughout the day (**Figure 24.d**). Likewise, the impact of a lane closure on crash duration worsens from 4 PM onwards (**Figure 24. e**). This could be because it may take longer to clear debris from the travel lanes as nighttime approaches. Ramp closure produced the largest impact on crash duration during the middle of the day (11 AM-3 PM) (**Figure 24. f)**. Lastly, the in-transit time of the first responder has a comparatively lesser impact on intensifying crash duration during peak hours (**Figure 24. g**), which may be attributed to the higher concentration of resources available during peak hours. These temporal trends imply a near-future focus for emergency operators who are responding to crashes and other incidents. The focus could be effectively setting dynamic message signs, allocating HELP truck resources dynamically, and so on.

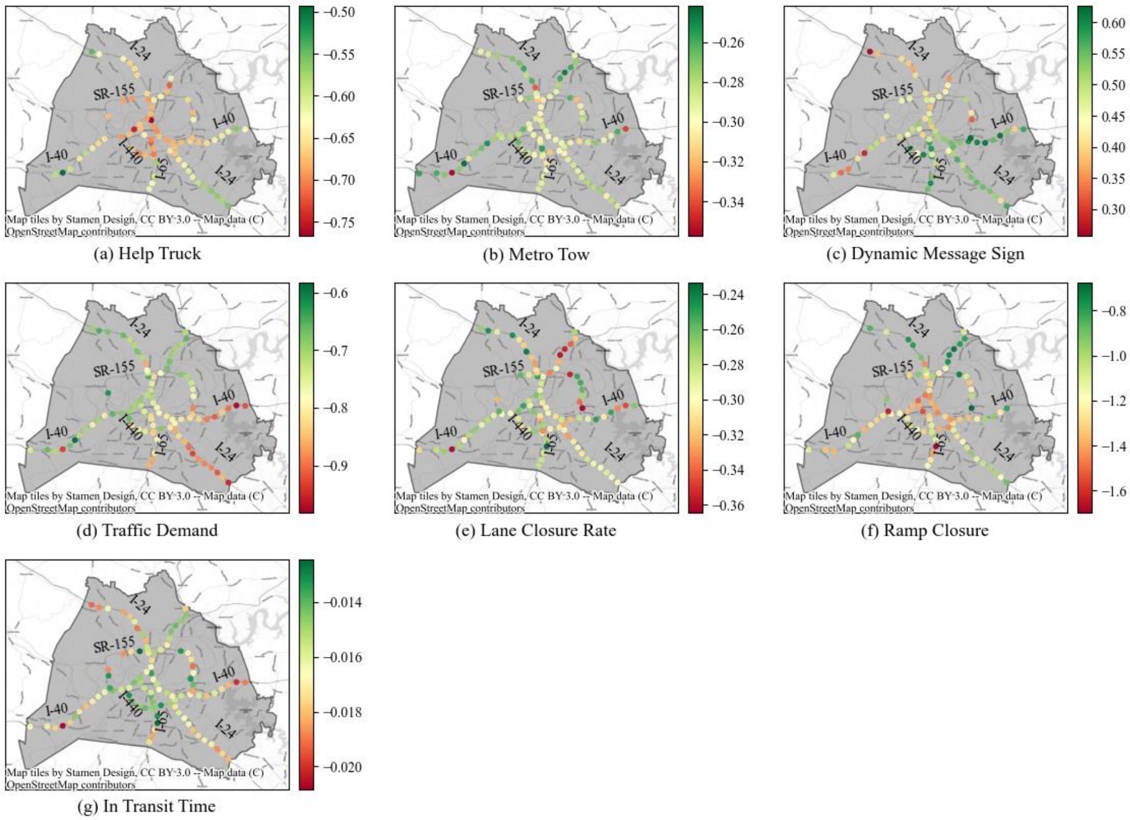

Figure 23. Spatial distribution of parameter estimates (aggregated by mile markers).

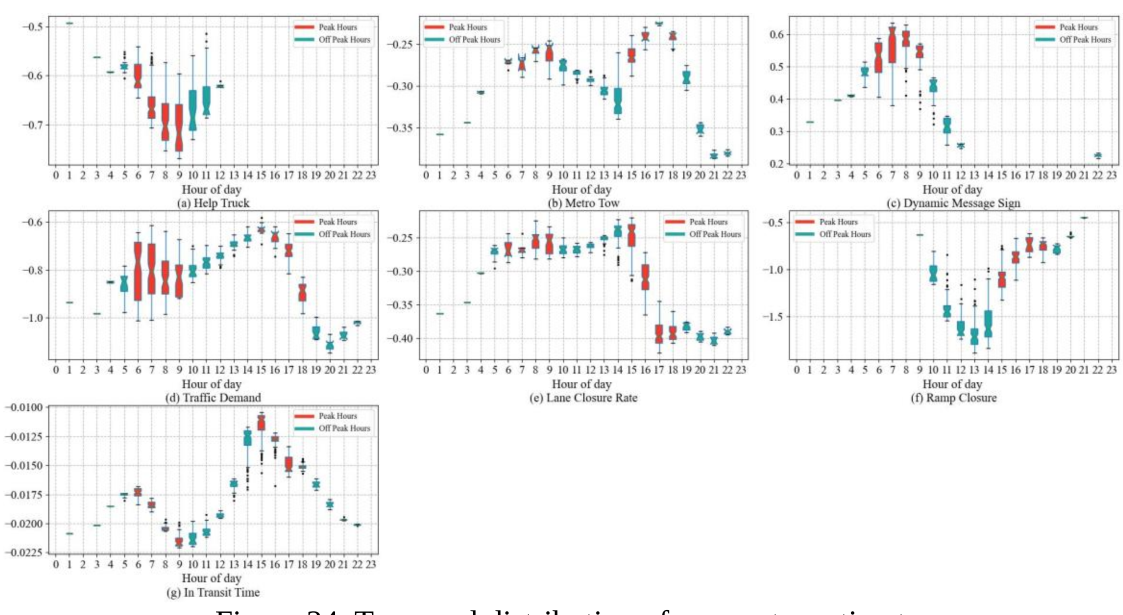

Figure 24. Temporal distribution of parameter estimate.

Limitations and future study

There are some limitations of this study. First, like normal regression, the proposed parametric model can only explain the correlation between crash and their covariates, yet the causality should be carefully examined. For instance, results show that the response of a HELP truck and a Tow truck to a crash is associated with a longer duration. This is because HELP trucks usually prioritize the major incidents which last longer than minor incidents, leading to data collection biased. Hence, the regression results cannot manifest the benefit of deploying HELP trucks. A causal inference model is needed in a future study to infer whether HELP trucks and other responders reduce or increase the crash duration. Besides, researchers are likely to apply Waze traffic jam reports estimating the detection time of the crash in future studies because previous studies have found that Wazers can detect the accident sooner than when responders are notified (*12; 64*). However, the proportional hazard model will become more complicated as both the start time and end time of the crash are only known to an interval, which is known as a doubly censoring mechanism (*155*).

Conclusions

To reduce non-recurrent congestion resulting from incidents, it is essential to have a thorough understanding of the factors that impact the incident duration. This study investigates the crash duration as the crash is the major concern among all incident types. The crash duration of this study comprises the crash response, clearance, and recovery time. Since crash response time and clearance time can be obtained from incident operation logs, this study starts with estimating recovery time using Waze traffic jam reports. Notably, the crash duration is interval-censored as the Wazers are not likely to capture the exact time that traffic backs to normal, and the transition of traffic status is usually fuzzy. A geographically and temporally weighted proportional hazard model is created to identify the factors that correlate with crash duration. The key findings of this study are:

- When using Waze traffic jam reports to eximate recovery time, it is found that 90% of traffic jam reports' headway about the same incident is less than 16 minutes.
- When modeling the covariates of crash duration, GTWPH outperforms the global PPH model in the explanatory power as well as the goodness of fit. GTWPH provides a more in-depth understanding of how covariates affect crash duration spatiotemporally.
- In a global PPH model, it is found that using DMS to distribute information about crashes is associated with a 32.8% reduction in crash duration when compared to situations where DMS is not used. GTWPH model further reveals that setting DMS on I-24 and in the morning peak hours is even more effective in reducing crash duration.

- Spatiotemporal test results show the effects of HELP trucks, utilization of dynamic message signs, in-transit time of the first responders, and traffic demand on the hazard function are heterogeneous across space and time.
- The average estimates of GTWPH are smaller than global PPH except for the traffic demand. The global PPH model seems to largely underestimate the impact of traffic demand compared to GTWPH.
- Although not varying spatiotemporally, other factors show a significant correlation with crash duration. For instance, an increase of one unit in lane block ratio is linked to a 59.1% longer crash duration, while ramp closures can cause an additional 28.7% increase in crash duration.

The study's outcomes can help incident operators in prioritizing resources for crash response and clearance when dealing with crashes that happen at different times and locations. The proposed crash duration model can also be expanded to other traffic incidents analysis such as disabled vehicles. Future studies could focus on comparing the predictive performance between the model established in this article and conventional models that account for unobserved heterogeneity.

CHAPTER IV. ESTIMATION OF TRUCK TRAFFIC VOLUME USING LOOP DETECTOR AND CROWDSOURCED SPEED DATA

The chapter is a modified version of a published paper:
Gu, Y., Liu, D., Stanford, J., & Han, L. D. (2022). Innovative Method for Estimating Large Truck Volume Using Aggregate Volume and Occupancy Data Incorporating Empirical Knowledge into Linear Programming. Transportation Research Record.

Abstract

Truck traffic monitoring is critical for the operation and planning of transportation and economics. Nowadays, many "sophisticated" traffic detectors equipped with infrared, microwave, and magnetic sensors can directly detect vehicle classifications, yet they are not widely available due to their high cost. Single loop detectors are widely deployed at early-stage development of transportation yet are limited to collecting traffic volume and occupancy. Hence, several studies have been conducted to use data from single loop detectors to restore truck traffic. However, these methods are susceptible to dynamic traffic conditions and necessary assumptions. To this end, this chapter developed two methods and compared them with two common literature methods. The first method established a linear optimization problem by minimizing the difference between observed occupancy and calculated occupancy. The length of short vehicles (SV) and large trucks (LT) are allowed to vary with speed. Another method applies Waze speed to estimate the total vehicle length, which is more straightforward. Three months of detector data and Weigh-in-motion (WIM) data from the California Freeway Performance Measurement System (PeMS) were collected and used to examine the performance of different methods. The results show that all methods are susceptible to low truck conditions. The optimization method outperforms when truck traffic increases at the station level and during the night-time period. The straightforward method may be affected by the quality of Waze speed. Nonetheless, it still performs better than dynamic estimation. Compared to the literature methods, the proposed two methods are less restricted by traffic conditions, and they are promising to be implemented to loop detectors for wide truck traffic monitoring.

Introduction

Large trucks and other long vehicles play an essential role in the United States logistics system and their activity level works as a good economic indicator (*156*). Meanwhile, LT causes many transportation-related issues because of their special characteristics such as the weight of the load. For example, studies (*157; 158*) show that high large truck volumes cause great damage to road pavement, so truck volume is a core consideration as transportation agencies budget pavement construction. From the emissions perspective, some heavy-duty diesel trucks produce nitrogen oxides and black carbon particles, significantly contaminating the air quality (*159*). In the Congestion Mitigation and Air Quality (CMAQ) program, the Federal Highway Administration (FHWA) requires states to monitor the percentage of non-single occupancy vehicle travel and total emission reduction (*160*). Research shows that the severity and frequency of crashes increase considerably when large trucks are involved (*161*). From the planning perspective, the proportion of truck volume is one of the major factors affecting road capacity in the

Highway Capacity Manual (*126*) (*162*). Therefore, monitoring LT volume has always been an important topic in transportation studies.

Literature Review

Single-loop detectors, along with dual-loop detectors, have played a fundamental role in measuring traffic since the 1960s. Although the sensor technology (e.g., infrared, microwave, etc.) evolves, most detectors still measure only time occupancy and total vehicle volume. A typical single-loop detector reports these measures aggregated over pre-set time intervals (e.g., the 20s or 30s) but cannot gauge the distance that a vehicle traveled. Hence, single-loop detectors are not directly useful for determining vehicle speed or distinguishing vehicle types. Nevertheless, with the relationship (Equation (40)) between volume N_i(the percentage of time that the detector is occupied by vehicles), speed v_i and mean effective vehicle length (MEVL) $\bar{l}_i$ at interval i, one can obtain the parameter of interest given the other three parameters (*163*). MEVL is defined as the average length of vehicles plus the longitudinal span of the detection area. This is because the actual distance a vehicle traversed over a detector encompasses the length of a vehicle and the detection region (e.g., loop wires or magnetic beam) (*164*). Based on MEVL, the LT volume can be further determined through the combination of vehicle classification with the maximum probability. With this logic, many studies have been conducted, and various models have been applied to improve the accuracy of MEVL and speed estimation, which are reviewed in this section below.

$$v_i = \frac{N_i}{T \cdot O_i} \cdot \bar{l}_i \tag{40}$$

In earlier studies, instead of considering the MEVL straightforward, the g-factor (denoted as *g*), as the reciprocal of MEVL in Equation 1, was used to indicate the composition of the vehicle population passing the detection area, as shown in Equation (41) (*165*).

$$v_i = \frac{N_i}{T \cdot O_i} \cdot \frac{1}{g} \tag{41}$$

In a fixed g-factor model (*166; 167*), MEVL is assumed constant, and the speed variance of vehicles within the interval is discarded (14). However, this method was verified viable only when the traffic condition is congested (*163*); otherwise, the MEVL may be biased under a free-flow state. However, in practice, the traffic congestion and LT volume could significantly affect the value of MEVL (*165*). Hence, a dynamic g-factor (or MEVL) was explored to account for the length variation. For example, Wang and Nihan (*168*) modeled the MEVL as a log-linear function of independent variables including volume, expectation of occupancy, low-volume dummy, etc. Low-volume dummy variables are set to one when the hourly volume is less than 30 for better regression. In such a way, the variation of MEVL was captured, which certainly presents the variation of vehicle composition across the day. Coifman (*163*) noticed that the relation of MEVL and rest parameters in Equation (40) becomes ambiguous in free-flow conditions. Thus, an exponential filtering method was imposed on MEVL when occupancy is less than 10% (free-flow condition). However, this approach is over-reliant

on empirical data because of the selection of a threshold for the free-flow state and the value of MEVL for the congested period. Notably, these studies realized that the estimation of MEVL is closely subject to the traffic status and should be dynamic. Wang and Nihan (*169*) proposed a method by applying volume and occupancy observed at each interval to adjust the MEVL during each short period (e.g., 5 minutes). To reduce the impact of LT on MEVL estimation, they first separated the SV and LT by critical MEVL. Then the basic SV length was updated by intervals without the presence of LT. However, their work relies on two important assumptions. One is that speed within a period (i.e., 5 minutes) is assumed constant to prevent the accumulated error from modification.
The other assumption is that at least two intervals only have short vehicles. With this assumption, the MEVL can be proportionally adjusted based on the length of SV. The results indicate that LT estimation had higher accuracy in uncongested conditions than in congested conditions. Although MEVL can be measured or adjusted through traffic volume or traffic conditions, previous methods still depend on empirical data on speed or vehicle length.

$$v_i = \frac{N_i}{T \cdot O_i} \cdot \frac{\bar{l}_i}{T}[\frac{\sigma_{v_i}^2}{v_i^2} + 1] \tag{42}$$

Considering the difficulty of obtaining the empirical data in some cases, pursuing accurate speed is another approach to getting MEVL. Using volume and occupancy data from a single loop detector, Dailey expanded **Equation** (40) by considering the variability of speed in each interval $sigma_{v_i}^2$ (*170*) as shown in **Equation** (42) Based on this non-linear relationship, an Extended Kalman Filter (EKF) was implemented to solve the speed at each interval. However, two unknown parameters, the variation of speed and MEVL, are needed in this filtering process. Furthermore, a later study found that the ratio $\sigma_{v_i}^2/v_i^2$ is small and consequently, it can be ignored (*168*). Nevertheless, Zhang, Xie and Ye (*171)* and Zhang, Wang and Wei (*172)* implemented Unscented Kalman Filtering (UKF) to generate speed estimation based on the formulation (Equation (42) derived by Dailey (*170)* Results show that speed estimated from UKF did work better than EKF under various traffic conditions. Instead of estimating speed from a complicated relationship described by the traffic fundamental stream model, Kwon, Varaiya and Skabardonis (*173)* proposed a simple method relying on the speed correlation between lanes. However, this approach only works for freeway locations with truck-free lanes which are easily violated. Given the MEVL, the speed of the truck-free lane can be obtained through **Equation** (40); then, by applying the correlation coefficients observed from empirical data, the other lanes' speeds were estimated indirectly. Thus, this approach is also subject to the coefficients between lanes, and the accuracy of speed estimation is highly dependent on the choice of coefficients. On top of using aggregate volume and occupancy directly, Hazelton (*174)* assumed a random walk by simulating the individual vehicles' speed at an interval. A Markov Chain Monte Carlo (MCMC) model was applied to estimate the aggregate speed over an interval. As Ye, Zhang and Middleton (*175)* and Dailey (*170)* stated, this approach considered the error of measurement (e.g., error of occupancy). However, it is subject to the prior information on vehicle length, error of speed, and error of occupancy, which could affect the posterior distribution of speed.

Once the MEVL for each detection interval is obtained, the problem of estimating LT becomes how to allocate the SV and LT given the aggregate volume. Wang and Nihan (*168)* assumed both SV and LT follow normal distributions, with MEVL of SV and LT obtained from empirical data. Wang and Nihan (*169)* determined the best combination of SV and LT in terms of minimizing the distance between the sample interval and category, given a limited combination of SV and LT within the rolling 30-second time window. However, in the real world, SV and LT would not always follow an exact normal distribution. Hence, supposing the distribution of SV and LT are independent, irrespective of distribution type, Zhang, Xie and Ye (*171)* and Kwon, Varaiya and Skabardonis (*173)* rearranged the MEVL by the expectation of average SV and LT length. Therefore, given the SV and LT length from historical data, and MEVL from the speed estimation, the numbers of SV and LT are directly solved. However, the lengths of SV and LT are fixed for all periods in a day, which is only suitable for the stations in which SV and LT lengths are highly proportional.

Unlike the above algebra approaches, Zhang, Wang and Wei (*172)* applied Artificial Neural Network (ANN) to link occupancy, volume, and timestamp from single loop detectors to the volume of different vehicle types (e.g., car, trucks, etc.) from dual loop detectors. With the supervised learning approach, various complex relations between occupancy, volume, and vehicle type volume can be captured. Notably, as they stated, this method can accommodate heavily congested traffic by retraining the ANN model using data collected under congestion conditions. Because of this training requirement, this approach highly relies on dual loop detectors, and the performance of the trained model in other locations is unknown due to the potential spatial heterogeneity of traffic flow.

In conclusion, two limitations were found in previous studies regarding LT volume estimation using occupancy and volume data. First, estimating MEVL heavily relies on exogenous data such as dual-loop data for vehicle classification or vehicle length distribution, which is hard to obtain without extra detectors. Second, most of the approaches cannot accommodate various traffic conditions. In a few cases where good performance is reached throughout the day, their work is limited to a specific situation or location (*127; 129; 137)*.

Methodology

Given sensor inputs of aggregate volume and occupancy during a 30-second interval, the best combination of SV and LT can be estimated according to their intrinsic relationship, as **Equation (40)** shows. This study developed two methods based on simple loop detector data and Waze speed, separately. In addition, two methods from existing literature were implemented to serve as a benchmark for the proposed techniques. The following section elaborates on different methods.

Method 1. Optimization based on traffic volume and occupancy.

Since we cannot capture individual vehicles' lengths through conventional loop detectors, we must assume the typical values for the length of LT and SV. However, the constant vehicle length is barely realistic and will undoubtedly produce a discrepancy between the estimated total vehicle length and the observed total vehicle length. Alternatively, we use the occupancy which is proportional to vehicle length because we can obtain occupancy from loop detectors directly. Therefore, this method comes down to minimizing the difference between estimated occupancy and observed occupancy, subjecting to a series of constraints. The objective function can be written as:

$$minimize: |O_o - O_c| \tag{43}$$

where O_o and O_c denote the observed occupancy and the calculated occupancy based on the "best guess" of vehicle combinations for an interval, respectively.

Given the assumed vehicle length for SV and LT, denoted as l_{SV} and l_{LT}, separately, O_c can be formulated as the sum of SV occupancy and LT occupancy, which takes the form:

$$\begin{aligned} O_c &= m \cdot O_{SV} + n \cdot O_{LT} \\ &= m \cdot O_l \cdot l_{sv} + n \cdot O_l \cdot l_{lt} \end{aligned} \tag{44}$$

where O_{sv} and O_{lt} denote the average occupancy of SV and LT for an interval. Furthermore, they are decomposed by unit occupancy O_l (i.e., occupancy per foot) so that the occupancy of SV and LT can be adjusted implicitly through the vehicle length variables. Furthermore, utilizing unit occupancy has the potential to decrease measurement errors in vehicle occupancy compared to estimating the average occupancy of SV or LT vehicles. In this study, the unit occupancy is inferred by the short vehicles. Equation (45) gives the calculation of unit occupancy. The numerator characterizes the distribution of occupancy for a typical SV. The coefficient 'a' can be interpreted as the fundamental occupancy, with other occupancies at varying speeds being exponentially related to this baseline value. For example, if a 15-feet SV (l_{sv}) is traveling at 60 mph (v_0), its occupancy would be 0.174 seconds, or 0.57% (a) (in accordance with typical detector output format) if the detector interval is 30 seconds. Parameter c is a constant value resultant from the unit translation. The coefficient b represents the typical occupancy of an SV traveling at 60 mph.

$$O_l = \frac{a \cdot e^{\frac{O_i}{b}}}{l_{sv}} = \frac{c \cdot \frac{v_0}{l_{sv}} \cdot e^{(\frac{O_i}{b})}}{l_{sv}} \tag{45}$$

We should notice that occupancy can be affected by vehicle speed. For instance, a short vehicle takes a longer time to traverse detector in a congested period than a free-flow period. Therefore, the unit occupancy should be represented concerning the vehicle speed to accommodate the different traffic conditions. Equation (46) further decomposed Equation (45) into:

$$\begin{aligned} O_c &= m \cdot O_l \cdot l_{sv} + n \cdot O_l \cdot l_{lt} \\ &= m \cdot \frac{c}{v} \cdot l_{sv} + n \cdot \frac{c}{v} \cdot l_{lt} \\ &= \frac{c}{v} \cdot (m \cdot l_{sv} + n \cdot l_{lt}) \\ &= \frac{c}{v_0} \cdot \frac{v_o}{v} \cdot (m \cdot l_{sv} + n \cdot l_{lt}) \\ &= \frac{c}{v_o} \cdot \alpha \cdot (m \cdot l_{sv} + n \cdot l_{lt}) \end{aligned} \tag{46}$$

$$= \frac{c}{v_o} \cdot (m \cdot (l_{sv} \cdot \alpha) + n \cdot (l_{lt} \cdot \alpha))$$

Where $\alpha = v_o/v$ serves as a regulator that can represent the varying traffic situations. By assuming $v_0 - \delta \leq v \leq v_0 + \delta$, where δ denotes the speed deviation (e.g., $\pm$ 5 mph), Given that theoretical speed may differ from the actual speed, the α is further refined by a lower bound value α^l and upper bound value α^u:

$$\alpha^l = \frac{v_o}{v_o + \delta} = \frac{v_0}{v_0 - \delta} \tag{47}$$

Where δ is speed deviation (e.g., $\pm$ 5 mph). Then, the ratios α^l and α^u are integrated into l_{SV} and l by extending the upper bounds and lower bounds of SV and LT length:

$$l_{SV}^l = \min\{l_{st} \times \alpha^l, l_{ST} - \Delta_{st}\} \tag{48}$$

$$l_{SV}^u = \max\{l_{st} \times \alpha^{\mathrm{u}}, l_{ST} + \Delta_{st}\} \tag{49}$$

$$l_{LT}^l = \min\{l_{lt} \times \alpha^l, l_{LT} - \Delta_{lt}\} \tag{50}$$

$$l_{LT}^u = \min\{l_{lt} \times \alpha^l, l_{LT} + \Delta_{lt}\} \tag{51}$$

Where Δ_{st} and Δ_{lt} denote the variation of vehicle length, separately. Hence, the vehicle length of SV and LT is allowed to vary within the range given by Equations (52)-(53), separately. Equation (54) gives an equality constraint that formulates that number of total vehicles should be equal to the observed traffic count from the detector. Besides, the number of SV and LT should be non-negative values and no greater than the observed traffic count, as Equation (55) shows.

$$l_{sv}^l \leq l_{sv} \leq l_{sv}^u \tag{52}$$

$$l_{lt}^l \leq l_{LT} \leq l_{lt}^u \tag{53}$$

$$m + n = N_i \tag{54}$$

$$0 \leq m, n \leq N_i, \{m, n\} \in N^+ \tag{55}$$

where (l_{sv}^l, l_{sv}^u), (l_{lt}^l, l_{lt}^u) are the boundary of the length of SV and LT.

Combining all information from **Equation** (43)-(55), the whole integer optimization is formulated. Some might claim that this is not a valid linear programming problem since two decision variables in **Equation (44)** are multiplied together, which violates the assumptions of linear programming. Others might claim that it is an integer programming problem because decision variables are integers instead of inclusive segments. Both claims are false by considering there are only *(N+1)* possible combinations for *N* vehicles in the 30-second time interval, the problem can be viewed as enumerating the LP problem *(N+1)* times by fixing decision variables m and n. Since *N* is restricted by the capacity, the problem can be solved in polynomial time complexity by enumerating LP *(N+1)* time (*176*). Similarly, the absolute error objective function is not of simple linear form but is piece-wise linear and therefore can be converted to the standard linear programming problem by adding auxiliary variables (*176*). By adding an auxiliary variable Δ, the original linear optimization problem with absolute difference objective function is reformulated by substituting the objective function to the (56) adding two more constraints (**Equations** (57) and (58)) for the auxiliary variable Δ, with everything else staying the same:

$$minimize: \Delta \tag{56}$$

$$O_o - O_c \leq \Delta \tag{57}$$

$$O_c - O_o \leq \Delta \tag{58}$$

Method 2. Lane-to-lane speed correlation

The method was proposed by Kwon et, al., in 2003 and is implemented by the PeMS system (*173*). Two conditions must be met for this approach to work: first, there must be a designated lane for trucks in the freeway locations; second, the speed must be strongly correlated between the lanes. With these two conditions, the authors start by calculating the speed for truck free lane by the following relationship:

$$\bar{v}(i,j) = \frac{N(i,j) \cdot \bar{l}_{sv}}{O(i,j)} \tag{59}$$

Where $\bar{v}(i,j)$ denotes the speed for truck-free lane *i* at *j* interval. $N(i,j)$ and $O(i,j)$ denote the volume and occupancy of a truck-free lane *i* at *j* interval. $\bar{l}_{sv}$ is the average length of short vehicles, which is a constant value in this study. Outer lanes usually exhibit slower speeds whereas we can infer the speed of outer lanes via the speed correlation $\beta(i', i)$. Hence, the outer lanes speed can be represented by:

$$\bar{v}(i',j) \approx \beta(i',i)\ \bar{v}(i,j) \tag{60}$$

Notably, i' represents the outer lanes which are truck-rich.

With the speed estimated above, the total vehicle length can be solved by:

$$\hat{L}(i',j) = \bar{v}(i,j) \cdot \frac{O(i',j)}{N(i',j)} \tag{61}$$

And then the truck proportion by:

$$\hat{p}(i',j) = \frac{\hat{L}(i',j) - \bar{l}_{sv}}{\bar{l}_{lt} - \bar{l}_{sv}} \tag{62}$$

The truck count for interval *j* is then estimated by:

$$\hat{n}_{lt}(i',j) = \hat{p}(i',j) \cdot N(i',j) \tag{63}$$

For further details about this approach, please refer to the original research paper (*173*).

Method 3. Dynamic estimation

This method is proposed by Wang and Nihan in 2004 (*169*). Likewise, this method targets discovering two types of vehicles including SV and LT using traffic volume and occupancy from a single loop detector. There are two fundamental assumptions underlying this method. The first is that the speed of vehicles remains constant within each defined period, which typically comprises several intervals (e.g., 30 seconds). The second assumption is that every period contains at least two intervals in which no LTs are present. The first two smallest occupancy-to-volume ratios are used to select the two intervals with no LTs as this ratio is linearly proportional to vehicle lengths, given speed *v* is constant within a period *j* (See Equation (64)).

$$\bar{l}(j) = \frac{O(j)}{N(j)} \cdot v(j) \cdot T \tag{64}$$

Therefore, the vehicle length of average SV length can be estimated by using these two intervals output, that is:

$$\bar{l}_{sv}(j) = \frac{O_{sv}(j)}{N_{sv}(j)} \cdot s(j) \cdot T = \frac{O_p(j) + O_{p+1}(j)}{N_p(j) + N_{p+1}(j)} \cdot s(j) \cdot T \tag{65}$$

As a result, for the intervals in period j that are not screened out, the total length of vehicles $\bar{l}_k(j)$ can be proportional to the length of shorter vehicles, because the constant speed can be canceled out between intervals.

$$\bar{l}_k(j) = \frac{O_k(j)}{N_k(j)} \cdot \frac{N_{sv}(j)}{O_{sv}(j)} \cdot \bar{l}_{sv} \tag{66}$$

To minimize the impact of random errors on the computation, the algorithm incorporates new occupancy and volume data obtained from intervals without LTs to update the short vehicle occupancy $O_{sv}(j)$ and volume $N_{sv}(j)$. Whether an interval contains no LTs is determined based on whether the average vehicle length within that interval is smaller than the length of any vehicle that includes at least one truck. Ultimately, the algorithm iterates all types of vehicle combinations and selects one that produces the minimum distance $d_{kx}(j)$ between the composite vehicle length $\bar{l}_k(j)$ and the mixed vehicle distribution (calculated by a Gaussian distribution with mean = $\mu_{kx}(j)$ and variance = $\sigma_{kx}(j)$), as Equation (67) shows.

$$d_{kx}(j) = \left| \frac{\bar{l}_k(j) - l_{loop} - \mu_{kx}(j)}{\sigma_{kx}(j)} \right| \tag{67}$$

Where l_{loop} is the length of the detector. In contrast to method 2, this approach improves truck estimation by accounting for the variation of vehicle length that follows a Gaussian distribution, which is more realistic. For more details about this approach, authors can refer to the original paper (*169*).

Method 4: straightforward estimation

Speed, as shown in Equation (40), is another crucial element in calculating the vehicle length. However, speed data is barely available because most detectors like single loop detectors are unable to measure the complete length of vehicles that pass over them. Nonetheless, some separate data sources such as probe vehicle data can provide coarse speed information around the detectors. When speed from a separate source is available, overall vehicle length $\bar{l}_i$ can be directly estimated by Equation (68).

$$\bar{l}_i = v_i \cdot O_i \tag{68}$$

Further, $\bar{l}_i$ is broken down into the total length of SV and LT, which can be expressed as:

$$\bar{l}_i = m \cdot \bar{l}_{sv} + n \cdot \bar{l}_{lt} \tag{69}$$

To address the potential misclassification of short vehicles in a congested period, the average length of short vehicles is modified based on the speed. Specifically,

$$\bar{l}'_{sv} = \frac{v_{sl}}{v_i} \cdot \bar{l}_{sv} \tag{70}$$

Where v_{sl} is the speed limit. The factor v_{sl}/v_i elongates the vehicle length when speed decreases thereby preventing the incorrect classification of short vehicles as long vehicles due to the longer presence on the detector.

Compared to the lane-to-lane speed correlation approach, this method eliminates the need for assumptions regarding the absence of trucks in a lane and the correlation of speeds between lanes. However, the speed comes from the exogenous data source, which may be biased.

Method evaluation

To evaluate the overall performance of proposed models, Mean Absolute Error (*37*) is computed:

$$MAE = \frac{1}{N}\sum_{n=1}^{n=N} |n_{est} - n_{obs}| \tag{71}$$

Where $|n_{est} - n_{obs}|$ calculates the absolute error (AE). n_{est} denotes the estimated number of trucks and n_{obs} represents the observed number of trucks from detectors. N denotes the number of samples, which could be the number of days, number of hours, and so on.

Data Description

The primary data of this study contains PeMS detector data and Waze Speed data. PeMS is maintained by the California Department of Transportation. It provides a large amount of traffic detector data and weigh-in-motion (WIM) vehicle classification data. This study selected four loop detector stations (*177*) that have WIM stations installed nearby to compare the effectiveness of various methods for estimating truck traffic volume. The detector data comprises information on traffic volume and occupancy for each lane for every 30-second interval. The WIM station provides hourly traffic volume data for each lane, segmented by vehicle types, which serves as the ground truth of truck traffic. Additionally, the study collected data on Waze speed for short segments that pass through these stations. The Waze speed is aggregated from crowdsourced Wazers' vehicle speeds by the Waze map itself and is reported at one-minute intervals, without distinctions between lanes. The quality of Waze speed may be affected by the population of Wazers at different times of day, as reported by an early study (*60*).

All the data were collected between November 15, 2022, and February 15, 2023. The configuration of selected detectors is shown in **Table 10**. Since truck traffic can be affected by economic activities, population density, land use, and many other factors, one station has been selected from an urbanized area and another station from a rural area, while ensuring that this selection is not biased toward any specific area. **Figure 25** shows the location and roadway geometry of WIM stations. Note that the Westbound section of station 34870 has WIM sensors installed in four out of five lanes, while the Eastbound section has WIM sensors installed in all five lanes. At station 34630, WIM sensors are installed in all lanes. Truck percentages are calculated based on all WIM observations during the study period. Stations in the urbanized areas are observed with relatively few trucks traffic coming in and out of the city. The city's inbound truck traffic is nearly half of the outbound truck traffic. Station 34630 recorded a significantly higher amount of truck traffic for both directions during the study period. Comparatively, it suggests that a fraction of trucks may circumvent the city area due to its higher levels of congestion compared to rural areas.

Table 10. Configuration of WIM and LDS stations

WIM station	LDS station	Highway	Direction	Lanes	Truck percentage	Population
34870	313405	I-80	W	4/5	1.7%	Urbanized
	313406	I-80	E	5/6	3.2%	Urbanized
34630	3412044	I-80	W	3	9.6%	Rural
	3412041	I-80	E	3	10.4%	Rural

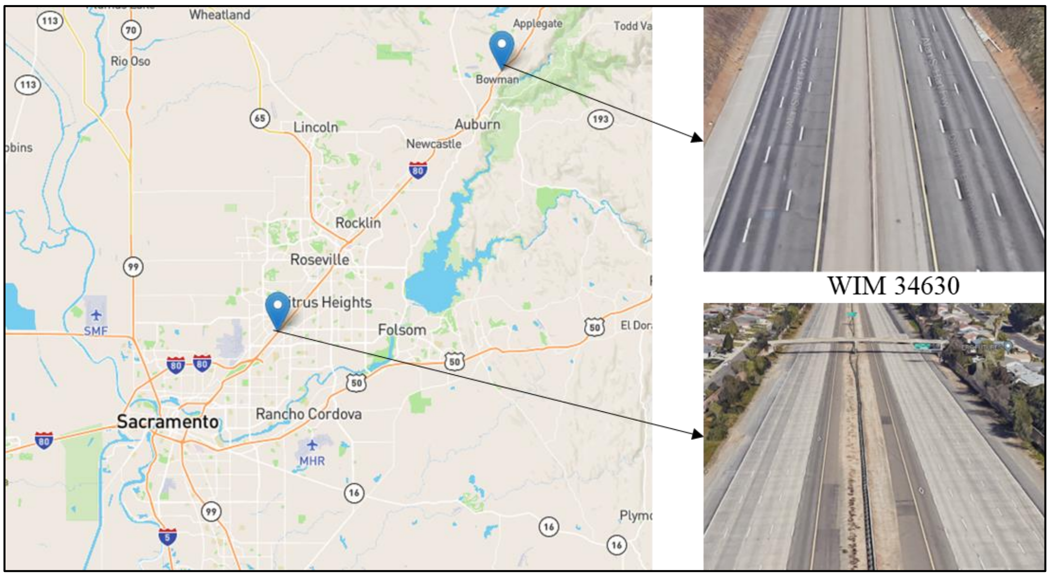

Figure 25. Location of WIM and LDS detector stations.

Results

Specification of parameters

As per the outlined methodology, it is essential to determine the average length of SV and LT for all approaches. The preliminary distribution of vehicle length was presented based on the three-month WIM data. As shown in **Figure 26**, two distinct modes can be observed, with the left mode corresponding to short vehicles and the right mode representing LT. However, it should be noted that the WIM system only measures the spacing between the vehicle's axles and may not necessarily record the whole length of the vehicle. Therefore, the distribution of actual vehicle lengths should be slightly shifted towards the right. By considering the vehicle head and tail, we choose 15 feet and 65 feet to be the average lengths of short vehicles and LT respectively. While a more proper value for two types of vehicles can reduce the error of estimation, there are many places where vehicle length is not readily available. When the proposed algorithm is implemented for these places, the average vehicle length of SV and LT can be determined by referring to the relevant local regulations about these vehicle types.

Besides the commonly used parameters, some method-specific parameters need to be carefully determined. Regarding method 1, to establish an exponential relationship between the occupancy of short vehicles and the observed occupancy of mixed vehicles, the parameter 'a' in Equation (45) is set to 0.58. This value is calculated based on the estimated time it takes for a typical short vehicle traveling at 60 mph to pass over a detector, which is 0.174 seconds or 0.58% of a 30-second interval. The parameter 'b' in Equation (45) reflects the typical traffic conditions that allow a short vehicle to drive at 60 mph consistently. The parameter 'b' is customized to each specific site as the degree of difficulty for a short vehicle to maintain a speed of 60 mph can vary depending on the location and characteristics of the roadway. As a result, the value of this parameter is selected based on the minimum estimation error for one day's training data. This ensures that the parameter accurately reflects the specific traffic conditions at each site and produces the most accurate estimates possible. Finally, 'b' is set to be 40 (%) for station 34630 and 22 (%) for station 34870. This makes sense as station 34870 is situated in urban areas where there is typically heavier traffic than station 34630 which is in rural areas. Turning to method 2, the additional parameters that need to be set are the lane-to-lane speed correlation. This study refers to the original paper (*173*) and applied the following values for the algorithm: $\beta(2,1) = 0.95$, $\beta(3,1) = 0.9$ and $\beta(4,1) = 0.85$. In relation to method 3, the standard deviation of the length of SV and LT are set at 2 and 5, respectively. Additionally, the length of the loop detector used in this method is 6 feet which is the same as the value applied in the original paper (*169*). In method 4, the speed limit v_{sl} is 70 mph. Waze speed was found to be noticeably different from traffic detectors speed conditional on traffic situations. As a result, this study adjusted the speed values based on the results of a prior evaluation study (*60*) to reduce the impact of bias on truck volume estimation. Specifically, the adjustments to the reported speeds are as follows: a 17.0% reduction was applied to speeds ranging from 0 to 45 mph, a 6.3% reduction was applied to speeds ranging from 45 to 55 mph, and a 14.6% increase was applied to speeds exceeding 55 mph. Further study is needed to clarify how much variance of Waze speed is acceptable for the proposed algorithm.

Estimation of truck volume

On most freeways that have three or more lanes, the left-most lane is typically designated as a lane for non-commercial vehicles only, prohibiting the access of trucks and other large vehicles. Although the truck-free lane regulations are in place, it is still possible to observe some trucks using the truck-free lane. Nevertheless, the overall volume of truck traffic in the truck-free lane is anticipated to be lower than in the other lanes. Hence, we compared the performance of methods on truck-free and truck-rich lanes. **Figure 27** and **Figure 28** show the hourly absolute error of different methods for WIM stations 34870 and 34630 separately. Notice that station 34870 has much less overall truck traffic than station 34630 (see **Table 10**). For each figure, the upper plot shows the truck-free lane's results and the bottom plot shows the truck-rich lanes' results. The box plot highlights the variation of error, and the pink line exhibits the hourly truck percentage. Comparing **Figure 27** and **Figure 28**, several observations can be made:

For estimation of the truck-free lane, Method 1 (optimization, green box) and Method 4 (straightforward, pink box) tend to overestimate the truck for the afternoon peak hour (i.e., 15-19). The degree of overestimation varies across different stations, primarily attributed to the traffic volume at peak hours. Station 34870 is located in an urbanized area that experiences higher traffic than station 34630 which is in a rural area. Noticeably, only Method 4 appears to be a slight overestimation for station 34630.

For estimation of the truck-rich lanes, all methods tend to produce larger errors and more outliers for station 34870 than 34630. It is important to highlight that all the methods demonstrate superior estimation performance for nighttime truck traffic in comparison to daytime truck traffic. This suggests that our proposed methods (i.e., Method 1 and 4), as well as the methods found in the literature (Method 2 and 3), are effective when the volume of truck traffic is high. In this regard, Method 3 (dynamic estimation, yellow box) shows a smaller estimation error than other methods. Method 1, method 2, and the literature methods generated similar error patterns. However, when it comes to daytime, our proposed Method 1 and Method 4 yield higher average absolute error and greater variation in error than the methods found in the literature. However, regarding station 34630, Method 1 generated a comparably low average error and exhibited less variation in errors than the other methods, regardless of the time of day. The error pattern generated by Method 4 appears the difference between daytime and nighttime. Method 4 performs similarly to Method 3, and both generated higher error rates than Method 2 (lane-to-lane speed correlation, highlighted by the blue box). This suggests that Method 1 is the most robust when the volume of truck traffic is high, followed by Method 2, Method 4, and Method 3. Method 3 produced the highest error rates, primarily because it assumes that there are at least two intervals that have no truck presence in a short period. However, this assumption is unlikely to hold during times and at stations with high levels of truck traffic. Violating this assumption undoubtedly causes large errors.

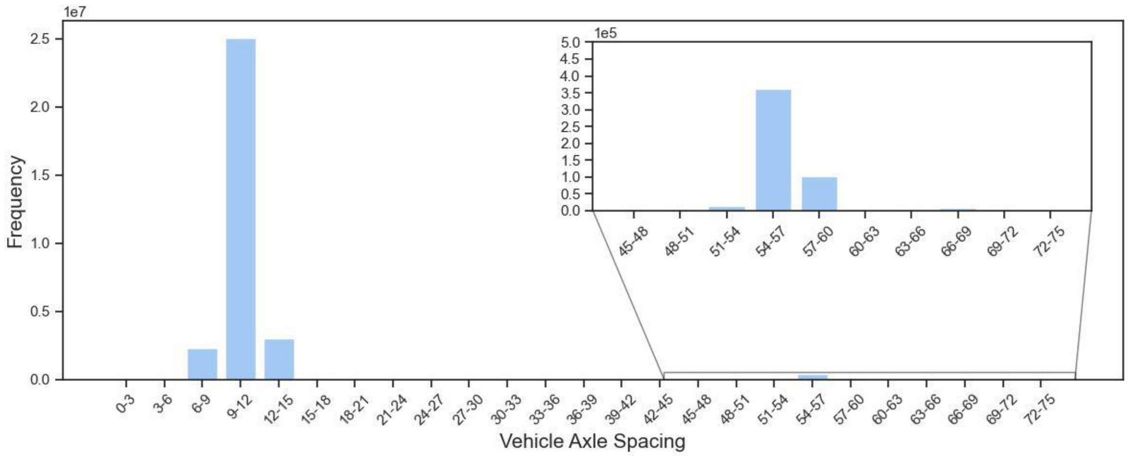

Figure 26. Histogram of vehicle axle spacing (feet)

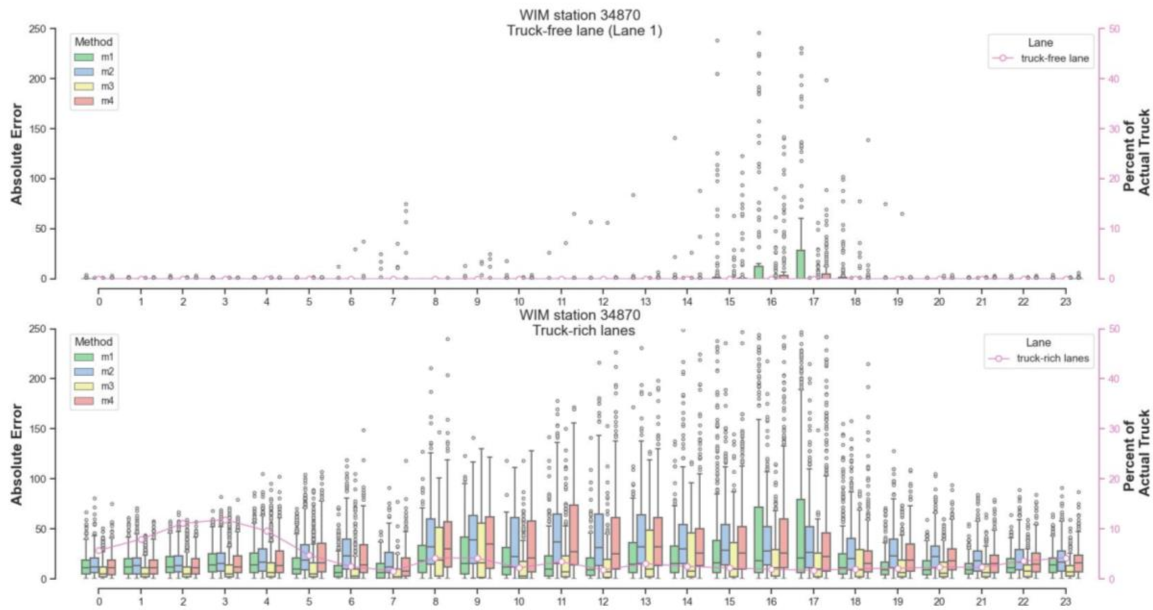

Figure 27. Hourly absolute error of WIM station 34870 (low truck traffic)

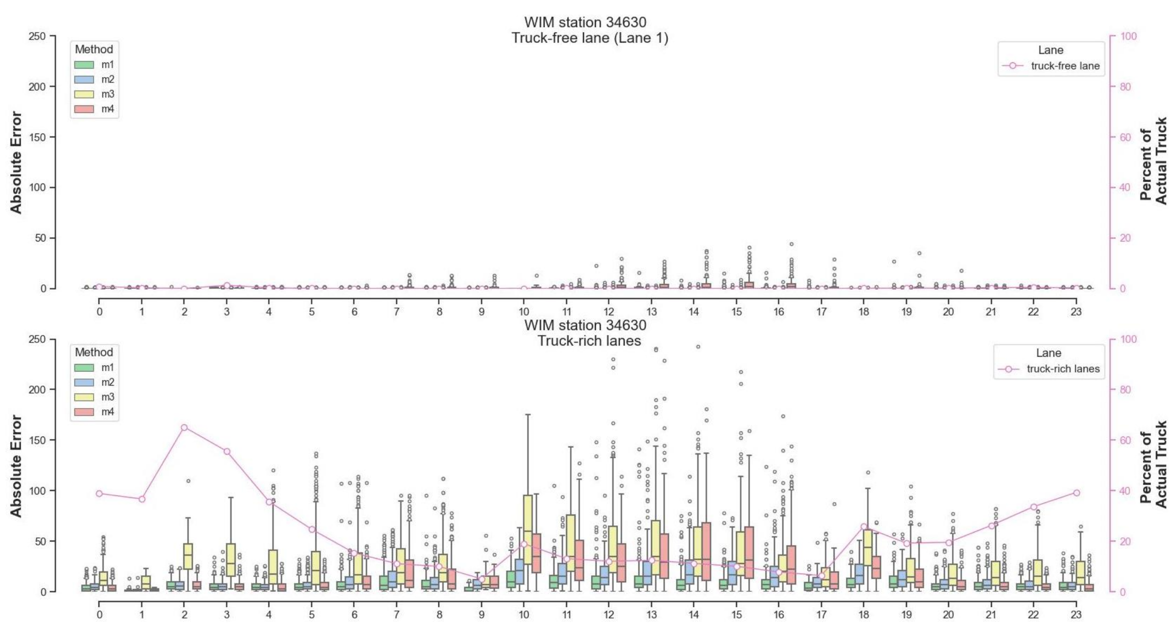

Figure 28. Hourly absolute error of WIM station 34630 (high truck traffic)

Table 11 and **Table 12** provide a summary of the absolute error on an hourly basis, classified according to peak and off-peak hours for WIM stations 34870 and 34630, respectively. Both tables reveal that peak hours' truck volume is much lower than off-peak hours. Regarding station 34870, the average error and variance during peak hours were found to be higher for the two proposed methods (Method 1 and 4) in comparison to the two literature methods (Method 2 and 3). In contrast, Method 1 demonstrates a considerable reduction in error when the percentage of trucks increases during off-peak hours. However, its performance is slightly inferior to Method 3 in this regard. Likewise, the reduction of error was observed for Method 4 in estimating off-peak hours truck traffic. The results show that Method 4 performs better than Method 2 regarding the average error, yet Method 4 yields a larger variance of error. During off-peak hours, the speed of traffic lanes can be closely matched, and adjusting the speed values using standard discount factors may negatively affect the accuracy of truck volume estimation. On the other hand, the larger variance of error produced by Method 4 may be attributed to the reduced Wazers' population during off-peak hours, especially for nighttime hours. Turning to station 34630, the truck proportion is increased for both peak and off-peak hours. Method 1 outperforms and generates the lowest average error and variance of error for both periods. Method 3 generates the largest error rates because the assumption of Method 3 is likely to be violated when truck traffic increases. Finally,

Table 13 shows the daily MAE for the study period. For station 34870, Method 3 outperforms, followed by Method 1, 4, and 2. For station 34630 Method 1 outperforms, followed by Method 2, 4, and 3. In the future, researchers could explore the possibility of combining different methods to enhance the accuracy of truck volume estimation. This is because the optimal estimation method tends to change with variations in the percentage of trucks.

Discussion

To calculate the total length of vehicles for a detection interval, the speed is typically needed in addition to the traffic volume and occupancy. As a result, the two methods described in the literature begin by estimating the speed for shorter vehicles, assuming different truck-free presence scenarios. After addressing the speed for beginning periods, then the following speed can be proportionally updated by incoming traffic occupancy and traffic volume because the vehicle speed is proportional to the inverse of occupancy. However, there are two limitations to this proportion idea. First, the assumption may not hold as the truck traffic increases. For the lane-to-lane speed correlation method, it may not be workable for two-lane freeways which is quite common in rural areas. Although the dynamic estimation method does not require a truck-free lane, the assumption that at least two intervals in a short period (e.g., 5 minutes) is barely possible for the areas with heavy truck traffic such as commercial or industrial zones. Second, the estimation result is prone to be correlated, and so is the error. It is the prominent issue of the proportion method. Both traffic volume and speed demonstrate autocorrelation. However, once the assumption is not satisfied, the error would be propagated and magnified forward. In addition to the limitations of proportion philosophy, another significant issue of existing methods is the fixed vehicle length, which is hard to accommodate the varying traffic status. Even though the dynamic estimation method considers the vehicle length

Table 11. The hourly absolute error of WIM station 34870 (low truck traffic).

Period	Method	Truck Pct.	Method 1	Method 2	Method 3	Method 4
Peak hours	Mean	2.38	34.02	35.04	25.01	35.72
	Std.	2.96	55.22	33.43	19.57	46.94
Off-peak hours	Mean	5.91	16.80	26.11	14.13	24.04
	Std.	9.78	18.85	26.63	20.63	30.21

*Note. a) Peak hours are defined as the time between 6-9 AM and 3-7 PM, while the remaining hours are off-peak hours. b). Truck Pct. is the percentage of trucks measured by each hour at peak or off-peak. c). Std. is the standard deviation.

Table 12. The hourly absolute error of WIM station 34630 (high truck traffic).

Period	Method	Truck Pct.	Method 1	Method 2	Method 3	Method 4
Peak hours	Mean	11.95	8.93	15.07	30.52	23.48
	Std.	11.64	10.61	14.96	27.84	25.86
Off-peak hours	Mean	26.70	8.40	12.02	30.72	16.92
	Std.	23.92	10.73	13.42	30.26	23.24

Table 13. Daily MAE of WIM stations.

WIM station	Statistics	Truck Pct.	Method 1	Method 2	Method 3	Method 4
34870	Mean	3.37	21.67	26.62	15.62	25.59
	Std.	4.02	16.98	16.69	16.03	17.49
34630	Mean	14.54	9.07	12.88	30.38	18.42
	Std.	11.23	6.79	8.14	22.31	12.73

distribution for assigning vehicle counts, the distribution itself is not linked to the speed. Hence, this type of model tends to overestimate the long trucks in peak hours. In comparison, the optimization method proposed in this study is free of truck-free assumptions. The optimization is performed for every individual interval. Hence, the estimation is independent of neighboring observations. Moreover, the optimization framework is compatible with errors arising from the assumed vehicle length, and the gross relation between speed and occupancy. The error, namely, the difference between observed and calculated total occupancy, is minimized by adjusting the vehicle length according to the speed. Therefore, short vehicles are prevented from being classified as long trucks when the vehicle speed is low (e.g., during peak hours).

It's undeniable that the accuracy of the total vehicle length calculation, based on the fundamental relationship between speed, length, and time, depends heavily on the accuracy of the speed measurement. While accurate speed estimation is crucial, it may not necessarily guarantee accurate vehicle classification. This is analogous to solving an equation with two variables, given total vehicle length (L) is known. For instance, the solutions of Equation (72) are not unique, given the constant length of short vehicles L_{sv} and long trucks L_{lt}. If L_{lt} is not connected to the vehicle speed, the number of long trucks is prone to be greater to match a larger total vehicle length in a congested period. In other words, a fraction of short vehicles is misclassified as long trucks. This study addressed this issue by allowing vehicle length to vary within a range concerning the vehicle speed (or occupancy). The upper bound of short vehicle length is virtually augmented proportional to the inverse of vehicle speed (or the occupancy). Therefore, the short vehicle is less likely to be classified as the long truck when the short vehicle occupies the detector for a while.

$$m \cdot L_{sv} + n \cdot L_{lt} = L \tag{72}$$

Many traditional detectors are not able to collect the speed and many external speed data sources are usually aggregated at a gross granularity. Obtaining accurate speed is barely possible. For instance, the crowdsourced speed exploited for method 4 is collected from probe vehicles. The speed is measured based on a fraction of road users and aggregated to a roadway section, without distinguishing the difference between lanes. The speed quality is likely to be affected by the penetration of probe vehicles. Hence, method 4 is not as sound as method 2 which applies the lane-to-lane speed correlation. On the other hand, with the aid of external speed, truck-free assumptions are no longer needed. Therefore, method 4 is better than method 3 (dynamic estimation) when truck traffic increases.

Conclusion

LT volume data are important for many purposes in transportation planning and economic development. During the early development of state transportation, single loop detectors were extensively implemented due to their cost-effectiveness and ease of installation and maintenance in comparison to other types of traffic detectors. However, single loop detectors are limited to collecting only traffic volume and occupancy data without the ability to distinguish vehicle types. Nowadays, many more “advanced” traffic detectors that are equipped with infrared, microwave, and magnetic techniques can directly identify LT, whereas they are not as widely available as single loop detectors. Therefore, enabling single loops to deliver long truck volume data is very practical and beneficial for the development of intelligent transportation systems.

In this chapter, we developed two models to estimate the long truck traffic and compared their performance with two literature methods. The first model innovatively formulates the truck estimation problem as an optimization problem. It modifies the vehicle lengths as a function of speed so that it can accommodate different traffic statuses. This method only used the traffic volume and occupancy data. If external speed is available in some cases, the truck estimation could be more straightforward, which is method 4 implemented in this study. With the speed information, the total vehicle length of each interval can be solved, and truck volume can be assigned based on the assumed vehicle length. Likewise, we used the ratio of the speed limit to real-time speed to adjust the average length of short vehicles to prevent them from being misclassified as large trucks. This method used the traffic volume, occupancy from loop detectors, and speed from Waze.

The experiment sites were intentionally selected to reflect the different roadway characteristics, with one WIM station in the urban area and one in the rural area. Three months of detector data obtained from these two stations were used to examine the performance of four methods. Several important findings can be concluded:

a. All methods are susceptible to low truck traffic. They tend to overestimate the truck traffic for truck-rich lanes of station 34870. Among them, the optimization method and straightforward method are more volatile than the two literature methods under low truck traffic contexts.
b. Similarly, all methods achieve higher error rates for daytime peak hours than off-peak hours due to relatively low truck proportion.
c. Turning to WIM station 34630 which has a higher truck proportion, the optimization method outperforms for all times of the day. It produces the smallest average error and variance of error.
d. Crowdsourced Waze speed shows the capability of estimating truck traffic when the truck proportion is high. The speed-based straightforward method produces a lower average daily MAE than dynamic estimation (method 3). Since Waze speed can be collected where there is Wazers' presence, it is very flexible to implement this method in other locations.

In sum, the truck proportion is found to be a key element influencing the estimation results for different methods, which also corroborates the study that was done early (*178*). The future study should reveal the minimum truck percentage that is needed to make optimization methods and straightforward methods warranted. It is also worth fusing different methods to accommodate complex traffic characteristics and to achieve higher estimation accuracy.

CONCLUSION

This dissertation compiled a series of studies to explore the use of crowdsourced data for smart transportation management and infrastructure maintenance. Four studies were conducted to discover pavement potholes and identify pothole hotspots, untangle the relationships between flat tire incidents and potholes, estimate the incident recovery time for complete incident time to normal traffic flow, and monitor truck traffic along with conventional loop detectors data, separately.

First, we exploited crowdsourced pothole reports for pavement evaluation. The study introduces two use cases for utilizing pothole reports - one for identifying pothole hotspots, and the other for discovering potholes. Some of Waze's pothole reports might be redundant and fake which is a common issue of crowdsourced data. Hence, the proposed two models are all density-based, which can accommodate duplicated and noisy reports. The first model, namely, the spatiotemporal kernel density model highlights the location and lifespan of pothole hotspots. It is found that the roads near the center of the city appear to have denser pothole clusters but with shorter lifespans, compared to rural areas. This finding may reflect the effectiveness and timeliness of pavement repair work. The second model, that is spatiotemporal DBSCAN clustered the pothole reports to identify the potholes. Through the clustering results, we found two types of potholes: single spot and pothole zones. This finding can assist in deciding between spot patching or road resurfacing. Moreover, Waze reports were found to be much sooner than the pothole repair work request. The study also found that Waze reports can contribute to 6.6% to 36.3% of potholes out of the PMS system for Nashville city. In sum, it is promising to apply Waze pothole reports to facilitate pavement management and maintenance.

Second, the study aims to untangle the associations and causation between flat tire frequencies and roadway potholes. The flat tire incidents are extracted from the incident operation logs, especially those related to disabled vehicles. Moreover, the Waze data is especially significant as it offers information on pavement conditions throughout the year, allowing for the possibility of making causal inferences. Considering that pothole occurrence varies spatiotemporally, a geographically and temporally weighted Poisson regression model was developed to understand how flat tire frequencies are associated with the severity of potholes. The results found that pothole severity is positively correlated with flat tire frequencies, with one unit increase in normalized pothole reports associating with 7.2% more flat tire incidents. Moreover, the correlation between potholes in the central area of the city and the frequency of flat tires appears to be stronger compared to rural areas, which could be attributed to the higher traffic volume in the city. From a temporal perspective, pothole has a comparatively large association with flat tire incidents during winter months (e.g., December, January, and February) in which potholes outbreak. Furthermore, a fixed effect Poisson Regression model is established to infer the causality between potholes and flat tire frequencies. It substantiates that more potholes can significantly result in more flat tire frequencies. The findings should serve as a warning to the pavement maintenance crews to repair pavement distress promptly and efficiently to avoid further damage to vehicles.

Third, the study exploited Waze jam and accident reports to estimate the crash recovery time to fulfill the total crash time to normal traffic flow (NFT). Different from the incident clearance time which can be monitored and recorded by responders, recovery time is barely available without the follow-up of responders. However, Waze reports can fill out this blank. The recovery time estimated is interval censored (e.g., the end time of crash impact is known only to an interval) because Waze users may not exactly capture the time boundary when traffic returns to normal, thereby leading crash time to normal traffic flow interval censored. Accordingly, a geographically and temporally weighted proportional hazard model is developed to address the spatiotemporally varying effects of covariates of crash time to normal traffic flow. The results found that HELP truck, Dynamic Message Signs, traffic demand, and in-transit time of first responders significantly correlate with crash NFT duration, and their association varies across the time of day and over the space of the study area. This study encourages the incident responders to deploy dynamic message signs after the incident occurs because it is found that disseminating crash information is associated with shorter total crash NFT duration. The proposed model can also be applied to other types of incidents such as disabled vehicles, road closures, and so on.

Fourth, the study proposed two methods to make single loop detectors capable of detecting truck traffic, given traffic volume, occupancy from detectors, and speed information from external data sources. Along with existing studies, we targeted two types of vehicles: short vehicles and large trucks. The first method is an optimization method, it aims to minimize the difference between observed occupancy and calculated occupancy. The objective function is subject to various constraints on the total number of vehicles and the length of individual vehicles. One significant modification involves adjusting the length of vehicles based on their estimated speed, which is done to account for the overestimation of trucks during congested periods. The second method incorporates the Waze speed along with the traffic volume and occupancy. This method is straightforward as the vehicle length can be directly estimated with volume, occupancy, speed, and assumed vehicle length. Besides, we implement two literature methods as benchmarking. Three-month loop detector data and weigh-in-motion data from the California PeMS system were employed to test the model performances. The results show that all methods are susceptible to low truck traffic and literature methods seem to perform better than our proposed methods. However, when truck traffic increases, the proposed optimization method outperforms significantly, with relatively small mean absolute error and variance. Compared to literature methods, the proposed optimization method is more flexible and tackles the issue of overestimation during low-speed periods. Although the straightforward method that applies Waze speed is not the best model, it outperforms the dynamic estimation method. The use of crowdsourced speed is less effective than the lane-to-lane speed correlation method, primarily because Waze speed can be influenced by the number of users and does not differentiate between lanes.

This dissertation demonstrates that crowdsourced data has significant potential to supplement or substitute conventional methods of gathering data and feedback from many Waze users, without imposing any extra financial or label costs.

In essence, crowdsourcing is not only an innovation but also a philosophy in data collection and problem solutions. Despite the advancement in various techniques applied in transportation data collection, crowdsourcing would never be altered due to many merits such as low-cost, extensive geographical coverage, and real-time feed. On the contrary, the efficacy of data collection can be amplified by implementing these advanced techniques in a crowdsourced manner. In the future development of transportation, crowdsourcing should be promoted to decrease the cost of data collection, fill out the conventional data collection blind spots, and facilitate real-time operation.

LIST OF REFERENCES

[1] Waze. *Waze Statistics and User Count (2023)*. https://expandedramblings.com/index.php/waze-statistics-facts/. Accessed 4/3/2023, 2023.

[2] ---. Under the Hood: Real-time ETA and How Waze Knows You're on the Fastest Route.In, *No. 2020*, 2020.

[3] VinZant, N. *Pothole Damage Costs US Drivers $3 Billion a Year*. https://quotewizard.com/news/posts/pothole-damage-costs-us-drivers-3-billion-dollars-per-year. Accessed 02-06, 2022.

[4] Praharaj, S., F. T. Zahura, T. D. Chen, Y. Shen, L. Zeng, and J. L. Goodall. Assessing trustworthiness of crowdsourced flood incident reports using Waze data: a Norfolk, Virginia case study. *Transportation research record,* Vol. 2675, No. 12, 2021, pp. 650-662 %@ 0361-1981.

[5] AAA. *Pothole damage.* American Automobile Association. http://publicaffairsresources.aaa.biz/wp-content/uploads/2016/02/Pothole-Fact-Sheet.pdf. Accessed 02-06, 2022.

[6] TDOT. *TDOT Launches Plan for Pothole Repair*. https://www.tn.gov/tdot/news/2022/1/21/tdot-launches-plan-for-pothole-repair.html. Accessed Feb, 12, 2022.

[7] Huang, B., and X. Jia. Quality Improvement and Application of TDOT Pavement Management Systems (PMS) Data.In, 2015.

[8] Waze. *Connected Citizens*. https://web-assets.waze.com/partners/ccp/WAZE-CCP-Factsheet.pdf. Accessed Feb 12, 2022.

[9] Hoseinzadeh, N., Y. Liu, L. D. Han, C. Brakewood, and A. Mohammadnazar. Quality of location-based crowdsourced speed data on surface streets: A case study of Waze and Bluetooth speed data in Sevierville, TN. *Computers, Environment and Urban Systems,* Vol. 83, 2020.

[10] Liu, Y., Z. Zhang, L. D. Han, and C. Brakewood. Automatic traffic queue-end identification using location-based Waze user reports. *Transportation research record,* Vol. 2675, No. 10, 2021, pp. 895-906 %@ 0361-1981.

[11] Li, X., B. Dadashova, S. Yu, and Z. Zhang. Rethinking highway safety analysis by leveraging crowdsourced waze data. *Sustainability,* Vol. 12, No. 23, 2020, p. 10127.

[12] Goodall, N., and E. Lee. Comparison of Waze crash and disabled vehicle records with video ground truth. *Transportation research interdisciplinary perspectives,* Vol. 1, 2019, pp. 100019 %@ 102590-101982.

[13] Liu, Y. Real-time Traffic State Assessment using Multi-source Data. 2020.

[14] Safaei Moghadam, A., B. E. Minsker, and D. G. Tarboton. Leveraging crowdsourced traffic data to detect the risk of urban pluvial flash flooding along streets.In, *No. 2019*, 2019. pp. H12B-02.

[15] Gu, Y., H. Zhang, C. Brakewood, and L. D. Han. WAZE Data Reporting.In, Tennessee. Department of Transportation, 2022.

[16] Roberts, R., G. Giancontieri, L. Inzerillo, and G. Di Mino. Towards low-cost pavement condition health monitoring and analysis using deep learning. *Applied Sciences*, Vol. 10, No. 1, 2020, pp. 319 %@ 2076-3417.

[17] Karimzadeh, A., O. Shoghli, S. Sabeti, and H. Tabkhi. Multi-Asset Defect Hotspot Prediction for Highway Maintenance Management: A Risk-Based Machine Learning Approach. *Sustainability,* Vol. 14, No. 9, 2022.
[18] Ann Myers, L., R. Roque, B. E. Ruth, and C. Drakos. Measurement of contact stresses for different truck tire types to evaluate their influence on near-surface cracking and rutting. *Transportation Research Record,* Vol. 1655, No. 1, 1999, pp. 175-184 %@ 0361-1981.
[19] Zhang, K., and Z. Wang. LTPP data-based investigation on asphalt pavement performance using geospatial hot spot analysis and decision tree models. *International Journal of Transportation Science and Technology*, 2022.
[20] Ali, H. A., and A. Lopez. Statistical analyses of temperature and moisture effects on pavement structural properties based on seasonal monitoring data. *Transportation Research Record,* Vol. 1540, No. 1, 1996, pp. 48-55 %@ 0361-1981.
[21] Yu, B., and X. Yu. Vibration-based system for pavement condition evaluation.In *Applications of advanced technology in transportation*, 2006. pp. 183-189.
[22] Lekshmipathy, J., S. Velayudhan, and S. Mathew. Effect of combining algorithms in smartphone based pothole detection. *International Journal of Pavement Research and Technology,* Vol. 14, No. 1, 2021, pp. 63-72 %@ 1997-1400.
[23] Bhatt, U., S. Mani, E. Xi, and J. Z. Kolter. Intelligent pothole detection and road condition assessment. *arXiv preprint arXiv:1710.02595*, 2017.
[24] Egaji, O. A., G. Evans, M. G. Griffiths, and G. Islas. Real-time machine learning-based approach for pothole detection. *Expert Systems with Applications,* Vol. 184, 2021, pp. 115562 %@ 110957-114174.
[25] Chang, K. T., J. R. Chang, and J. K. Liu. Detection of pavement distresses using 3D laser scanning technology.In *Computing in civil engineering (2005)*, 2005. pp. 1-11.
[26] Zhang, Z., X. Ai, C. K. Chan, and N. Dahnoun. An efficient algorithm for pothole detection using stereo vision.In, IEEE, 2014. pp. 564-568 %@ 1479928933.
[27] Jog, G. M., C. Koch, M. Golparvar-Fard, and I. Brilakis. Pothole properties measurement through visual 2D recognition and 3D reconstruction.In, 2012. pp. 553-560.
[28] Moazzam, I., K. Kamal, S. Mathavan, S. Usman, and M. Rahman. Metrology and visualization of potholes using the microsoft kinect sensor.In, IEEE, 2013. pp. 1284-1291 %@ 147992914X.
[29] Buza, E., S. Omanovic, and A. Huseinovic. Pothole detection with image processing and spectral clustering.In, *No. 810*, 2013. p. 4853.
[30] Huidrom, L., L. K. Das, and S. K. Sud. Method for automated assessment of potholes, cracks and patches from road surface video clips. *Procedia-Social and Behavioral Sciences,* Vol. 104, 2013, pp. 312-321 %@ 1877-0428.
[31] Koch, C., and I. Brilakis. Pothole detection in asphalt pavement images. *Advanced Engineering Informatics*, Vol. 25, No. 3, 2011, pp. 507-515 %@ 1474-0346.
[32] Pereira, V., S. Tamura, S. Hayamizu, and H. Fukai. A deep learning-based approach for road pothole detection in timor leste.In, IEEE, 2018. pp. 279-284 %@ 153864522X.
[33] Ukhwah, E. N., E. M. Yuniarno, and Y. K. Suprapto. Asphalt pavement pothole detection using deep learning method based on YOLO neural network.In, IEEE, 2019. pp. 35-40 %@ 1728137497.

[34] Ye, W., W. Jiang, Z. Tong, D. Yuan, and J. Xiao. Convolutional neural network for pothole detection in asphalt pavement. *Road materials and pavement design,* Vol. 22, No. 1, 2021, pp. 42-58 %@ 1468-0629.
[35] Liu, J., X. Yang, S. Lau, X. Wang, S. Luo, V. C. S. Lee, and L. Ding. Automated pavement crack detection and segmentation based on twoâ€• step convolutional neural network. *Computerâ€• Aided Civil and Infrastructure Engineering,* Vol. 35, No. 11, 2020, pp. 1291-1305 %@ 1093-9687.
[36] Zhang, A. A., K. C. P. Wang, Y. Liu, Y. Zhan, G. Yang, G. Wang, E. Yang, H. Zhang, Z. Dong, and A. He. Intelligent pixel-level detection of multiple distresses and surface design features on asphalt pavements. *Computerâ€• Aided Civil and Infrastructure Engineering,* Vol. 37, No. 13, 2022, pp. 1654-1673 %@ 1093-9687.
[37] Maeda, H., T. Kashiyama, Y. Sekimoto, T. Seto, and H. Omata. Generative adversarial network for road damage detection. *Computer-Aided Civil and Infrastructure Engineering,* Vol. 36, No. 1, 2021, pp. 47-60 %@ 1467-8667.
[38] Patra, S., A. I. Middya, and S. Roy. PotSpot: Participatory sensing based monitoring system for pothole detection using deep learning. *Multimedia Tools and Applications,* Vol. 80, No. 16, 2021, pp. 25171-25195 %@ 21573-27721.
[39] Kulkarni, A., N. Mhalgi, S. Gurnani, and N. Giri. Pothole detection system using machine learning on Android. *International Journal of Emerging Technology and Advanced Engineering,* Vol. 4, No. 7, 2014, pp. 360-364.
[40] Sander, J. r., M. Ester, H.-P. Kriegel, and X. Xu. Density-based clustering in spatial databases: The algorithm gdbscan and its applications. *Data mining and knowledge discovery,* Vol. 2, No. 2, 1998, pp. 169-194 %@ 1573-1756X.
[41] Hu, Y., F. Wang, C. Guin, and H. Zhu. A spatio-temporal kernel density estimation framework for predictive crime hotspot mapping and evaluation. *Applied geography,* Vol. 99, 2018, pp. 89-97 %@ 0143-6228.
[42] Nakaya, T., and K. Yano. Visualising crime clusters in a spaceâ€• time cube: An exploratory dataâ€□analysis approach using spaceâ€□time kernel density estimation and scan statistics. *Transactions in GIS,* Vol. 14, No. 3, 2010, pp. 223-239 %@ 1361-1682.
[43] Li, Y., M. Abdel-Aty, J. Yuan, Z. Cheng, and J. Lu. Analyzing traffic violation behavior at urban intersections: A spatio-temporal kernel density estimation approach using automated enforcement system data. *Accident Analysis & Prevention,* Vol. 141, 2020, pp. 105509 %@ 100001-104575.
[44] Romano, B., and Z. Jiang. Visualizing traffic accident hotspots based on spatial-temporal network kernel density estimation.In, 2017. pp. 1-4.
[45] Robert, P. W. On the choice of smoothing parameters for Parzen estimators of probability density functions. *IEEE Trans. Comput,* Vol. 25, No. 11, 1976, pp. 1175-1179.
[46] Hart, T., and P. Zandbergen. Kernel density estimation and hotspot mapping: Examining the influence of interpolation method, grid cell size, and bandwidth on crime forecasting. *Policing: An International Journal of Police Strategies & Management,* Vol. 37, No. 2, 2014, pp. 305-323 %@ 1363-1951X.
[47] Birant, D., and A. Kut. ST-DBSCAN: An algorithm for clustering spatial–temporal data. *Data & Knowledge Engineering,* Vol. 60, No. 1, 2007, pp. 208-221.

[48] Zhang, Z., Y. Liu, L. D. Han, and P. B. Freeze. Secondary crash identification using crowdsourced Waze user reports. *Transportation research record*, Vol. 2675, No. 10, 2021, pp. 853-862 %@ 0361-1981.
[49] Amin-Naseri, M. Adopting and incorporating crowdsourced traffic data in advanced transportation management systems.In, Iowa State University, 2018.
[50] Zhang, Y., L. D. Han, and H. Kim. Dijkstras-DBSCAN: Fast, Accurate, and Routable Density Based Clustering of Traffic Incidents on Large Road Network. *Transportation research record*, Vol. 2672, No. 45, 2018, pp. 265-273 %@ 0361-1981.
[51] Schubert, E., J. r. Sander, M. Ester, H. P. Kriegel, and X. Xu. DBSCAN revisited, revisited: why and how you should (still) use DBSCAN. *ACM Transactions on Database Systems (TODS)*, Vol. 42, No. 3, 2017, pp. 1-21 %@ 0362-5915.
[52] Hinneburg, A., and H.-H. Gabriel. Denclue 2.0: Fast clustering based on kernel density estimation.In, Springer, 2007. pp. 70-80.
[53] Wang, B., and X. Wang. Bandwidth selection for weighted kernel density estimation. *arXiv preprint arXiv:0709.1616*, 2007.
[54] Xu, L., M.-P. Kwan, S. McLafferty, and S. Wang. Predicting demand for 311 non-emergency municipal services: An adaptive space-time kernel approach. *Applied geography*, Vol. 89, 2017, pp. 133-141 %@ 0143-6228.
[55] Amin-Naseri, M., P. Chakraborty, A. Sharma, S. B. Gilbert, and M. Hong. Evaluating the reliability, coverage, and added value of crowdsourced traffic incident reports from Waze. *Transportation Research Record*, Vol. 2672, No. 43, 2018, pp. 34-43 %@ 0361-1981.
[56] Di Martino, F., and S. Sessa. The extended fuzzy C-means algorithm for hotspots in spatio-temporal GIS. *Expert Systems with Applications*, Vol. 38, No. 9, 2011, pp. 11829-11836 %@ 10957-14174.
[57] Rahman, M. M., M. M. Uddin, and S. L. Gassman. Pavement performance evaluation models for South Carolina. *KSCE Journal of Civil Engineering*, Vol. 21, No. 7, 2017, pp. 2695-2706 %@ 1976-3808.
[58] Mulyono, A. T., D. Parikesit, M. Antameng, and R. Rahim. Analysis of loss cost of road pavement distress due to overloading freight transportation.In, Eastern Asia Society for Transportation Studies, 2009. pp. 139-139.
[59] Ahn, S., S. Kandala, J. Uzan, and M. El-Basyouny. Impact of traffic data on the pavement distress predictions using the mechanistic empirical pavement design guide. *Road Materials and Pavement Design*, Vol. 12, No. 1, 2011, pp. 195-216 %@ 1468-0629.
[60] Zhang, Z., L. D. Han, and Y. Liu. Exploration and evaluation of crowdsourced probe-based Waze traffic speed. *Transportation letters*, Vol. 14, No. 5, 2022, pp. 546-554 %@ 1942-7867.
[61] GEICO. How Potholes Can Damage Your Car.In, *No. 2022*.
[62] Firestone. POTHOLE DAMAGE TO TIRES AND VEHICLES.In *POTHOLE DAMAGE TO TIRES AND VEHICLES, No. 2022*, 2016.
[63] Waze. *Waze for Cities*, Wazeopedia. https://wazeopedia.waze.com/wiki/USA/Waze_for_Cities. Accessed 07.04, 2022.

[64] Liu, Y., N. Hoseinzadeh, L. D. Han, and C. Brakewood. Evaluation of Crowdsourced Event Reports for Real Time IMplementationâ€"Spatial and Temporal Accuracy Analyses. 2019.
[65] Hoseinzadeh, N., Y. Gu, L. D. Han, C. Brakewood, and P. B. Freeze. Estimating freeway level-of-service using crowdsourced data.In*,* *No. 8*, MDPI, 2021. pp. 17 %@ 2227-9709.
[66] Li, X., B. Dadashova, S. Yu, and Z. Zhang. Rethinking highway safety analysis by leveraging crowdsourced waze data. *Sustainability,* Vol. 12, No. 23, 2020, pp. 10127 %@ 12071-11050.
[67] Yang, C., Y. Tsai, and Z. Wang. Algorithm for spatial clustering of pavement segments. *Computerâ€• Aided Civil and Infrastructure Engineering,* Vol. 24, No. 2, 2009, pp. 93-108 %@ 1093-9687.
[68] Wang, W., S. Qiu, S. Wang, P. Wang, and J. Zhang. Investigation of seasonal variations of Beijing pavement condition data using unevenly spaced dynamic panel data model. *International Journal of Pavement Engineering,* Vol. 19, No. 9, 2018, pp. 851-856 %@ 1029-8436.
[69] Zang, L., Y. Cai, B. Wang, R. Yin, F. Lin, and P. Hang. Optimization design of heat dissipation structure of inserts supporting run-flat tire. *Proceedings of the Institution of Mechanical Engineers, Part D: Journal of Automobile Engineering,* Vol. 233, No. 14, 2019, pp. 3746-3757 %@ 0954-4070.
[70] Sathishkumar, P., R. Wang, L. Yang, and J. Thiyagarajan. Trajectory control for tire burst vehicle using the standalone and roll interconnected active suspensions with safety-comfort control strategy. *Mechanical Systems and Signal Processing,* Vol. 142, 2020, pp. 106776 %@ 100888-103270.
[71] Anastasopoulos, P., and F. L. Mannering. A note on modeling vehicle accident frequencies with random-parameters count models. *Accid Anal Prev,* Vol. 41, No. 1, 2009, pp. 153-159.
[72] Al-Masaeid, H. R. Impact of pavement condition on rural road accidents. *Canadian Journal of Civil Engineering,* Vol. 24, No. 4, 1997, pp. 523-531 %@ 0315-1468.
[73] Zeng, H., M. D. Fontaine, and B. L. Smith. Estimation of the Safety Effect of Pavement Condition on Rural, Two-Lane Highways. *Transportation Research Record: Journal of the Transportation Research Board,* Vol. 2435, No. 1, 2014, pp. 45-52.
[74] Kaplan, S., and C. G. Prato. Impact of BAC limit reduction on different population segments: a Poisson fixed effect analysis. *Accident Analysis & Prevention,* Vol. 39, No. 6, 2007, pp. 1146-1154 %@ 0001-4575.
[75] Joshua, S. C., and N. J. Garber. Estimating truck accident rate and involvements using linear and Poisson regression models. *Transportation planning and Technology,* Vol. 15, No. 1, 1990, pp. 41-58 %@ 0308-1060.
[76] Miaou, S.-P., P. S. Hu, T. Wright, A. K. Rathi, and S. C. Davis. Relationship between truck accidents and highway geometric design: a Poisson regression approach. *Transportation Research Record,* No. 1376 %@ 0309054176, 1992.
[77] Michener, R., and C. Tighe. A Poisson regression model of highway fatalities. *The American Economic Review,* Vol. 82, No. 2, 1992, pp. 452-456 %@ 0002-8282.

[78] Farmer, C. M. Relationship of traffic fatality rates to maximum state speed limits. *Traffic injury prevention,* Vol. 18, No. 4, 2017, pp. 375-380 %@ 1538-9588.
[79] Li, Z., W. Wang, P. Liu, J. M. Bigham, and D. R. Ragland. Using geographically weighted Poisson regression for county-level crash modeling in California. *Safety science,* Vol. 58, 2013, pp. 89-97 %@ 0925-7535.
[80] Xu, P., and H. Huang. Modeling crash spatial heterogeneity: Random parameter versus geographically weighting. *Accident Analysis & Prevention,* Vol. 75, 2015, pp. 16-25 %@ 0001-4575.
[81] Arvin, R., M. Kamrani, and A. J. Khattak. How instantaneous driving behavior contributes to crashes at intersections: extracting useful information from connected vehicle message data. *Accident Analysis & Prevention,* Vol. 127, 2019, pp. 118-133 %@ 0001-4575.
[82] Mohammadnazar, A., I. Mahdinia, N. Ahmad, A. J. Khattak, and J. Liu. Understanding how relationships between crash frequency and correlates vary for multilane rural highways: Estimating geographically and temporally weighted regression models. *Accident Analysis & Prevention,* Vol. 157, 2021, pp. 106146 %@ 100001-104575.
[83] Finkel, S. E. *Causal analysis with panel data*. Sage, 1995.
[84] Imbens, G. W., and D. B. Rubin. *Causal inference in statistics, social, and biomedical sciences*. Cambridge University Press, 2015.
[85] Oppewal, H. Concept of causality and conditions for causality. *Wiley International Encyclopedia of Marketing*, 2010.
[86] Glass, G. V. Analysis of data on the Connecticut speeding crackdown as a time-series quasi-experiment. *Law and Society Review*, 1968, pp. 55-76 %@ 0023-9216.
[87] Li, H., D. J. Graham, and A. Majumdar. The effects of congestion charging on road traffic casualties: A causal analysis using difference-in-difference estimation. *Accident Analysis & Prevention,* Vol. 49, 2012, pp. 366-377 %@ 0001-4575.
[88] De Chaisemartin, C. m., and X. d'Haultfoeuille. Two-way fixed effects estimators with heterogeneous treatment effects. *American Economic Review,* Vol. 110, No. 9, 2020, pp. 2964-2996 %@ 0002-8282.
[89] Wagenaar, A. C., D. M. Murray, and T. L. Toomey. Communities Mobilizing for Change on Alcohol (CMCA): Effects of a randomized trial on arrests and traffic crashes. *Addiction,* Vol. 95, No. 2, 2000, pp. 209-217 %@ 0965-2140.
[90] L Morgan, S. *Handbook of causal analysis for social research*. Springer, 2007.
[91] Huang, B., B. Wu, and M. Barry. Geographically and temporally weighted regression for modeling spatio-temporal variation in house prices. *International journal of geographical information science,* Vol. 24, No. 3, 2010, pp. 383-401 %@ 1365-8816.
[92] Liu, J., A. Hainen, X. Li, Q. Nie, and S. Nambisan. Pedestrian injury severity in motor vehicle crashes: an integrated spatio-temporal modeling approach. *Accident Analysis & Prevention,* Vol. 132, 2019, pp. 105272 %@ 100001-104575.
[93] Ma, X., J. Zhang, C. Ding, and Y. Wang. A geographically and temporally weighted regression model to explore the spatiotemporal influence of built environment on transit ridership. *Computers, Environment and Urban Systems,* Vol. 70, 2018, pp. 113-124 %@ 0198-9715.

[94] Brewer, M. J., A. Butler, and S. L. Cooksley. The relative performance of AIC, AICC and BIC in the presence of unobserved heterogeneity. *Methods in Ecology and Evolution*, Vol. 7, No. 6, 2016, pp. 679-692 %@ 2041-2210X.
[95] Hausman, J. A., B. H. Hall, and Z. Griliches. Econometric models for count data with an application to the patents-R&D relationship.In, national bureau of economic research Cambridge, Mass., USA, 1984.
[96] Halaby, C. N. Panel models in sociological research: Theory into practice. *Annual review of sociology*, 2004, pp. 507-544 %@ 0360-0572.
[97] Wooldridge, J. M. *Econometric analysis of cross section and panel data*. MIT press, 2010.
[98] Tippetts, A. S., R. B. Voas, J. C. Fell, and J. L. Nichols. A meta-analysis of. 08 BAC laws in 19 jurisdictions in the United States. *Accident Analysis & Prevention,* Vol. 37, No. 1, 2005, pp. 149-161 %@ 0001-4575.
[99] Allison, P. D., and R. P. Waterman. Fixed effects negative binomial regression models. *Sociological methodology*, Vol. 32, No. 1, 2002, pp. 247-265 %@ 0081-1750.
[100] Cavanaugh, J. E. Unifying the derivations for the Akaike and corrected Akaike information criteria. *Statistics & Probability Letters,* Vol. 33, No. 2, 1997, pp. 201-208 %@ 0167-7152.
[101] Cameron, A. C., and F. A. G. Windmeijer. R-squared measures for count data regression models with applications to health-care utilization. *Journal of Business & Economic Statistics*, Vol. 14, No. 2, 1996, pp. 209-220 %@ 0735-0015.
[102] *6 Flat Tire Causes and How to Prevent Them*, Desjardins Insurance. https://www.desjardinsgeneralinsurance.com/blog/-/6-flat-tire-causes-and-how-to-prevent-them. Accessed 07.04, 2022.
[103] Abatzoglou, J. T. Development of gridded surface meteorological data for ecological applications and modelling. *International Journal of Climatology,* Vol. 33, No. 1, 2013, pp. 121-131 %@ 0899-8418.
[104] Adlinge, S. S., and A. K. Gupta. Pavement deterioration and its causes. *International Journal of Innovative Research and Development,* Vol. 2, No. 4, 2013, pp. 437-450.
[105] Miles, J. Tolerance and variance inflation factor. *Wiley statsref: statistics reference online,* 2014.
[106] TDOT. *TDOT Launches Plan for Pothole Repair*. https://www.tn.gov/tdot/news/2022/1/21/tdot-launches-plan-for-pothole-repair.html. Accessed March 5, 2023.
[107] Agarwal, D. K., A. E. Gelfand, and S. Citron-Pousty. Zero-inflated models with application to spatial count data. *Environmental and Ecological statistics,* Vol. 9, No. 4, 2002, pp. 341-355 %@ 1573-3009.
[108] Gu, Y., D. Liu, R. Arvin, A. J. Khattak, and L. D. Han. Predicting intersection crash frequency using connected vehicle data: A framework for geographical random forest. *Accident Analysis & Prevention,* Vol. 179, 2023, pp. 106880 %@ 100001-104575.
[109] *HCM 2010 : highway capacity manual*. Fifth edition. Washington, D.C. : Transportation Research Board, c2010-, 2010.

[110] FHWA. *Traffic Incident Management*.
https://ops.fhwa.dot.gov/aboutus/one_pagers/tim.htm. Accessed August 04, 2022.
[111] Administration, N. H. T. S. The Economic and Societal Impact of Motor Vehicle Crashes, 2019 (Revised).In, 2023.
[112] Smith, K., and B. L. Smith. Forecasting the clearance time of freeway accidents. 2002.
[113] Haule, H. J., T. Sando, R. Lentz, C.-H. Chuan, and P. Alluri. Evaluating the impact and clearance duration of freeway incidents. *International journal of transportation science and technology,* Vol. 8, No. 1, 2019, pp. 13-24 %@ 2046-0430.
[114] Chimba, D., B. Kutela, G. Ogletree, F. Horne, and M. Tugwell. Impact of abandoned and disabled vehicles on freeway incident duration. *Journal of Transportation Engineering,* Vol. 140, No. 3, 2014, pp. 04013013 %@ 04010733-04013947X.
[115] FHWA. *Traffic Incident Management (TIM) Performance Measurement: On the Road to Success.* Federal Highway Administration Office of Operations.
https://ops.fhwa.dot.gov/publications/fhwahop10009/tim_fsi.htm. Accessed October 3, 2022.
[116] Khattak, A. J., J. L. Schofer, and M.-H. Wang. A simple time sequential procedure for predicting freeway incident duration. *Journal of Intelligent Transportation Systems,* Vol. 2, No. 2, 1995, pp. 113-138 %@ 1065-5123.
[117] Zhan, C., A. Gan, and M. Hadi. Identifying secondary crashes and their contributing factors. *Transportation research record,* Vol. 2102, No. 1, 2009, pp. 68-75 %@ 0361-1981.
[118] Wang, J., W. Xie, B. Liu, and D. R. Ragland. Identification of freeway secondary accidents with traffic shock wave detected by loop detectors. *Safety science,* Vol. 87, 2016, pp. 195-201 %@ 0925-7535.
[119] Zeng, X., and P. Songchitruksa. Empirical method for estimating traffic incident recovery time. *Transportation research record,* Vol. 2178, No. 1, 2010, pp. 119-127 %@ 0361-1981.
[120] Jeihani, M., P. James, A. A. Saka, and A. Ardeshiri. Traffic recovery time estimation under different flow regimes in traffic simulation. *Journal of Traffic and Transportation Engineering (English Edition),* Vol. 2, No. 5, 2015, pp. 291-300 %@ 2095-7564.
[121] Hojati, A. T., L. Ferreira, S. Washington, P. Charles, and A. Shobeirinejad. Modelling total duration of traffic incidents including incident detection and recovery time. *Accident Analysis & Prevention,* Vol. 71, 2014, pp. 296-305 %@ 0001-4575.
[122] Islam, N., E. K. Adanu, A. M. Hainen, S. Burdette, R. Smith, and S. Jones. A comparative analysis of freeway crash incident clearance time using random parameter and latent class hazard-based duration model. *Accident Analysis & Prevention,* Vol. 160, 2021, pp. 106303 %@ 100001-104575.
[123] Chand, S., Z. Li, A. Alsultan, and V. V. Dixit. Comparing and Contrasting the Impacts of Macro-Level Factors on Crash Duration and Frequency. *International Journal of Environmental Research and Public Health,* Vol. 19, No. 9, 2022, pp. 5726 %@ 1660-4601.

[124] Patwary, A. L., and A. J. Khattak. Crash harm before and during the COVID-19 pandemic: Evidence for spatial heterogeneity in Tennessee. *Accident Analysis & Prevention,* Vol. 183, 2023, pp. 106988 %@ 100001-104575.
[125] Zhou, H., and Z. Tian. Modeling analysis of incident and roadway clearance time. *Procedia-social and behavioral sciences,* Vol. 43, 2012, pp. 349-355 %@ 1877-0428.
[126] HCM2010. Highway Capacity Manual. 5th ed. *Transportation Research Board*, 2010.
[127] Nam, D., and F. Mannering. An exploratory hazard-based analysis of highway incident duration. *Transportation Research Part A: Policy and Practice,* Vol. 34, No. 2, 2000, pp. 85-102 %@ 0965-8564.
[128] Li, X., J. Liu, A. Khattak, and S. Nambisan. Sequential prediction for large-scale traffic incident duration: application and comparison of survival models. *Transportation research record,* Vol. 2674, No. 1, 2020, pp. 79-93 %@ 0361-1981.
[129] Junhua, W., C. Haozhe, and Q. Shi. Estimating freeway incident duration using accelerated failure time modeling. *Safety science,* Vol. 54, 2013, pp. 43-50 %@ 0925-7535.
[130] Zhang, Z., J. Liu, X. Li, and A. J. Khattak. Do Larger Sample Sizes Increase the Reliability of Traffic Incident Duration Models? A Case Study of East Tennessee Incidents. *Transportation research record,* Vol. 2675, No. 6, 2021, pp. 265-280.
[131] Park, H., A. Haghani, and X. Zhang. Interpretation of Bayesian neural networks for predicting the duration of detected incidents. *Journal of Intelligent Transportation Systems,* Vol. 20, No. 4, 2016, pp. 385-400 %@ 1547-2450.
[132] Chung, Y. Development of an accident duration prediction model on the Korean Freeway Systems. *Accident Analysis & Prevention,* Vol. 42, No. 1, 2010, pp. 282-289 %@ 0001-4575.
[133] Margiotta, R. A., R. Dowling, and J. Paracha. Analysis, Modeling, and Simulation for Traffic Incident Management Applications.In, United States. Federal Highway Administration, 2012.
[134] Hojati, A. T., L. Ferreira, S. Washington, and P. Charles. Hazard based models for freeway traffic incident duration. *Accident Analysis & Prevention,* Vol. 52, 2013, pp. 171-181 %@ 0001-4575.
[135] Tirtha, S. D., S. Yasmin, and N. Eluru. Modeling of incident type and incident duration using data from multiple years. *Analytic Methods in Accident Research,* Vol. 28, 2020, pp. 100132 %@ 102213-106657.
[136] Zeng, Q., F. Wang, T. Chen, and N. N. Sze. Incorporating real-time weather conditions into analyzing clearance time of freeway accidents: A grouped random parameters hazard-based duration model with time-varying covariates. *Analytic Methods in Accident Research*, 2023, pp. 100267 %@ 102213-106657.
[137] Khattak, A. J., J. Liu, B. Wali, X. Li, and M. Ng. Modeling traffic incident duration using quantile regression. *Transportation research record,* Vol. 2554, No. 1, 2016, pp. 139-148 %@ 0361-1981.
[138] Wali, B., A. J. Khattak, and J. Liu. Heterogeneity assessment in incident duration modelling: Implications for development of practical strategies for small & large scale incidents. *Journal of Intelligent Transportation Systems,* 2021, pp. 1-16 %@ 1547-2450.

[139] Hamad, K., R. Al-Ruzouq, W. Zeiada, S. Abu Dabous, and M. A. Khalil. Predicting incident duration using random forests. *Transportmetrica A: transport science,* Vol. 16, No. 3, 2020, pp. 1269-1293 %@ 2324-9935.
[140] Wu, W.-w., S.-y. Chen, and C.-j. Zheng. Traffic incident duration prediction based on support vector regression.In *ICCTP 2011: Towards Sustainable Transportation Systems,* 2011. pp. 2412-2421.
[141] Tang, J., L. Zheng, C. Han, F. Liu, and J. Cai. Traffic incident clearance time prediction and influencing factor analysis using extreme gradient boosting model. *Journal of Advanced Transportation,* Vol. 2020 %@ 0197-6729, 2020.
[142] Tang, J., L. Zheng, C. Han, W. Yin, Y. Zhang, Y. Zou, and H. Huang. Statistical and machine-learning methods for clearance time prediction of road incidents: A methodology review. *Analytic Methods in Accident Research,* Vol. 27, 2020, pp. 100123 %@ 102213-106657.
[143] Gourieroux, C., A. Monfort, and A. Trognon. Pseudo maximum likelihood methods: Theory. *Econometrica: journal of the Econometric Society,* 1984, pp. 681-700 %@ 0012-9682.
[144] Huang, Y., X. Wang, and D. Patton. Examining spatial relationships between crashes and the built environment: A geographically weighted regression approach. *Journal of transport geography,* Vol. 69, 2018, pp. 221-233 %@ 0966-6923.
[145] Pulugurtha, S. S., and S. Mathew. Modeling AADT on local functionally classified roads using land use, road density, and nearest nonlocal road data. *Journal of transport geography,* Vol. 93, 2021, pp. 103071 %@ 100966-106923.
[146] Pan, Y., S. Chen, S. Niu, Y. Ma, and K. Tang. Investigating the impacts of built environment on traffic states incorporating spatial heterogeneity. *Journal of transport geography,* Vol. 83, 2020, pp. 102663 %@ 100966-106923.
[147] Zhang, Z., and J. Sun. Interval censoring. *Statistical methods in medical research,* Vol. 19, No. 1, 2010, pp. 53-70 %@ 0962-2802.
[148] Cox, D. R. Partial likelihood. *Biometrika,* Vol. 62, No. 2, 1975, pp. 269-276 %@ 1464-3510.
[149] Finkelstein, D. M. A proportional hazards model for interval-censored failure time data. *Biometrics*, 1986, pp. 845-854 %@ 0006-0341X.
[150] Li, R., F. C. Pereira, and M. E. Ben-Akiva. Overview of traffic incident duration analysis and prediction. *European transport research review,* Vol. 10, No. 2, 2018, pp. 1-13 %@ 1866-8887.
[151] TDOT. *How does the HELP Program work?* https://www.tn.gov/tdot/traffic-operations-division/how-does-the-help-program-work-.html. Accessed 10.03, 2022.
[152] Zhang, H., Y. Gu, R. Huang, and L. D. Han. Quantify Freeway Safety Service Patrol and Protect the Queue Impact on Transportation Network Reliability.In, Tennessee. Department of Transportation, 2022.
[153] Chou, C., E. Miller-Hooks, and I. Promisel. Benefit-cost analysis of freeway service patrol programs: Methodology and case study. *Advances in transportation studies*, Vol. 20, 2010, pp. 81-96 %@ 1824-5463.

[154] Salum, J. H., A. E. Kitali, T. Sando, and P. Alluri. Evaluating the impact of Road Rangers in preventing secondary crashes. *Accident Analysis & Prevention,* Vol. 156, 2021, pp. 106129 %@ 100001-104575.
[155] Yu, Q., L. Li, and G. Y. C. Wong. On consistency of the selfâ€• consistent estimator of survival functions with intervalâ€• censored data. *Scandinavian Journal of Statistics,* Vol. 27, No. 1, 2000, pp. 35-44 %@ 0303-6898.
[156] Coifman, B., and S. Kim. Speed estimation and length based vehicle classification from freeway single-loop detectors. *Transportation research part C: emerging technologies,* Vol. 17, No. 4, 2009, pp. 349-364 %@ 0968-0090X.
[157] Bai, Y., S. D. Schrock, T. E. Mulinazzi, W. Hou, C. Liu, and U. Firman. Estimating highway pavement damage costs attributed to truck traffic. 2010.
[158] Gillespie, T. D., and S. M. Karamihas. Heavy truck properties significant to pavement damage. *ASTM Special Technical Publication,* Vol. 1225, 1994, pp. 52-52 %@ 0066-0558.
[159] Huai, T., S. D. Shah, J. W. Miller, T. Younglove, D. J. Chernich, and A. Ayala. Analysis of heavy-duty diesel truck activity and emissions data. *Atmospheric Environment,* Vol. 40, No. 13, 2006, pp. 2333-2344 %@ 1352-2310.
[160] Administration, F. H. *Computation Guidance for Congestion Mitigation and Air Quality Improvement (CMAQ) Program Total Emissions Reduction Measure*. https://www.fhwa.dot.gov/tpm/guidance/emission_reduction_guide.pdf. Accessed 05.06, 2021.
[161] Dong, C., Q. Dong, B. Huang, W. Hu, and S. S. Nambisan. Estimating factors contributing to frequency and severity of large truckâ€“involved crashes. *Journal of Transportation Engineering, Part A: Systems,* Vol. 143, No. 8, 2017, pp. 04017032 %@ 04012473-04012907.
[162] Adminstration, F. H. *Traffic Data Computation Method*. https://www.fhwa.dot.gov/policyinformation/pubs/pl18027_traffic_data_pocket_guide.pdf. Accessed July 31, 2021.
[163] Coifman, B. Improved velocity estimation using single loop detectors. *Transportation Research Part A: Policy and Practice,* Vol. 35, No. 10, 2001, pp. 863-880 %@ 0965-8564.
[164] Klein, L. A., M. K. Mills, and D. R. P. Gibson. Traffic detector handbook: Volume I.In, Turner-Fairbank Highway Research Center, 2006.
[165] Hall, F. L., and B. N. Persaud. Evaluation of speed estimates made with single-detector data from freeway traffic management systems. *Transportation Research Record*, No. 1232 %@ 0309049601, 1989.
[166] Courage, K. G., C. S. Bauer, and D. W. Ross. Operating parameters for main-line sensors in freeway surveillance systems. *Transportation Research Record,* Vol. 601, 1976, pp. 19-28.
[167] Mikhalkin, B., H. J. Payne, and L. Isaksen. Estimation of speed from presence detectors.In, 1972.
[168] Wang, Y., and N. L. Nihan. Freeway traffic speed estimation with single-loop outputs. *Transportation Research Record,* Vol. 1727, No. 1, 2000, pp. 120-126 %@ 0361-1981.

[169] ---. Dynamic estimation of freeway large-truck volumes based on single-loop measurements.In, *No. 8*, Taylor & Francis, 2004. pp. 133-141 %@ 1547-2450.
[170] Dailey, D. J. A statistical algorithm for estimating speed from single loop volume and occupancy measurements. *Transportation Research Part B: Methodological,* Vol. 33, No. 5, 1999, pp. 313-322 %@ 0191-2615.
[171] Zhang, Y., Y. Xie, and Z. Ye. Estimation of large truck volume using single loop detector data.In, 2008.
[172] Zhang, G., Y. Wang, and H. Wei. Artificial neural network method for length-based vehicle classification using single-loop outputs. *Transportation Research Record,* Vol. 1945, No. 1, 2006, pp. 100-108 %@ 0361-1981.
[173] Kwon, J., P. Varaiya, and A. Skabardonis. Estimation of truck traffic volume from single loop detectors with lane-to-lane speed correlation. *Transportation Research Record,* Vol. 1856, No. 1, 2003, pp. 106-117 %@ 0361-1981.
[174] Hazelton, M. L. Estimating vehicle speed from traffic count and occupancy data. *Journal of Data Science,* Vol. 2, No. 3, 2004, pp. 231-244 %@ 1683-8602.
[175] Ye, Z., Y. Zhang, and D. R. Middleton. Unscented Kalman filter method for speed estimation using single loop detector data. *Transportation Research Record,* Vol. 1968, No. 1, 2006, pp. 117-125 %@ 0361-1981.
[176] Bertsimas, D., and J. N. Tsitsiklis. *Introduction to linear optimization*. Athena Scientific Belmont, MA, 1997.
[177] Mednis, A., G. Strazdins, R. Zviedris, G. Kanonirs, and L. Selavo. Real time pothole detection using android smartphones with accelerometers.In, IEEE, 2011. pp. 1-6 %@ 1457705133.
[178] Gu, Y., D. Liu, J. Stanford, and L. D. Han. Innovative Method for Estimating Large Truck Volume Using Aggregate Volume and Occupancy Data Incorporating Empirical Knowledge Into Linear Programming. *Transportation research record,* Vol. 2676, No. 11, 2022, pp. 648-663 %@ 0361-1981.

VITA

Yangsong Gu was born and raised in a village in Nantong, China. In 2019, he graduated from Changsha University of Science and Technology with a bachelor's degree in Transportation Engineering. He was awarded National Scholarship two times during his undergraduate period. In the fall of 2019, he joined Dr. Lee D. Han's research group as a graduate research assistant. In August 2022, he became a Ph.D. candidate with a concentration in transportation in Civil Engineering. He also concurrently pursues a master's degree in Statistics.

In Dr. Han's group, he participated in multiple research projects collaborating with TDOT, including measurement of effectiveness for TSMO (traffic system management and operation), benefits of freeway service patrol, exploring Waze use scenarios, and so on. Meanwhile, he also serves as a reviewer for academic journals such as Transportation Research Record and Accident Analysis and Prevention.

Over the past four years, Yangsong received many scholarships and awards, including middle Tennessee ASHE general academic scholarships, ITSTN first place winner, TSITE student paper competition first place winner for the academic year of 2021 and 2022, SDITE student paper competition first place winner, T. Darcy Sullivan scholarship, finalist of NOCOE transportation tournament, graduate student senate travel award and so on.